

Development of Analytical Methods for the Determination of Methylarginines in Serum

Thomas Linz

B.S. Chemistry, Truman State University, 2007

Submitted to the Department of Chemistry and the Graduate School of the University of Kansas
in partial fulfillment of the requirements for the degree of Doctor of Philosophy.

Susan Lunte – Chair

Robert Dunn

Craig Lunte

David Weis

Brian Ackley

Dissertation Defense: April 12, 2012

The Dissertation Committee for Thomas Linz certifies that this is the
approved version of the following dissertation:

Development of Analytical Methods for the Determination of Methylarginines in Serum

Susan Lunte – Chair

April 12, 2013

Date Approved

Abstract

Nitric oxide (NO) plays a crucial role in numerous physiological pathways including the regulation of the endothelium that lines blood vessels throughout the body. Therefore, in order to maintain good endothelial health, there must be a careful homeostasis of NO. Under pathological conditions that impair the production of NO, endothelial function is disrupted which can result in various pathologies including cardiovascular diseases (CVDs) and respiratory disorders. A class of endogenous compounds that inhibit the enzyme responsible for NO synthesis *in vivo* are the methylated arginines (MAs). Given their propensity for attenuating NO production, it comes as no surprise that MAs have been implicated in several diseases. Increased blood concentrations of asymmetric dimethylarginine (ADMA), symmetric dimethylarginine (SDMA), and monomethylarginine (MMA) have been reported in patients suffering from CVDs. However, despite evidence demonstrating the link between MAs and these diseases, no diagnostic concentrations have yet been established. The goal of this work was to develop an analytical method capable of rapidly determining the concentrations of MAs in blood samples so that threshold concentrations indicative of disease could be established. Further efforts were then made to fabricate a point-of-care device that could be used in a clinical setting to measure MAs as a means of preventative diagnostics.

Analyzing components in a serum sample is a very challenging endeavor because of the incredible complexity of the sample matrix. To alleviate matrix interferences, a method was developed to rapidly isolate MAs from serum using a newly developed heating procedure. The sample was immersed in a boiling water bath which caused it to solidify. Solvent was then added to the congealed serum and briefly homogenized to permit solid-liquid extraction to take place.

After a brief incubation period at room temperature, the sample was centrifuged to sediment the aggregated serum proteins, leaving the small molecules of interest in the supernatant. The supernatant was then derivatized with naphthalene-2,3-dicarboxaldehyde to label the MAs for analysis by capillary electrophoresis (CE) with fluorescence detection. A CE method was developed using sulfobutylether- β -cyclodextrin and dimethylsulfoxide as buffer modifiers to obtain good resolution between the MAs and the other components in serum-derived samples. Under optimized conditions, baseline resolution was achieved which allowed precise quantitation of the MAs. The separation method was then transferred to a microchip electrophoresis (MCE) device that made it possible to perform the same analysis more rapidly on a smaller, portable device. MAs were separated using this MCE platform as a first step towards the development of a point-of-care device to perform clinical analyses on-chip.

I would like to dedicate this dissertation to the chemistry faculty at Truman State University, especially Dr. Brian Lamp. At the time in my life when I was most uncertain about what I wanted in the future, you provided me with intense clarity. I learned that pushing one's limits was not something to fear, but rather something to strive for.

Acknowledgements

No accomplishment is truly achieved by a single individual. It is through the effort and dedication of our mentors, both personal and professional, that we are able to be successful in our ventures. Therefore, while this dissertation is devoted to my work, it is only fitting that I begin by bidding thanks to all of those who helped me reach this point.

I would first like to thank my advisor, Sue Lunte, for allowing me to pursue my degree in her lab. The freedom she granted me in the lab to achieve the goals of my project were instrumental in advancing my critical thinking and troubleshooting skills, which have made me into a stronger scientist. I also need to thank Sue for the vast opportunities she provided me with during grad school that most students are not fortunate enough to get. In addition to allowing me to expand my breadth of knowledge by attending numerous conferences during my time at KU, I also received a rare opportunity to lobby federal congress for research funding. Not many professors are able to gain that experience themselves, let alone provide a student with that opportunity, so for this, I am grateful.

Given Sue's hectic travel schedule and countless meetings over the years, I would also like to thank the members of the group that came before me for providing me with suggestions and troubleshooting advice when I was first getting started. The knowledge and wisdom I received from Drs. Dave Fischer, Pradyot Nandi, Matt Hulvey, and Courtney Kuhnline helped make my life so much easier in way that I never fully appreciated until after they left. I tried to emulate their helpfulness in my own way when giving instruction to the younger students once I became the senior lab member. To that end, I am happy to have gotten the chance to work with Dulan Gunasekara, Rachel Saylor, Joe Siegel, and Christa Snyder, and I hope that I have aided

their development into capable scientists. I consider all of these people to be friends, and wish them the best of luck in the future.

Although most of my time in graduate school was probably spent in the lab, I am grateful for the people that made the time I spent out of it so enjoyable. While there is no way to list everyone, I would like to single out the Livanecs, my boyfriends, and my girlfriend as amazing people whose friendships I am grateful for. Phil and Maggie, thank you for hosting all those KU basketball games and bonfires at your house. I loved all of them, and things were nowhere near as fun when you left for Texas. Dan Clark and Carl Cooley (and to a lesser extent Chuck Norris), while all those lunch dates gave me the rotund figure I have today, my sanity would never have lasted without you guys. Finally, Cassie Ward, I truly appreciate you putting up with me over the years. I know most of the time when I said that I needed one more hour to finish my experiments that often turned into two or three more hours. I am thankful for your understanding nature and for all the support you have given me.

Lastly, I need to thank my family for their encouragement over the years. Although they probably never really understood my work and could not completely comprehend the struggles associated with graduate school, their support has been unwavering. They were proud of me and believed in me, and although that didn't necessarily make the work any easier, it certainly helped lift my spirits. Thanks guys.

Table of Contents

1. Chapter One: Research Objectives and Chapter Summaries.....	1
1.1 Research Objectives.....	2
1.2 Chapter Summaries.....	3
1.2.1 Chapter Two.....	3
1.2.2 Chapter Three.....	3
1.2.3 Chapter Four.....	3
1.2.4 Chapter Five.....	4
1.2.5 Chapter Six.....	5
1.2.6 Chapter Seven.....	5
2. Chapter Two: Biological and Analytical Background: Setting the Stage.....	6
2.1 Nitric Oxide Synthase Physiology.....	7
2.2 Methylarginines and NO Production.....	10
2.3 Methylarginine Involvement in Disease States.....	15
2.3.1 Cardiovascular Disease.....	15
2.3.2 Respiratory Disorders.....	17
2.4 Analytical Methods to Monitor NOS Activity.....	19
2.4.1 Nitric Oxide Analysis.....	20
2.4.2 Methylarginine Analysis.....	21
2.4.2.1 Antibody-Based Analyses.....	21
2.4.2.2 Separations-Based Analyses.....	23

2.4.2.2.1 Liquid Chromatography.....	23
2.4.2.2.2 Capillary Electrophoresis.....	24
2.4.2.3 Derivatization Chemistry.....	29
2.5 Conclusions.....	32
2.6 References.....	34
3. Chapter Three: Optimization of a Capillary Electrophoresis Separation Method for the Determination of NDA-Derivatized Methylarginines.....	47
3.1 Introduction.....	48
3.2 Materials and Methods.....	50
3.2.1 Reagents.....	50
3.2.2 Capillary Electrophoresis.....	51
3.3 Results and Discussion.....	52
3.3.1 Run Buffer Modifiers.....	52
3.3.2 Separation Optimization.....	58
3.3.3 Internal Standard Identification and Peak Capacity Improvement.....	60
3.3.3.1 Dimethylsulfoxide Addition.....	62
3.3.4 CE-LIF Method Characterization.....	67
3.3.5 NDA Derivatization.....	71
3.3.6 Other Separation Considerations.....	80
3.4 Conclusions.....	83
3.5 References.....	84

4. Chapter Four: Development of a Heat-Assisted Extraction Sample Preparation Method for the Determination of Methylarginines in Serum.....	86
4.1 Introduction.....	87
4.2 Materials and Methods.....	89
4.2.1 Reagents.....	89
4.2.2 Capillary Electrophoresis.....	89
4.2.3 Heat-Assisted Extraction Procedure.....	90
4.2.4 Solid-Phase Extraction Procedure.....	90
4.3 Results and Discussion.....	90
4.3.1 NDA Derivatization.....	93
4.3.2 Capillary Electrophoresis Characterization.....	97
4.3.3 Solid-Phase Extraction Characterization.....	99
4.3.4 Sample Preparation Considerations.....	106
4.3.5 Heat-Assisted Extraction Optimization.....	107
4.3.6 Sample Preparation Method Comparison.....	114
4.3.7 Determination of Serum MAs.....	117
4.4 Conclusions.....	122
4.5 References.....	123
5. Chapter Five: Determination of Methylarginines in Clinical Samples.....	128
5.1 Introduction.....	129
5.2 Materials and Methods.....	130
5.2.1 Reagents.....	130

5.2.2 Patient Populations.....	130
5.2.3 Heat-Assisted Extraction Procedure.....	131
5.2.4 Capillary Electrophoresis.....	132
5.2.5 Liquid Chromatography-Tandem Mass Spectrometry (LC-MS/MS).....	133
5.3 Results and Discussion.....	134
5.3.1 CE Separation Optimization.....	134
5.3.2 Analysis of Cardiovascular Disease Serum Samples.....	137
5.3.2.1 Determination of Clinical Methylarginine Concentrations.....	137
5.3.2.2 Arginine Methylation Index.....	139
5.3.2.3 Interfering Species.....	141
5.3.3 Analysis of Respiratory Disease Plasma Samples.....	147
5.3.3.1 Clinical Methylarginine Concentrations.....	148
5.3.3.2 Arginine Methylation Index.....	152
5.4 Conclusions.....	154
5.5 References.....	155
6. Chapter Six: Development of a Microchip Electrophoresis Point-of-Care Device for the Determination of Methylarginines.....	157
6.1 Introduction.....	158
6.2 Methods and Materials.....	159
6.2.1 Reagents.....	159
6.2.2 Microchip Fabrication.....	160
6.2.2.1 PDMS Microchips.....	160

6.2.2.2 Glass Microchips.....	162
6.2.4 Microchip Operation.....	168
6.2.4.1 PDMS Microchip Operation.....	168
6.2.4.2 Glass Microchip Operation.....	170
6.3 Results and Discussion.....	171
6.3.1 Microchip Electrophoresis with Electrochemical Detection.....	171
6.3.1.1 Electrochemical Response of NDA-Labeled Analytes.....	173
6.3.1.2 Evaluation of Alternative Nucleophiles.....	175
6.3.1.2.1 Electrokinetic Flow Injection Analysis.....	176
6.3.1.2.2 Cyclic Voltammetry.....	181
6.3.1.2.3 Microchip Electrophoresis.....	184
6.3.2 Microchip Electrophoresis with Fluorescence Detection.....	191
6.4 Conclusions.....	193
6.5 References.....	195
7. Chapter Seven: Conclusions and Future Directions.....	198
7.1 Dissertation Summary.....	199
7.2 Future Directions.....	201
7.2.1 Analytical Advances.....	201
7.2.2 Biochemical Mechanism Elucidation Studies.....	202
7.2.2.1 Cardiovascular Disease.....	202
7.2.2.2 Respiratory Disease.....	203
7.3 References.....	205

Chapter One

Research Objectives and Chapter Summaries

1.1 Research Objectives

Nitric oxide (NO) is a small, reactive molecule that is involved in cell signaling, immune response, and vasodilation. Without sufficient NO production, these processes are disrupted resulting in a number of disease states. One such example is with regards to diseases related to the endothelium. Since NO is central to regulating endothelial cells throughout the body, including in blood vessels and the lungs, improper concentrations of NO can impair endothelial function and cause pathologies including cardiovascular disease (CVD) and respiratory disorders.

Maintaining proper NO homeostasis is dependent on the activity of the NO-producing enzyme nitric oxide synthase (NOS) and the concentrations of methylarginines (MAs). MAs are small molecule inhibitors of NOS that serve to regulate *in vivo* NO production. Under normal conditions, MAs are present in plasma in the mid-nanomolar range; however, under pathological conditions, the concentrations of these species can be elevated above 1 μM . Since increased amounts of MAs lead to reduced endogenous NO production, these species could alter endothelial function and stimulate disease onset. Studies have shown that patients suffering from diseases involving endothelial dysfunction, such as CVDs and respiratory diseases, have higher systemic MA concentrations. Because MAs are directly involved in the NO pathway that is believed to be responsible for pathogenesis, serum concentrations of these compounds could potentially serve as biomarkers for disease diagnosis.

The goal of this dissertation project was the development of analytical methods for the determination of MAs in serum samples. The following chapters will explain in detail the experiments that were undertaken to develop novel sample preparation and separations methods to enable extraction of MAs from complex sample matrices and their subsequent quantitation.

1.2 Chapter Summaries

1.2.1 Chapter Two

This chapter provides a review of the relevant biological and analytical background information central to the goals of this dissertation. An account of the pathways involved in the *in vivo* production of NO is described along with information regarding the involvement of MAs in these processes. This information provides the rationale and significance of the project. A description of the analytical methods which were used to conduct the research in subsequent chapters is also given. This includes generic information on the theoretical basis behind the analytical methods as well as a review of other methods that have been previously utilized to measure MAs.

1.2.2 Chapter Three

This chapter describes the optimization of a capillary electrophoresis method designed to separate the individual MA species. The systematic evaluation of the various run buffer modifiers is discussed to explain which additives were necessary to achieve a good separation. This discussion was also expanded to describe the process undertaken to select a suitable internal standard for the analysis, and the separation modifications necessary for its inclusion. Additional information describing optimal conditions for the derivatization procedure is also provided.

1.2.3 Chapter Four

Sample preparation concerns are always great when analyzing complex samples such as serum. Therefore, this chapter presents details on the rationale and optimization of a novel heat-

assisted extraction method. Emphasis was placed on minimizing cost while maximizing throughput to enable this method to be practical in a clinical setting. During development of this procedure, several different parameters were evaluated to determine the conditions that produced the most efficient extraction. Following optimization, the heat-assisted extraction was compared to a traditional solid-phase extraction method, and the results obtained from each were found to be in good agreement. However, the new method significantly expedited sample processing while also diminishing the cost associated with sample preparation.

1.2.4 Chapter Five

The sample preparation and separation methods described in Chapters 3 and 4 were combined here and applied to the analysis of clinical samples. The results of two small-scale clinical studies are reported in this chapter which were designed to investigate the diagnostic potential of MAs for different disease states related to reduced NO bioavailability. In the first study, serum samples were analyzed from patients with and without coronary artery disease to determine whether a difference in MA concentrations existed between the two populations. The purpose of this experiment was to determine threshold concentrations indicative of disease that could be used in preventative diagnostics. A second study was also performed to determine whether respiratory distress in newborns was caused by poor vasodilation stemming from increased concentrations of MAs. To that end, a preliminary study was conducted to establish baseline MA concentrations in babies over the first six months of life.

1.2.5 Chapter Six

A long-term goal of this project was to develop a miniature analysis system that would enable rapid and inexpensive measurements of MAs. This chapter describes the progress made in the development of a point-of-care device capable of quickly measuring MAs in low-volume samples. Microchip electrophoresis (MCE) was coupled to both electrochemical (EC) and laser-induced fluorescence (LIF) detection modes to determine which better allowed endogenous MA concentrations to be determined. The MCE-EC separation was found to have inadequate limits of detection (LODs) using the conditions from the previous chapters. Given this, an additional study was performed to improve the derivatization chemistry to better facilitate EC analysis. A novel nucleophile was identified for the derivatization reaction which imparted several advantages; however, even with the use of this reagent, the LODs of MCE-EC were still too high to enable quantitation of MAs from serum samples. Therefore, an investigation was made into the use of MCE-LIF to separate MAs. A preliminary separation of MAs was performed with promising results. It was found that this platform provided baseline resolution between standards and had a sufficient LOD to monitor endogenous MA concentrations.

1.2.6 Chapter Seven

This chapter summarizes the research completed at the time of the dissertation defense. Additional experiments are also described to give future direction to the project. These entail both applications-based experiments and technology-driven improvements that address important advances that could still be made with regard to MA analysis.

Chapter Two

Biological and Analytical Background: Setting the Stage

2.1 Nitric Oxide Synthase Physiology

Nitric oxide (NO) is an interesting molecule whose role in numerous physiological pathways makes it essential to life [1]. It is a small, gaseous molecule that diffuses freely within cells and the extracellular space. Therefore, it can produce physiological responses distal to the site of production and serve as a signaling molecule and neurotransmitter in a variety of tissues [2]. NO also plays an important role in endothelial physiology [3]. Its potent, immediate action on platelets in the blood stream prevents aggregation [4]. Additionally, once NO is synthesized, it can bind to the heme center of guanylate cyclase, which induces the production of cyclic guanosine monophosphate [5]. This stimulates the relaxation of vascular smooth muscle which in turn increases vasodilation in blood vessels [6]. This helps to lower blood pressure and improve blood oxygenation [1]. It has also been shown that NO is involved in the formation of reactive nitrogen and oxygen species (RNOS) [7]. This can serve both beneficial and detrimental purposes in the body whereby these RNOS can either damage native cells or can attack foreign cells during an immune response [8]. Because of these factors, achieving proper NO homeostasis is crucial for healthy survival.

The production of NO *in vivo* is carried out by a family of enzymes termed nitric oxide synthases (NOSs). NOS catalyzes the oxidation of arginine in the presence of tetrahydrobiopterin (BH₄), oxygen, and NADPH to form citrulline and NO [9]. There are three different isoforms of NOS: endothelial (eNOS), neuronal (nNOS), and inducible (iNOS). eNOS and nNOS, both constitutively expressed in cells throughout the body (not strictly in endothelial and neuronal cells [10]), are modulated by calcium/calmodulin (CAM) and dependent on their local concentrations [11]. iNOS is expressed throughout the body as well; however, it is calcium-independent. The output of NO from iNOS is dependent on the surrounding environment and can

vary greatly. Under normal conditions, very little NO is produced. However, under pathological conditions, iNOS rapidly stimulates NO production and is capable of producing far higher concentrations than either eNOS or nNOS. These differences in NO production govern the physiological function of the different isoforms. eNOS and nNOS primarily serve to synthesize NO for vasodilation or signaling purposes while iNOS predominantly produces NO in immune response pathways [8].

Tetrahydrobiopterin is a cofactor that is critical for maintaining proper activity of all NOSs. Studies have shown that NOS uncouples without adequate concentrations of BH₄ resulting in a decrease in NO production and an increase in superoxide (O₂^{•-}) [12, 13]. This shift in NOS production leads to vasoconstriction from the lack of NO as well as an increase in oxidative stress damage resulting from the formation of reactive oxygen species [11, 14]. However, it is not simply the BH₄ concentration that dictates the progression of this physiologically harmful pathway. The oxidation state of BH₄ *in vivo* is crucial to its biological activity. Reports in the literature have shown that BH₄ is extremely susceptible to oxidation [15, 16]. When present in its partially oxidized form, dihydrobiopterin (BH₂), or its completely oxidized form, biopterin, the molecule is no longer capable of serving as a cofactor for NOS but rather causes enzyme uncoupling which leads to the production of O₂^{•-} [12]. It is the ratio of BH₄ to BH₂ and biopterin, not merely the endogenous BH₄ concentration, that determines biological function [17, 18]. Structures of these molecules are shown in Figure 2.1.

The uncoupling of NOS not only decreases NO production but also stimulates the production of reactive molecules like O₂^{•-}. Once formed, O₂^{•-} can react with NO to form peroxynitrite (ONOO⁻) which has been shown to react with lipids and proteins and is capable of causing apoptosis [19, 20]. Once these destructive reactive species are produced, a feed-forward

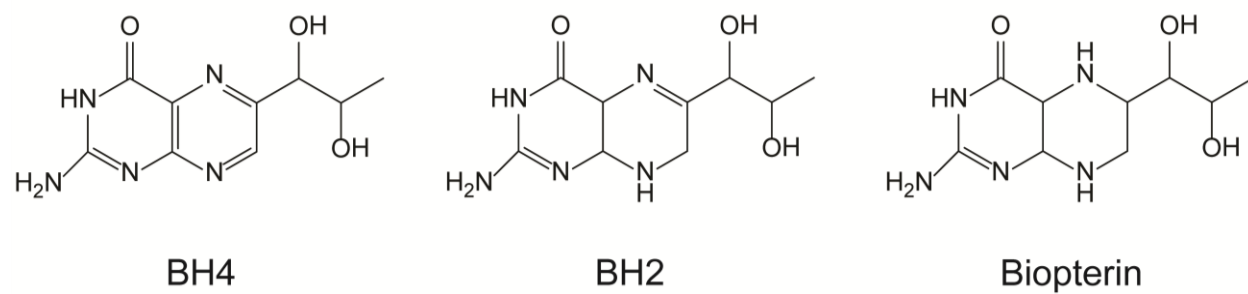


Figure 2.1 Structures of the bipterins involved in the NOS pathway.

mechanism is initiated which propagates the cycle shown in Figure 2.2. This causes even more harmful species to be synthesized which in turn causes further cellular damage. Therefore, it is critical that NOS functions properly *in vivo* or serious health consequences could arise.

2.2 Methylarginines and NO Production

While NOS utilizes arginine as a substrate for the synthesis of NO, certain methylated arginines (MAs) regulate NO production through competitive inhibition. Specifically, asymmetric N^G, N^G -dimethylarginine (ADMA) and N^G -monomethyl-L-arginine (MMA) have been shown to prevent NO generation and cause vasoconstriction and increased platelet adhesion in humans as well as in animal models [6, 21, 22]. The related molecule symmetric N^G, N^G -dimethylarginine (SDMA) does not competitively inhibit NOS. However, SDMA along with the other two MAs compete with arginine for cellular uptake via cationic amino acid transporters, and thus all impact the amount of NO that is produced [23]. As a result, research has been performed to elucidate the role of these compounds in various pathologies where NO bioavailability is believed to play a significant role. Structures of the different MA analogues along with their average human plasma concentrations are shown in Figure 2.3.

MAs are found endogenously in most cell types as well as in plasma [24, 25]. They are not synthesized *de novo* but rather are formed through methylation of arginine residues in proteins [23, 26, 27]. Protein arginine methyltransferases (PRMTs) are a class of enzymes that covalently attach one or two methyl groups to the guanidine nitrogens of an arginine residue. Two types of PRMT have been reported in the literature. PRMT-I asymmetrically dimethylates arginine residues to form ADMA, while PRMT-II symmetrically dimethylates arginines to form SDMA. Both isoforms are capable of producing MMA [21, 23, 26]. During the course of normal

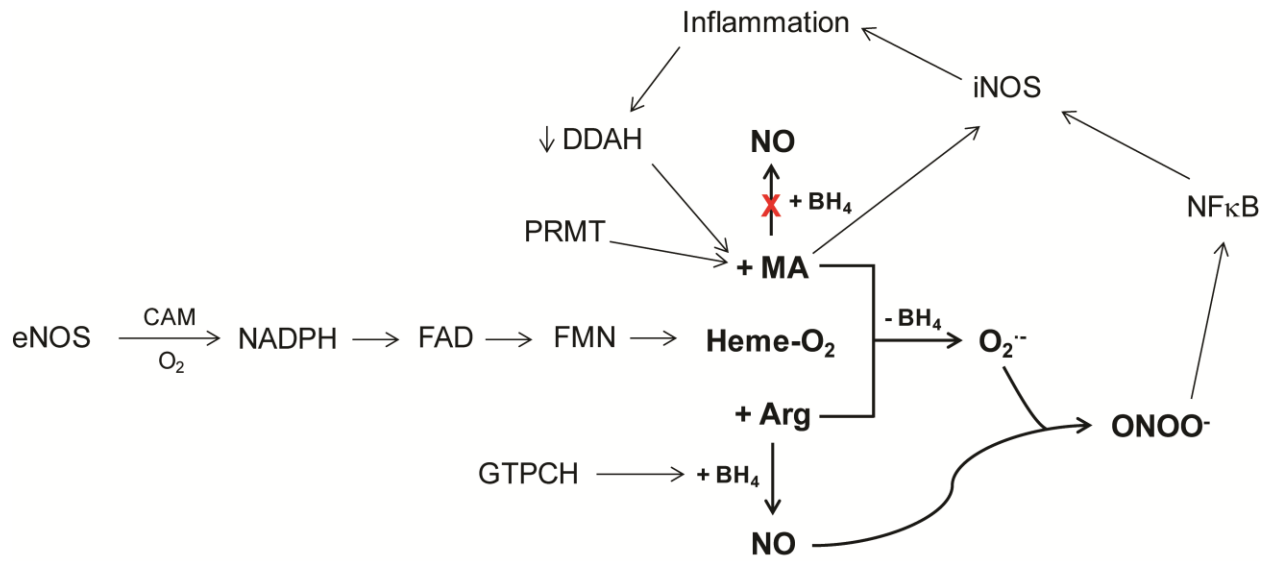


Figure 2.2 The eNOS pathway. Nitric oxide is synthesized when adequate concentrations of arginine and BH₄ are present. NO production ceases under conditions of BH₄ depletion or increased levels of MAs. FAD: flavin adenine dinucleotide; FMN: flavin mononucleotide; NFκB: nuclear factor kappa B; GTPCH: guanosine triphosphate cyclohydrolase.

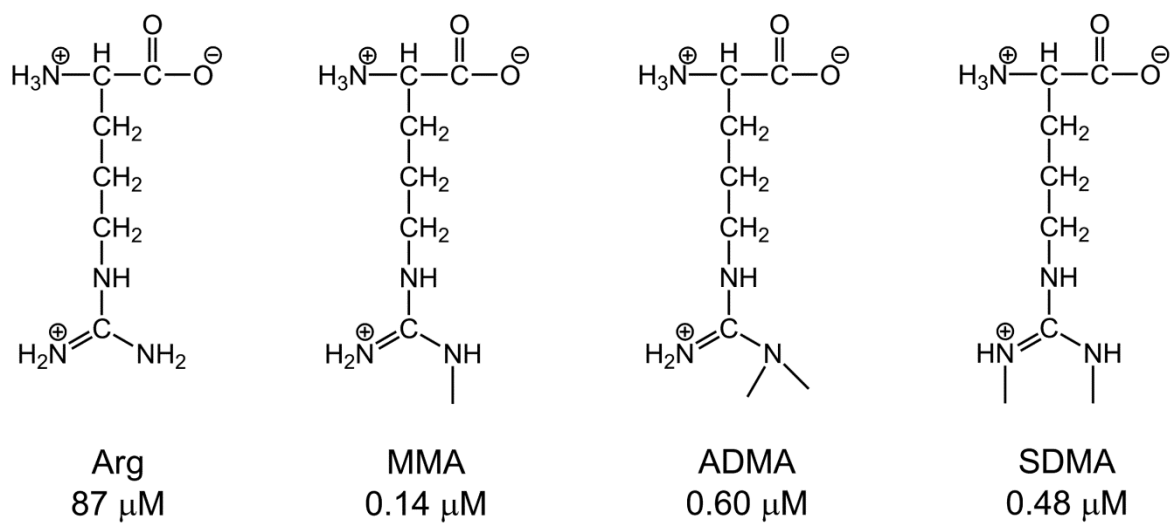


Figure 2.3 Structures of the methylarginines and their average plasma concentrations.

protein turnover, MAs are liberated and can then exit the cell via cationic amino acid transporters and enter systemic circulation [23].

Serum arginine concentrations are 30-100 μM while MA concentrations are typically 100-800 nM. Despite the relatively low amounts of MAs compared arginine, these NOS inhibitors are quite potent and can affect vasodilation. Inhibition constants for ADMA and MMA range from 500 nM to 1.1 μM depending on the cell type [28-30]. While normal physiological concentrations of these species are too low to significantly inhibit NO production because of the vast excess of arginine present, the intracellular amounts can be rapidly upregulated. Under pathological conditions, a significant increase of MAs has been reported inside the cell indicating that cells are capable of storing MAs. This influx of MAs is capable of having a substantial effect on NO production and has been shown to impair vascular relaxation [28].

Free MAs can have a profound effect on vasodilation by preventing the synthesis of NO and are therefore well-regulated *in vivo*. The exact mechanism of MA degradation is dependent upon the MA species. ADMA and MMA are predominantly metabolized by the enzyme dimethylarginine dimethylaminohydrolase (DDAH) where each species is broken down to form dimethylamine and methylamine, respectively, and citrulline. There are two isoforms of DDAH (DDAH-I and DDAH-II) but both enzymes perform the same function. The primary difference is the localization of the enzyme in certain tissues [31]. It should be noted that DDAH has no effect on the metabolism of SDMA. SDMA is cleared exclusively via renal excretion, while this pathway only plays a minor role in the elimination of ADMA and MMA. The two asymmetric MA analogues are primarily broken down by DDAH (~90%) with only small amounts cleared renally (~10%) [24]. The physiological pathways involving MAs are illustrated in Figure 2.4.

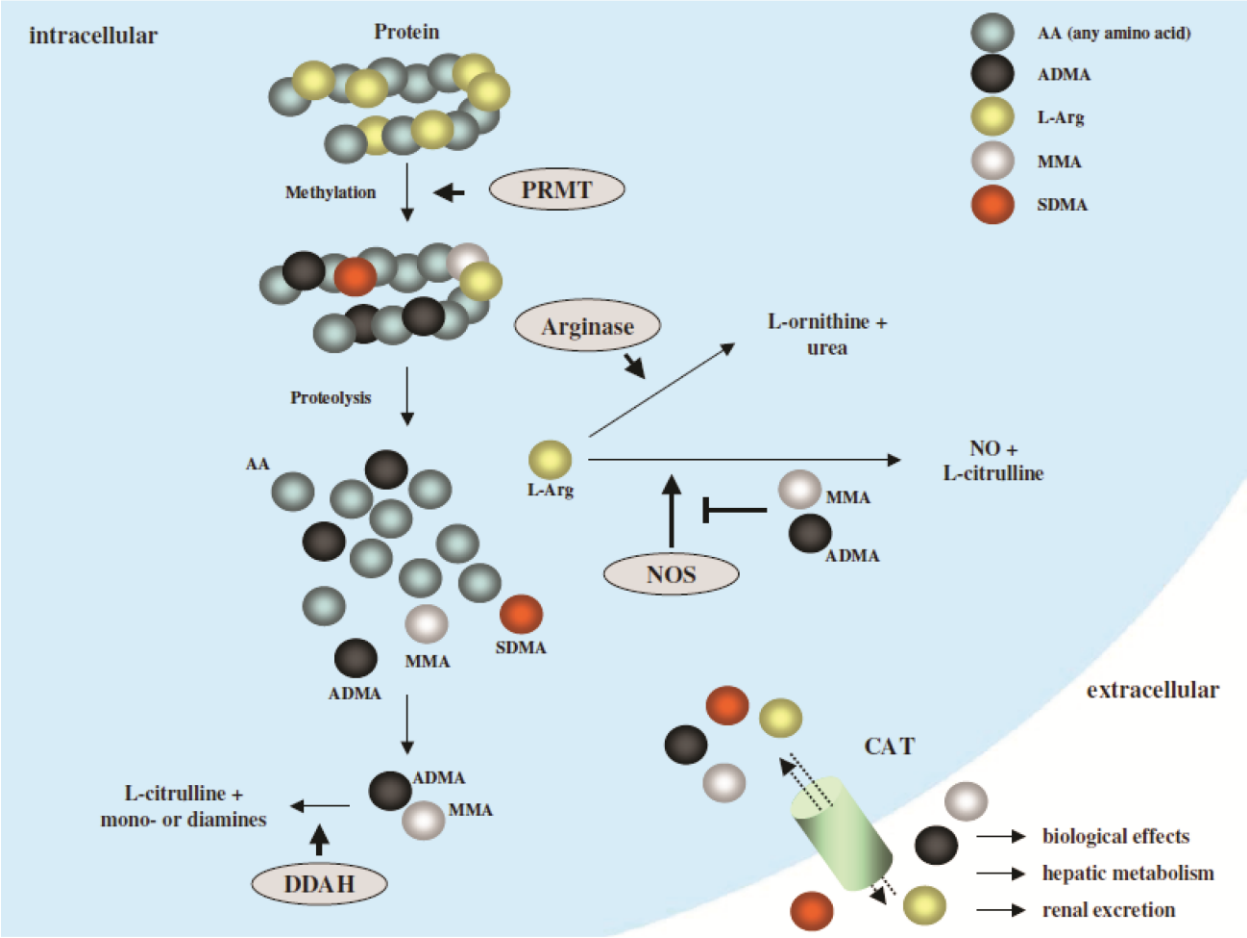


Figure 2.4 Biochemical pathways of MAs. Image from reference [23].

2.3 Methylarginine Involvement in Disease States

2.3.1 Cardiovascular Disease

Cardiovascular disease (CVD) is a broad term encompassing diseases such as high blood pressure, coronary artery disease, and stroke. It is estimated that 80 million people in the United States currently suffer from one or more forms of CVD. Due to its high prevalence, 35.3% of all deaths in the US are CVD-related, making it the leading cause of mortality in the nation [32]. Although there are many factors that contribute to the onset of CVD, disruption of the endothelium and a reduced bioavailability of NO are believed to play central roles and could be responsible for disease onset [33].

The physiological function of MAs is to ensure that proper vasodilation is maintained. If this careful homeostasis is disrupted, potentially severe health consequences can result. Recent literature has shown that increased amounts of MAs have been found in patients suffering from pathologies such as stroke [34, 35], various heart diseases [36-45], and renal failure [46, 47]. The biochemical mechanisms behind the progression of these diseases are not yet well understood, but all have been linked to disrupted endothelium function [48]. Given that MAs reduce the bioavailability of NO, it has been suggested that an abundance of MAs may be responsible for disease onset and progression.

Miyazaki *et al.* first showed that the plasma concentration of ADMA can be correlated to intima-media thickness (IMT), where IMT values indicate the extent of a blockage in blood vessels. It was reported that patients with higher ADMA concentrations had larger IMTs. This was the first evidence that ADMA could be used as a clinical marker for predicting atherosclerosis in humans [49]. Similar results were obtained in a larger study that showed that

elevated concentrations of both ADMA and MMA were predictors of IMT after adjustments for cardiovascular risk factors and renal function were made [50]. Other studies have shown that patients who were in the quintile with the highest plasma concentrations of ADMA were significantly more likely to have a myocardial infarction or stroke than those in the bottom four quintiles [34]. It has also been shown that patients with significantly higher concentrations of ADMA and SDMA are more likely to die within a year from the beginning of the study than those who had lower levels. This study found that the threshold ADMA concentration that maximized sensitivity and specificity to predict all-cause mortality was 1.16 μM [43].

Despite the fact that all MAs affect the synthesis of NO, most research has focused strictly on ADMA. This is predominantly because ADMA is present at higher endogenous concentrations than MMA, and because SDMA does not competitively inhibit NOS. A recent study performed at the Cleveland Clinic, however, demonstrated that the most robust independent predictor of coronary artery disease was not the quantity of ADMA present but rather the arginine methylation index (ArgMI). The ArgMI is comprised of the sum of the dimethylated species concentrations divided by the concentration of the monomethylated form ($\text{ArgMI} = (\text{ADMA} + \text{SDMA}) / \text{MMA}$) [51]. This index accurately predicted the extent of disease progression even without adjusting for traditional risk factors giving rise to the need for analytical methods capable of detecting all the MA analogues.

The studies summarized above demonstrate the link between MA concentrations and the onset of CVDs. Although the exact mechanism is unclear, it is highly plausible that these elevated MA concentrations are responsible for reducing NO production leading to the development of CVDs. This brings about an interesting question as to whether MAs could therefore be utilized as diagnostic markers for CVD. Since conventional methods of diagnosing

heart disease are highly invasive and costly (*e.g.* angiography), an inexpensive alternative screening method to determine the extent of CVD would be quite valuable. This screen for MAs could be performed in conjunction with the measurement of more traditional markers, such as cholesterol and lipids, to provide a more comprehensive panel for disease diagnosis. If threshold concentrations of MAs could be established to diagnose patients with CVD before any symptoms are exhibited, this could be of tremendous benefit to society.

2.3.2 Respiratory Disorders

Respiratory disorders impact a large number of newborns in the United States each year, especially those born prematurely [52]. The development of diseases such as respiratory distress syndrome (RDS) and bronchopulmonary dysplasia (BPD) often results in increased morbidity or death [53]. Although it has been established that the lungs are amongst the last fetal organs to mature, the exact mechanism by which newborns develop these respiratory disorders is unknown. One hypothesis is that infants lack sufficient levels of NO [54]. Insufficient concentrations of NO cause vasoconstriction and poor blood oxygenation which can result in hypoxic respiratory failure and the onset of other respiratory diseases.

One of the most important functions of NO *in vivo* is its ability to regulate the endothelium and induce vasodilation [55, 56]. These beneficial effects provided by NO have caused it to be exploited in therapeutic applications. Inhaled nitric oxide (iNO) therapy has been used to treat pulmonary disorders because it increases blood flow to the lungs and improves oxygenation in patients experiencing hypoxia, including infants suffering from hypoxic respiratory failure [57-61]. Newborns suffering from this affliction exhibit increased airway resistances that result in oxygen deficiency. The FDA has approved iNO for the treatment of full-

term babies experiencing hypoxia although it has also been explored for preterm infants suffering from BPD [53, 62-64].

It has been found that iNO therapy is not efficacious for all newborns experiencing respiratory distress. The use of iNO has been shown to be effective for 62% of full term infants [65] and 49% of preterm infants [62]. Another study reported that 64% of infants with hypoxic respiratory failure in the untreated control group either died or required ECMO in comparison to only 46% of those who underwent iNO treatment [66]. It has also been reported that very low birth-weight infants successfully treated with iNO were significantly less likely to use bronchodilators, steroids, diuretics or oxygen one year after NICU discharge [67]. Despite the relatively high rates of non-improvement and high cost of treatment, babies with hypoxic respiratory failure are frequently treated with iNO in order to aid in the sustainment of normal breathing [53, 68].

The results of the clinical studies described above indicate that the lack of NO is a central cause of the respiratory problems in a large percentage of newborns. Supplemental NO in the form of iNO helped improve health; however, the success rate of iNO therapy was limited to only about half the patients who underwent treatment. The reason for this is not well understood but one hypothesis is that iNO is most successful in infants who do not produce adequate amounts of NO due to an immature pulmonary endothelium. Nitric oxide is produced by the NOS enzymes with eNOS being the primary form in the pulmonary system [10]. It is hypothesized that the lack of NO production in infants with hypoxic respiratory failure could be caused by several possible mechanisms including (1) eNOS not yet being fully expressed *in vivo*, (2) PRMT being up-regulated or DDAH down-regulated in these infants causing increased MAs

that inhibit eNOS, or (3) endogenous BH₄ concentrations being diminished leading to an uncoupling of eNOS and the formation of O₂[•] instead of NO.

Since the prominent physiological role of MAs is to regulate NO production, it is likely that these species are involved in the onset of NO-related respiratory pathologies. Given that iNO therapy only alleviates severe respiratory failure in approximately half of the patients who receive treatment, the development of an assay to screen for MAs could serve as a viable predictor of clinical improvement. Those infants who have elevated MA concentrations, and therefore low NO production, would benefit from the administration of supplemental NO. The development of an assay to screen for MAs could help physicians immediately administer an appropriate therapy on an individual case-by-case basis depending on the result of the screening. This would facilitate faster health improvements while obviating costly non-efficacious treatments.

2.4 Analytical Methods to Monitor NOS Activity

Before any conclusions can be drawn regarding the involvement of MAs in the onset of various endothelium-derived pathologies, it would be beneficial to monitor *in vivo* NOS activity. Unfortunately, the only direct way to directly monitor NOS activity is with an enzymatic staining kit which requires the excision of tissue from an organism. Given that the goal of this dissertation is the development of non-invasive methods to screen for disease progression, tissue biopsy is not an option, which precludes staining. In order to determine whether MAs are impacting the ability of NOS to actively produce NO, analytical methods for the indirect measurement of NOS activity are required.

2.4.1 Nitric Oxide Analysis

Given that the function of NOS is to produce NO, measuring NO should provide insight into its activity. NO is essential to numerous physiological processes, so quantitation of its endogenous concentrations can provide insight into its involvement in disease onset. However, the detection of NO is not trivial. It is a highly reactive molecule with a half-life of only a few seconds *in vivo*. Furthermore, it is gaseous so care must be taken to prevent the analyte from diffusing out of solution. Although direct detection of NO is possible, it is very difficult due to the reasons described above. Therefore, many common methods for NO measurement rely on indirect methods.

Various approaches have been used to detect NO in biological samples. Historically, the most common indirect method for determining NO production *in vivo* has been by monitoring its oxidation products, nitrite and nitrate [69]. Ambient oxygen readily oxidizes NO into these more stable products that can then be directly detected by either UV absorbance or electrochemical methods [70] or indirectly via the Griess reaction [71]. An alternative method for the indirect measurement of NO production is to monitor the change in arginine and citrulline concentrations as an indicator of NOS activity *in vivo* [72, 73]. By observing the fluctuations in the amounts of these species, a correlation can be made to NOS activity and the amount of NO produced.

Although difficult, NO can also be measured directly. One such method utilizes recently developed NO-selective fluorescent probes. These tags can highlight intra-cellular localization of NO. However, these labels are expensive, and studies have shown that their selectivity can be a concern due to the cross-reactivity with other RNOS [74, 75]. A different approach is with the use of electrochemical sensors. Electrodes can be coated with a selective

polymeric membrane that allows NO to diffuse to the electrode surface while restricting access to other molecules in a sample [76].

2.4.2 Methylarginine Analysis

This dissertation will focus primarily on monitoring MAs as an alternative method for the indirect determination of NOS function. Since these species regulate NO production, they can serve as indicators of endogenous NO concentrations and the extent of NOS inhibition. MAs are amino acids that are cationic at physiological pH. Numerous methods have been developed for the determination of MAs using a multitude of different techniques [77]. Since a diversity of methods exist that are capable of quantifying these compounds in biological samples, a brief overview will be given here.

2.4.2.1 Antibody-Based Analyses

A standard workhorse method for the quantitation of biomolecules relies on antibody-based methods. Enzyme-linked immunosorbent assays (ELISAs) have been very popular in clinical labs for decades due to the relative simplicity of the method and its high-throughput capability. Multiple varieties of ELISAs exist, but competitive ELISAs are used for MA analyses [78, 79]. This method entails adding sample and MA-specific antibodies to a well with MA derivatives (tracers) immobilized on the well surface. The MAs in the sample compete with the tracer MAs to bind to the anti-MA antibodies. Following a rinse step, only anti-MAs bound to the tracers remain. A secondary peroxidase-conjugated antibody specific to anti-MA is then added to the well. The addition of a peroxidase substrate then causes a colorimetric change that can be measured with absorbance detection. Since the absorbance signal is dependent upon the

number of antibodies bound to the immobilized tracer MAs (not the MAs in the sample), the analytical signal is inversely proportional to the amount of antigen originally present. Although this method involves several pipetting and incubation steps, the ability to perform analyses in parallel by the use of a multi-well plate makes this an efficient analysis technique.

ELISA kits for the three MAs of interest are commercially available from several vendors. Such assays would allow the concentrations of MAs to be determined; however, there are problems associated with analyses using this platform [80]. First, measuring MAs by ELISA is quite costly. Each kit costs ~\$1000 and is only designed to quantify one MA. Therefore, three kits (one for each MA of interest) would be required to gather the desired information from each clinical sample. Additionally, there exists some degree of cross-reactivity between the intended MA and the other MA analogues. Although this should be minimal (all manufacturers claim < 2% cross-reactivity), it still may bias the results. Another potential problem is that the reported limits of detection (LODs) are 50 nM for each manufacturer's ELISA kits [79]. While this should not be problematic for ADMA and SDMA since their expected endogenous concentrations are above that, MMA has been reported at levels comparable to the LOD. If the endogenous concentrations are too similar to the LOD for the method, this would preclude meaningful quantitative data from being gathered. Interestingly, the only manufacturers that produce kits for MMA do not list their LODs or any other product information. To overcome the limitations of the ELISA-based methods in the determination of MA concentrations, alternative methods should be explored.

2.4.2.2 Separations-Based Analyses

Samples derived from biological matrices are highly complex. Numerous components are present whose concentrations can span multiple orders of magnitude. This environment makes the detection of select compounds within a sample extremely difficult. Unless selectivity can be gained for the analytes of interest using an antibody or a highly specific dye, discrete components cannot be quantified in a static assay. To overcome this problem, however, a separation step can be employed to separate individual analytes in a sample mixture in space and time. Resolving each component from others in this manner allows each individual analyte to be quantified free from interference of other compounds.

2.4.2.2.1 Liquid Chromatography

High-performance liquid chromatography (HPLC) is the most common technique for performing analytical separations in a variety of industries. HPLC experiments are performed by introducing a sample mixture into a column densely packed with a stationary phase (SP). As high pressure pumps force the sample through the column, individual analyte molecules either remain in the mobile phase (MP) or interact with the SP particles. The pseudo-equilibrium that analytes establish between the MP and SP determine how long each analyte dwells on-column. Analytes that have limited interaction with the SP elute relatively quickly, whereas analytes that have a high affinity for the SP have much longer retention times. The extent of interaction with the SP governs the separation and dictates when an analyte plug will elute.

The analysis of MAs by LC is challenging but methods have been previously reported [81]. A problem with achieving a good separation of the MAs is that they are small, amphoteric species, and therefore, do not retain well on many SPs. The majority of small molecule LC

separations in the literature are reversed-phase and employ a C18 column; however, MAs are very polar and consequently do not interact with the SP. This results in poor or no retention and very limited resolution between the analytes. To overcome this problem, methods have been reported using reversed-phase separations after first derivatizing the MAs with either an alkyl moiety [82] or a non-polar fluorescent tag [83-85]. This increased retention on-column because of the ability of the hydrophobic derivatization group to interact with the C18 SP. An alternative means of obtaining chromatographic resolution can be obtained by utilizing more polar SPs such as HILIC (hydrophilic interaction) silica columns [86-89]. However, despite the improved retention with these packing materials, some coelution was still observed.

2.4.2.2.2 Capillary Electrophoresis

Capillary electrophoresis (CE) is a separation technique that separates analytes based on their charges and hydrodynamic radii [90]. To conduct a capillary zone electrophoresis (CZE) experiment, a background electrolyte is introduced into a capillary followed by a small volume of sample (~1% of the total volume). A high voltage is then applied across the capillary. The application of an electric field causes the species in the sample plug to migrate based on both their innate electrophoretic mobilities and an electroosmotic flow (EOF) force. Electrophoretic mobilities are dependent on the charge and size of the molecules where species with the highest charge density migrate the fastest. In this setup, cations migrate towards the cathode, anions migrate towards the anode, and neutral molecules are unaffected.

While the electrophoretic mobilities of analytes are important considerations in CE separations, this description is incomplete because it does not factor in the charge of the substrate surface. Since most electrophoretic separations are performed in glass, the charge on the surface

is typically highly anionic. This creates layers of counter-ions next to the surface to maintain electroneutrality, which gives rise to the EOF. The EOF is often the dominant factor affecting analyte migration. In normal polarity CE, a mobile layer of cations is positioned next to the channel surface. Upon application of an electric field, these ions are attracted to the cathode which draws the bulk solution towards the cathode as well. The rate of this fluid flow is often greater than the electrophoretic mobilities of the analytes in the sample so that all species, regardless of charge, migrate towards the cathode. This is often beneficial because it allows all analytes in a sample to be monitored with a single detector. Because the EOF is governed by the surface charge of the channel substrate, its rate is highly pH dependent. Under more acidic conditions, the channel walls become protonated and therefore diminish the rate of bulk fluid transport. The combination of electrophoretic mobility and EOF dictate the net migration of a given analyte. An illustration of this is depicted in Figure 2.5.

Due to the limitations of CZE to resolve the components of more complex sample mixtures, micellar electrokinetic chromatography (MEKC) is frequently employed to enhance the separation. A MEKC experiment is set-up in an analogous manner to CZE. A capillary is filled with a background electrolyte solution, but for this experiment, surfactant is also added to the run buffer. At low surfactant concentrations, surfactant molecules line the surface of the capillary in an attempt to withdraw their hydrophobic tail groups from contact with the aqueous solution. At sufficiently high surfactant concentrations (above the critical micelle concentration), however, it is thermodynamically favorable for the surfactant to aggregate into micelles. The arrangement of surfactant molecules into micelles allows the polar headgroups to be in contact with the aqueous solution while allowing the hydrophobic tails to be in the interior. A picture of a micelle can be seen in Figure 2.6.

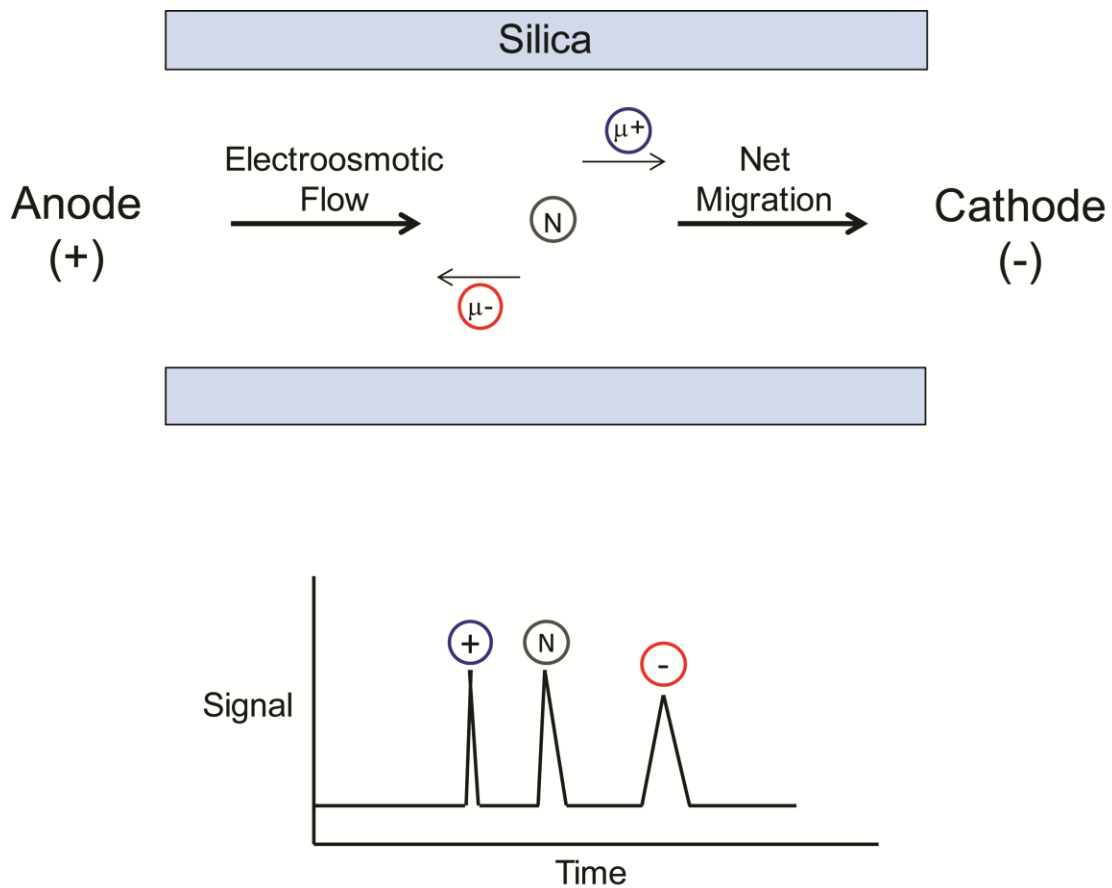


Figure 2.5 Schematic of the forces involved in electrophoretic separations and a theoretical electropherogram.

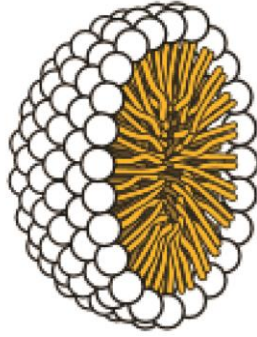


Figure 2.6 The configuration of a micelle. Image adapted from

<http://en.wikipedia.org/wiki/Micelle>.

Micelles serve as a pseudo-stationary phase in electrophoretic separations which can aid the separation. The migration of analytes in MEKC is determined by not only the electrophoretic mobilities of the analytes and the EOF as in CZE, but is now also impacted by the affinity of each analyte for the micelle. Molecules are able to partition into and out of the micelles which influences their net migrations. In normal polarity CE separations, anionic surfactants are employed for MEKC to elongate analyte migration times. In such a system, the migration time of a neutral analyte will fall between that of the EOF and that of the micelle depending on the analyte's affinity for the micelle. Molecules that have a strong electrostatic interaction with the surfactant headgroup or hydrophobic interactions with the core will have longer migration times.

Separating MAs with electrophoresis is very challenging due to the similar size and charge of the MA analogues. However, methods have been previously reported utilizing MEKC in the separation of MAs (see 3.1). These papers were able to obtain a reasonable separation between the MAs although comigration was observed in some instances. A drawback to these methods is that they utilized very high ionic strength buffers that can cause substantial Joule heating and hinder the analysis. These methods also required lengthy or complex derivatization steps to fluorescently label the analytes, which diminished throughput. Furthermore, the LODs of these methods were fairly high which could prevent endogenous MA concentrations from being detected. Given these drawbacks, there is still much room for improvement in the optimization of CE separations of MAs.

An additional benefit of CE in the measurement of MAs is its ability to be readily miniaturized. Electrophoretic separations can be conducted in microfluidic devices only a fraction of the size of a conventional CE instrument. This enables a more rapid separation and utilizes smaller volumes of sample and other reagents. Of particular benefit is that despite being

a smaller platform with a reduced separation distance, the separation efficiency in such devices is not normally diminished. Higher field strengths can be employed with the shorter channels preserving good separations. The major benefit of the microchip electrophoresis platform is that it could be incorporated as part of a point-of-care (POC) analysis system for the determination of MAs. LC cannot be easily miniaturized making it impractical in POC analyses, so future discussions herein will only pertain to CE-based methods.

2.4.2.3 Derivatization Chemistry

Unlabeled MAs can be measured by mass spectrometric (MS) detection or UV detection regardless of the choice of separation technique. However, CE-MS instruments are not extensively utilized because of their high cost. Furthermore, CE-MS suffers from limited separation capacity due to the incompatibility of MS with common surfactants required to achieve reasonable separations. Also, UV detection lacks the sensitivity of other detection methods. Given this, many CE analyses designed for amino acid measurements rely on derivatization of the analytes of interest with a fluorescent tag to enable laser-induced fluorescence (LIF) detection.

A large variety of fluorescent derivatization reagents are commercially available. These tags vary based on their spectral properties, size, and reactivity. These labels have been designed to attach to a number of different reactive sites on a molecule. Currently, dyes are available that react with a number of different functional groups including amines, thiols, carboxylic acids, and aldehydes. The ability of different dyes to label different functional groups on a molecule can impart some specificity into the analysis since not all analytes in a sample mixture contain the

same reactive sites. Choosing a derivatization reagent that only tags the class of compounds of interest will yield less complex separations and improve peak identification and quantitation.

The choice of labeling reagent is also affected by the method to be used for analysis. Although most analyses employ pre-column derivatization to provide optimal conditions for analyte labeling, forethought must be given to the analytical technique. Large hydrophobic dyes may not be soluble in aqueous run buffers and precipitate out of solution. Not only will this decrease the sensitivity of the analysis, it may completely halt it if large aggregates form and clog the capillary. Additionally, the kinetics of the reaction must be considered when selecting a derivatization reagent. Some labels react quickly under ambient conditions but others either require lengthy reaction times or an incubation step [91]. These requirements can drastically increase the sample preparation time which will diminish throughput.

The selection of a derivatization reagent is also frequently dictated by other practical concerns. For example, when utilizing LIF detection, the excitation wavelength of a dye must correspond to an available laser line. Given the relatively high cost of lasers, it is most practical to select a dye based on the laser equipment available. If fluorescence detection is to be achieved with a broadband source, cost must still be considered because of the necessity of the optic cubes required to allow the proper excitation and emission wavelengths through. Based on the excitation source available, a wide variety of derivatization reagents can be selected with excitation maxima throughout the near-UV and visible spectra. Other properties to note when reviewing the optical properties of the labels are their fluorescent efficiencies. The higher the quantum yield of a dye, the more fluorescent emission is produced. This is a beneficial trait in an analytical method because it increases the sensitivity of the analysis.

Another concern regarding the choice of fluorescent dye is the impact it will have on the analysis. The size and charge of the tag can have a large impact on the maximum attainable peak resolution in electrophoretic separations. Larger fluorescent tags will make the relative sizes of the derivatized complexes more similar which may hinder the separation. This effect will be especially pronounced in the analysis of small molecules; larger peptides and proteins will be less affected. For the analysis of small molecules, such as MAs, it is most beneficial to use the smallest labels possible to attain the best separation. Smaller fluorescent tags tend to be blue-shifted as compared to their larger counterparts due to the restricted range for electron delocalization. Therefore, lower wavelength excitation sources are required to utilize these labels. Another consideration is the charge on the molecule. Many derivatization reagents contain an anionic functional group. This ionizable moiety will alter the electrophoretic mobility of a labeled analyte and therefore impact the electrophoretic separation. This does not necessarily imply that the separation resolution will be worse, but it will be different. Additionally, once a label bonds to a functional group on a molecule, that functional group will be altered. For example, if a dye labels a carboxylic acid, following derivatization, it typically forms an ester group that is non-ionizable, thereby changing the charge of the molecule.

A wide variety of dyes with different properties are available but most have the significant disadvantage of being fluorescent themselves. This can be problematic because excess dye must be introduced into the sample mixture to ensure that all of analytes become labeled. Unfortunately, this often leaves a large amount of unreacted dye in the sample, which complicates the analysis by producing reagent peaks much larger than those for the analytes of interest [91]. For this reason, it is beneficial to use fluorogenic derivatization reagents that are not fluorescent until they label an analyte molecule.

Naphthalene-2,3-dicarboxaldehyde (NDA) is the derivatization reagent that was used throughout this dissertation because of the many benefits it imparts onto an analysis. NDA is a fluorogenic dye that derivatizes primary amines in the presence of cyanide to form stable 1-cyanobenz[f]isoindole (CBI) products under ambient conditions [92]. Because of its fast reaction kinetics (NDA labels compounds within minutes), the use of NDA is advantageous in methods employing precolumn derivatization [93]. The reaction of NDA with arginine is shown in Figure 2.7. NDA is a relatively small tag which minimizes its contribution to the size of the derivatized complex. This allows NDA-labeled analytes to be separated more easily by CE compared to those labeled with larger dyes. There are two excitation maxima for NDA-derivatized species at 420 nm and 445 nm, while the emission maximum is at 490 nm. LIF detection is typically employed when derivatizing analytes with NDA because it provides the best detection limits for the determination of CBI derivatives [94, 95].

2.5 Conclusions

This chapter has outlined the function of NOS and its significance to maintaining human health. It also addressed the role MAs play in NOS physiology. MAs can have both beneficial and detrimental impacts on the endothelium because of their abilities to modulate NO production. It is hypothesized that these species could serve as valuable markers to screen patients for the progression of diseases of the endothelium stemming from a reduced NO bioavailability. Background information was then given on various analytical methods that could be used to measure markers of NOS function, specifically NO and the MAs. It was concluded that CE-based separations would be the most beneficial for MA analyses long-term since they are capable of being miniaturized into a point-of-care screening system.

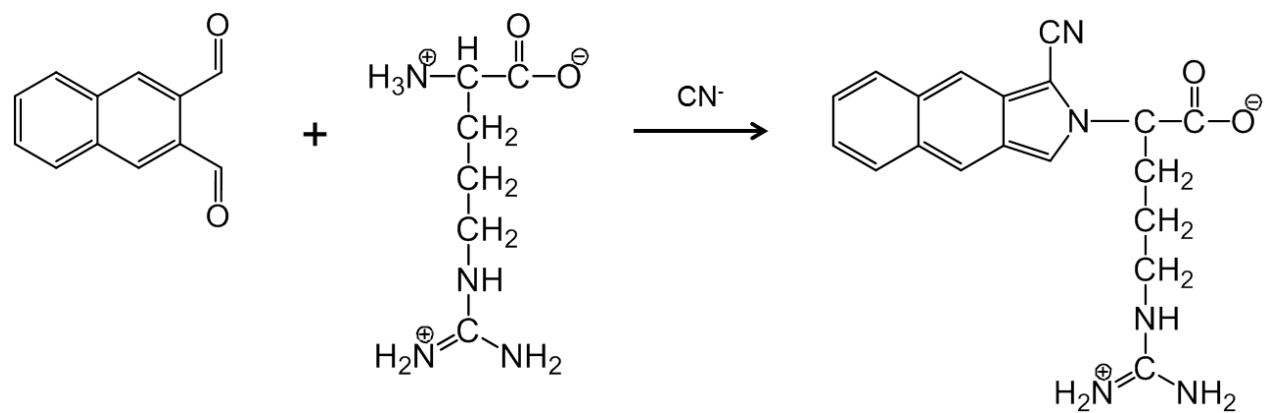


Figure 2.7 Derivatization scheme of arginine with NDA/ CN^- .

2.6 References

- [1] E. Culotta, D.E. Koshland, Jr., NO news is good news, *Science*, 258 (1992) 1862-1865.
- [2] J. Garthwaite, Concepts of neural nitric oxide-mediated transmission, *Eur. J. Neurosci.*, 27 (2008) 2783-2802.
- [3] J.A. Angus, Role of the endothelium in the genesis of cardiovascular disease, *Clin. Exp. Pharmacol. Physiol.*, 23 (1996) S16-S22.
- [4] A. Wennmalm, Endothelial nitric oxide and cardiovascular disease, *J. Intern. Med.*, 235 (1994) 317-327.
- [5] F. Murad, C.K. Mittal, W.P. Arnold, S. Katsuki, H. Kimura, Guanylate cyclase: activation by azide, nitro compounds, nitric oxide, and hydroxyl radical and inhibition by hemoglobin and myoglobin, *Advances in Cyclic Nucleotide Research*, 9 (1978) 145-158.
- [6] G.J. Dusting, Nitric oxide in cardiovascular disorders, *J. Vasc. Res.*, 32 (1995) 143-161.
- [7] F.L.M. Ricciardolo, S.A. Di, F. Sabatini, G. Folkerts, Reactive nitrogen species in the respiratory tract, *Eur. J. Pharmacol.*, 533 (2006) 240-252.
- [8] U. Foerstermann, W.C. Sessa, Nitric oxide synthases: regulation and function, *Eur. Heart J.*, 33 (2012) 829-837.
- [9] A.K. Nath, J.A. Madri, The roles of nitric oxide in murine cardiovascular development, *Dev. Biol.*, 292 (2006) 25-33.
- [10] K.A. Fagan, R.C. Tyler, K. Sato, B.W. Fouty, K.G. Morris, Jr., P.L. Huang, I.F. McMurtry, D.M. Rodman, Relative contributions of endothelial, inducible, and neuronal NOS to tone in the murine pulmonary circulation, *Am. J. Physiol.*, 277 (1999) L472-L478.

- [11] U. Foerstermann, H. Li, Therapeutic effect of enhancing endothelial nitric oxide synthase (eNOS) expression and preventing eNOS uncoupling, *Br. J. Pharmacol.*, 164 (2011) 213-223.
- [12] J. Vasquez-Vivar, P. Martasek, J. Whitsett, J. Joseph, B. Kalyanaraman, The ratio between tetrahydrobiopterin and oxidized tetrahydrobiopterin analogues controls superoxide release from endothelial nitric oxide synthase: An EPR spin trapping study, *Biochem. J.*, 362 (2002) 733-739.
- [13] Y. Xia, A.-L. Tsai, V. Berka, J.L. Zweier, Superoxide generation from endothelial nitric-oxide synthase. A Ca²⁺/calmodulin-dependent and tetrahydrobiopterin regulatory process, *J. Biol. Chem.*, 273 (1998) 25804-25808.
- [14] U. Landmesser, S. Dikalov, S.R. Price, L. McCann, T. Fukai, S.M. Holland, W.E. Mitch, D.G. Harrison, Oxidation of tetrahydrobiopterin leads to uncoupling of endothelial cell nitric oxide synthase in hypertension, *J. Clin. Invest.*, 111 (2003) 1201-1209.
- [15] J. Vásquez-Vivar, Tetrahydrobiopterin, superoxide, and vascular dysfunction, *Free Radical Bio. Med.*, 47 (2009) 1108-1119.
- [16] U. Landmesser, S. Dikalov, S.R. Price, L. McCann, T. Fukai, S.M. Holland, W.E. Mitch, D.G. Harrison, Oxidation of tetrahydrobiopterin leads to uncoupling of endothelial cell nitric oxide synthase in hypertension, *J. Clin. Invest.*, 111 (2003) 1201-1209.
- [17] M.J. Crabtree, C.L. Smith, G. Lam, M.S. Goligorsky, S.S. Gross, Ratio of 5,6,7,8-tetrahydrobiopterin to 7,8-dihydrobiopterin in endothelial cells determines glucose-elicited changes in NO vs. superoxide production by eNOS, *Am. J. Physiol. Heart Circ. Physiol.*, 294 (2008) H1530-1540.

- [18] M.J. Crabtree, A.L. Tatham, Y. Al-Wakeel, N. Warrick, A.B. Hale, S. Cai, K.M. Channon, N.J. Alp, Quantitative Regulation of Intracellular Endothelial Nitric-oxide Synthase (eNOS) Coupling by Both Tetrahydrobiopterin-eNOS Stoichiometry and Biopterin Redox Status: INSIGHTS FROM CELLS WITH TET-REGULATED GTP CYCLOHYDROLASE I EXPRESSION, *J. Biol. Chem.*, 284 (2009) 1136-1144.
- [19] G. Ferrer-Sueta, R. Radi, Chemical Biology of Peroxynitrite: Kinetics, Diffusion, and Radicals, *ACS Chem. Biol.*, 4 (2009) 161-177.
- [20] W.A. Pryor, K.N. Houk, C.S. Foote, J.M. Fukuto, L.J. Ignarro, G.L. Squadrito, K.J.A. Davies, Free radical biology and medicine: it's a gas, man!, *Am. J. Physiol. Regul. Integr. Comp. Physiol.*, 291 (2006) R491-511.
- [21] J.P. Cooke, Asymmetrical dimethylarginine: The uber marker?, *Circulation*, 109 (2004) 1813-1819.
- [22] P. Vallance, Importance of asymmetrical dimethylarginine in cardiovascular risk, *Lancet*, 358 (2001) 2096-2097.
- [23] D. Zakrzewicz, O. Eickelberg, From arginine methylation to ADMA: a novel mechanism with therapeutic potential in chronic lung diseases, *BMC Pulm. Med.*, 9 (2009) 5.
- [24] P. Bulau, D. Zakrzewicz, K. Kitowska, J. Leiper, A. Gunther, F. Grimminger, O. Eickelberg, Analysis of methylarginine metabolism in the cardiovascular system identifies the lung as a major source of ADMA, *Am. J. Physiol. Lung Cell Mol. Physiol.*, 292 (2007) L18-24.
- [25] M. Davids, A.J. van Hell, M. Visser, R.J. Nijveldt, P.A.M. van Leeuwen, T. Teerlink, Role of the human erythrocyte in generation and storage of asymmetric dimethylarginine, *Am. J. Physiol. Heart Circ. Physiol.*, 302 (2012) H1762-1770.

- [26] C.T.L. Tran, J.M. Leiper, P. Vallance, The DDAH/ADMA/NOS pathway, *Atheroscler. Suppl.*, 4 (2003) 33-40.
- [27] P. Vallance, J. Leiper, Cardiovascular Biology of the Asymmetric Dimethylarginine: Dimethylarginine Dimethylaminohydrolase Pathway, *Arterioscler. Thromb. Vasc. Biol.*, 24 (2004) 1023-1030.
- [28] A.J. Cardounel, H. Cui, A. Samouilov, W. Johnson, P. Kearns, A.-L. Tsai, V. Berka, J.L. Zweier, Evidence for the Pathophysiological Role of Endogenous Methylarginines in Regulation of Endothelial NO Production and Vascular Function, *J. Biol. Chem.*, 282 (2007) 879-887.
- [29] A.J. Cardounel, J.L. Zweier, Endogenous Methylarginines Regulate Neuronal Nitric-oxide Synthase and Prevent Excitotoxic Injury, *J. Biol. Chem.*, 277 (2002) 33995-34002.
- [30] D.W. Reif, S.A. McCreedy, N-Nitro-L-arginine and N-monomethyl-L-arginine exhibit a different pattern of inactivation toward the three nitric oxide synthases, *Arch. Biochem. Biophys.*, 320 (1995) 170-176.
- [31] C. Wadham, A.A. Mangoni, Dimethylarginine dimethylaminohydrolase regulation: a novel therapeutic target in cardiovascular disease, *Expert Opin. Drug Metab. Toxicol.*, 5 (2009) 303-319.
- [32] Cardiovascular disease statistics,
<http://www.americanheart.org/presenter.jhtml?identifier=4478>, American Heart Association, 2006.
- [33] G. Noll, T.F. Luscher, The endothelium in acute coronary syndromes, *Eur. Heart J.*, 19 (1998) C30-C38.

- [34] T. Leong, D. Zylberstein, I. Graham, L. Lissner, D. Ward, J. Fogarty, C. Bengtsson, C. Bjorkelund, D. Thelle, Asymmetric Dimethylarginine Independently Predicts Fatal and Nonfatal Myocardial Infarction and Stroke in Women, *Arterioscler. Thromb. Vasc. Biol.*, 28 (2008) 961-967.
- [35] J.H. Yoo, S.C. Lee, Elevated levels of plasma homocyst(e)ine and asymmetric dimethylarginine in elderly patients with stroke, *Atherosclerosis*, 158 (2001) 425-430.
- [36] Z. Wang, W.H.W. Tang, L. Cho, D.M. Brennan, S.L. Hazen, Targeted Metabolomic Evaluation of Arginine Methylation and Cardiovascular Risks: potential mechanisms beyond nitric oxide synthase inhibition, *Arterioscler. Thromb. Vasc. Biol.*, 29 (2009) 1383-1391.
- [37] C.D. Goonasekera, D.D. Rees, P. Woolard, A. Freund, V. Shah, M.J. Dillon, Nitric oxide synthase inhibitors and hypertension in children and adolescents, *J. Hypertens.*, 15 (1997) 901-909.
- [38] C. Dueckelmann, F. Mittermayer, D.G. Haider, J. Altenberger, J. Eichinger, M. Wolzt, Asymmetric dimethylarginine enhances cardiovascular risk prediction in patients with chronic heart failure, *Arterioscler. Thromb. Vasc. Biol.*, 27 (2007) 2037-2042.
- [39] C. Dueckelmann, F. Mittermayer, D.G. Haider, J. Altenberger, M. Wolzt, Plasma asymmetric dimethylarginine and cardiovascular events in patients with acute decompensated heart failure, *Transl. Res.*, 152 (2008) 24-30.
- [40] R. Schnabel, S. Blankenberg, E. Lubos, K.J. Lackner, H.J. Rupprecht, C. Espinola-Klein, N. Jachmann, F. Post, D. Peetz, C. Bickel, F. Cambien, L. Tiret, T. Muenzel, Asymmetric Dimethylarginine and the Risk of Cardiovascular Events and Death in Patients With

- Coronary Artery Disease. Results from the AtheroGene Study, *Circ. Res.*, 97 (2005) e53-e59.
- [41] H. Miyazaki, H. Matsuoka, J.P. Cooke, M. Usui, S. Ueda, S. Okuda, T. Imaizumi, Endogenous nitric oxide synthase inhibitor: a novel marker of atherosclerosis, *Circulation*, 99 (1999) 1141-1146.
- [42] L. Lee, R.C. Webb, Endothelium-dependent relaxation and L-arginine metabolism in genetic hypertension, *Hypertension*, 19 (1992) 435-441.
- [43] M. Zeller, C. Korandji, J.-C. Guillard, P. Sicard, C. Vergely, L. Lorgis, J.-C. Beer, L. Duvillard, A.-C. Lagrost, D. Moreau, P. Gambert, Y. Cottin, L. Rochette, Impact of Asymmetric Dimethylarginine on Mortality After Acute Myocardial Infarction, *Arterioscler. Thromb. Vasc. Biol.* 28 (2008) 954-960.
- [44] T.K. Krempl, R. Maas, K. Sydow, T. Meinertz, R.H. Boeger, J. Kaehler, Elevation of asymmetric dimethylarginine in patients with unstable angina and recurrent cardiovascular events, *Eur. Heart J.*, 26 (2005) 1846-1851.
- [45] Z. Ajtay, F. Scalera, A. Cziraki, I. Horvath, L. Papp, E. Sulyok, C. Szabo, J. Martens-Lobenhoffer, F. Awiszus, S.M. Bode-Boeger, Stent placement in patients with coronary heart disease decreases plasma levels of the endogenous nitric oxide synthase inhibitor ADMA, *Int. J. Mol. Med.*, 23 (2009) 651-657.
- [46] C. Zoccali, S.M. Bode-Boger, F. Mallamaci, F.A. Benedetto, G. Tripepi, L.S. Malatino, A. Cataliotti, I. Bellanuova, I. Fermo, J.C. Frolich, R.H. Boger, Plasma concentration of asymmetrical dimethylarginine and mortality in patients with end-stage renal disease: a prospective study, *Lancet*, 358 (2001) 2113-2117.

- [47] C. Fleck, A. Janz, F. Schweitzer, E. Karge, M. Schwertfeger, G. Stein, Serum concentrations of asymmetric (ADMA) and symmetric (SDMA) dimethylarginine in renal failure patients, *Kidney Int.*, 59 (2001) S14-S18.
- [48] F. Arrigoni, B. Ahmetaj, J. Leiper, The biology and therapeutic potential of the DDAH/ADMA pathway, *Curr. Pharm. Des.*, 16 (2010) 4089-4102.
- [49] H. Miyazaki, H. Matsuoka, J.P. Cooke, M. Usui, S. Ueda, S. Okuda, T. Imaizumi, Endogenous nitric oxide synthase inhibitor: A novel marker of atherosclerosis, *Circulation*, 99 (1999) 1141-1146.
- [50] J.A. Chirinos, R. David, J.A. Bralley, H. Zea-Diaz, E. Munoz-Atahualpa, F. Corrales-Medina, C. Cuba-Bustinza, J. Chirinos-Pacheco, J. Medina-Lezama, Endogenous nitric oxide synthase inhibitors, arterial hemodynamics, and subclinical vascular disease: The PREVENCIÓN study, *Hypertension*, 52 (2008) 1051-1059.
- [51] Z. Wang, W.H.W. Tang, L. Cho, D.M. Brennan, S.L. Hazen, Targeted metabolomic evaluation of arginine methylation and cardiovascular risks: Potential mechanisms beyond nitric oxide synthase inhibition, *Arterioscler. Thromb. Vasc. Biol.*, 29 (2009) 1383-1391.
- [52] Respiratory Distress Syndrome, <http://newsmomsneed.marchofdimes.com/?tag=respiratory-distress-syndrome>, March of Dimes, 2010.
- [53] W.E. Truog, Inhaled nitric oxide for the prevention of bronchopulmonary dysplasia, *Expert Opin. Pharmacother.*, 8 (2007) 1505-1513.
- [54] D. Lutman, A. Petros, Inhaled nitric oxide in neonatal and paediatric transport, *Early Hum. Dev.*, 84 (2008) 725-729.

- [55] B.R. Weil, B.L. Stauffer, J.J. Greiner, C.A. DeSouza, Prehypertension is associated with impaired nitric oxide-mediated endothelium-dependent vasodilation in sedentary adults, *Am. J. Hypertens.*, 24 (2011) 976-981.
- [56] R.A. Dweik, The lung in the balance: arginine, methylated arginines, and nitric oxide, *Am. J. Physiol. Lung Cell Mol. Physiol.*, 292 (2007) L15-17.
- [57] R.H. Steinhorn, Neonatal pulmonary hypertension, *Pediatr. Crit. Care Med.*, 11 (2010) S79-84.
- [58] A. Bin-Nun, M.D. Schreiber, Role of iNO in the modulation of pulmonary vascular resistance, *J. Perinatol.*, 28 (2008) S84-92.
- [59] B.C. Creagh-Brown, M.J. Griffiths, T.W. Evans, Bench-to-bedside review: Inhaled nitric oxide therapy in adults, *Crit. Care*, 13 (2009) 221.
- [60] R.F. Soll, Inhaled nitric oxide in the neonate, *J. Perinatol.*, 29 (2009) S63-67.
- [61] R.H. Steinhorn, Nitric oxide and beyond: New insights and therapies for pulmonary hypertension, *J. Perinatol.*, 28 (2008) S67-71.
- [62] R.A. Ballard, W.E. Truog, et al., Inhaled nitric oxide in preterm infants undergoing mechanical ventilation, *New Engl. J. Med.*, 355 (2006) 343-353.
- [63] M.A. Posencheg, A.J. Gow, W.E. Truog, R.A. Ballard, A. Cnaan, S.G. Golombek, P.L. Ballard, Inhaled nitric oxide in premature infants: effect on tracheal aspirate and plasma nitric oxide metabolites, *J. Perinatol.*, 30 (2010) 275-280.
- [64] S.S. Miller, W.D. Rhine, Inhaled nitric oxide in the treatment of preterm infants, *Early Hum. Dev.*, 84 (2008) 703-707.
- [65] W.E. Truog, G. Kurth, B. Haney, H.W. Kilbride, Hypoxic respiratory failure: etiology and outcomes at one referral center 2000 through 2005, *J. Perinatol.*, 27 (2007) 371-374.

- [66] N.I.N.O.S. group, Inhaled nitric oxide in full-term and nearly full-term infants with hypoxic respiratory failure, *New Engl. J. Med.*, 336 (1997) 597-604.
- [67] A.M. Hibbs, M.C. Walsh, R.J. Martin, W.E. Truog, S.A. Lorch, E. Alessandrini, A. Cnaan, L. Palermo, S.R. Wadlinger, C.E. Coburn, P.L. Ballard, R.A. Ballard, One-year respiratory outcomes of preterm infants enrolled in the Nitric Oxide (to prevent) Chronic Lung Disease trial, *J. Pediatr.*, 153 (2008) 525-529.
- [68] Committee on Fetus and Newborn, Use of inhaled nitric oxide, *Pediatrics*, 106 (2000) 344-345.
- [69] R.A. Hunter, W.L. Storm, P.N. Coneski, M.H. Schoenfisch, Inaccuracies of Nitric Oxide Measurement Methods in Biological Media, *Anal. Chem.*, 85 (2013) 1957-1963.
- [70] W.S. Jobgen, S.C. Jobgen, H. Li, C.J. Meininger, G. Wu, Analysis of nitrite and nitrate in biological samples using high-performance liquid chromatography, *J. Chromatogr., B: Anal. Technol. Biomed. Life Sci.*, 851 (2007) 71-82.
- [71] D.L. Granger, R.R. Taintor, K.S. Boockvar, J.B. Hibbs, Jr., Measurement of nitrate and nitrite in biological samples using nitrate reductase and Griess reaction, *Methods Enzymol.*, 268 (1996) 142-151.
- [72] I. Perez-Neri, E. Castro, S. Montes, M.-C. Boll, J. Barges-Coll, J.L. Soto-Hernandez, C. Rios, Arginine, citrulline and nitrate concentrations in the cerebrospinal fluid from patients with acute hydrocephalus, *J. Chromatogr., B: Anal. Technol. Biomed. Life Sci.*, 851 (2007) 250-256.
- [73] X. Ye, W.-S. Kim, S.S. Rubakhin, J.V. Sweedler, Ubiquitous presence of argininosuccinate at millimolar levels in the central nervous system of *Aplysia californica*, *J. Neurochem.*, 101 (2007) 632-640.

- [74] E.R. Mainz, D.B. Gunasekara, G. Caruso, D.T. Jensen, M.K. Hulvey, J.A.F. da Silva, E.C. Metto, A.H. Culbertson, C.T. Culbertson, S.M. Lunte, Monitoring intracellular nitric oxide production using microchip electrophoresis and laser-induced fluorescence detection, *Anal. Methods*, 4 (2012) 414-420.
- [75] W.-S. Kim, X. Ye, S.S. Rubakhin, J.V. Sweedler, Measuring Nitric Oxide in Single Neurons by Capillary Electrophoresis with Laser-Induced Fluorescence: Use of Ascorbate Oxidase in Diaminofluorescein Measurements, *Anal. Chem.*, 78 (2006) 1859-1865.
- [76] B.J. Privett, J.H. Shin, M.H. Schoenfisch, Electrochemical nitric oxide sensors for physiological measurements, *Chem. Soc. Rev.*, 39 (2010) 1925-1935.
- [77] E. Schwedhelm, Quantification of ADMA: analytical approaches, *Vasc. Med.*, 10 Suppl 1 (2005) S89-95.
- [78] F. Schulze, R. Wesemann, E. Schwedhelm, K. Sydow, J. Albsmeier, J.P. Cooke, R.H. Boeger, Determination of asymmetric dimethylarginine (ADMA) using a novel ELISA assay, *Clin. Chem. Lab. Med.*, 42 (2004) 1377-1383.
- [79] ADMA (human) ELISA Kit product insert, Enzo Life Sciences, 2009.
- [80] P. Valtonen, J. Karppi, K. Nyyssoenen, V.-P. Valkonen, T. Halonen, K. Punnonen, Comparison of HPLC method and commercial ELISA assay for asymmetric dimethylarginine (ADMA) determination in human serum, *J. Chromatogr., B: Anal. Technol. Biomed. Life Sci.*, 828 (2005) 97-102.
- [81] J. Martens-Lobenhoffer, S.M. Bode-Boeger, Chromatographic-mass spectrometric methods for the quantification of L-arginine and its methylated metabolites in biological fluids, *J. Chromatogr., B: Anal. Technol. Biomed. Life Sci.*, 851 (2007) 30-41.

- [82] M. Davids, E. Swieringa, F. Palm, D.E.C. Smith, Y.M. Smulders, P.G. Scheffer, H.J. Blom, T. Teerlink, Simultaneous determination of asymmetric and symmetric dimethylarginine, L-monomethylarginine, L-arginine, and L-homoarginine in biological samples using stable isotope dilution liquid chromatography tandem mass spectrometry, *J. Chromatogr., B: Anal. Technol. Biomed. Life Sci.*, 900 (2012) 38-47.
- [83] Y. Hui, M. Wong, J.-o. Kim, J. Love, D.M. Ansley, D.D.Y. Chen, A new derivatization method coupled with LC-MS/MS to enable baseline separation and quantification of dimethylarginines in human plasma from patients to receive on-pump CABG surgery, *Electrophoresis*, 33 (2012) 1911-1920.
- [84] M. Marra, A.R. Bonfigli, R. Testa, I. Testa, A. Gambini, G. Coppa, High-performance liquid chromatographic assay of asymmetric dimethylarginine, symmetric dimethylarginine, and arginine in human plasma by derivatization with naphthalene-2,3-dicarboxaldehyde, *Anal. Biochem.*, 318 (2003) 13-17.
- [85] T. Teerlink, R.J. Nijveldt, S. de Jong, P.A.M. van Leeuwen, Determination of arginine, asymmetric dimethylarginine, and symmetric dimethylarginine in human plasma and other biological samples by high-performance liquid chromatography, *Anal. Biochem.*, 303 (2002) 131-137.
- [86] J.M. El-Khoury, D.R. Bunch, E. Reineks, R. Jackson, R. Steinle, S. Wang, A simple and fast liquid chromatography-tandem mass spectrometry method for measurement of underivatized L-arginine, symmetric dimethylarginine, and asymmetric dimethylarginine and establishment of the reference ranges, *Anal. Bioanal. Chem.*, 402 (2012) 771-779.
- [87] J. Martens-Lobenhoffer, S.M. Bode-Boeger, Fast and efficient determination of arginine, symmetric dimethylarginine, and asymmetric dimethylarginine in biological fluids by

- hydrophilic-interaction liquid chromatography-electrospray tandem mass spectrometry, *Clin. Chem.*, 52 (2006) 488-493.
- [88] I. Squellerio, E. Tremoli, V. Cavalca, Quantification of arginine and its metabolites in human erythrocytes using liquid chromatography-tandem mass spectrometry, *Anal. Biochem.*, 412 (2011) 108-110.
- [89] C.M. Brown, J.O. Becker, P.M. Wise, A.N. Hoofnagle, Simultaneous determination of 6 L-arginine metabolites in human and mouse plasma by using hydrophilic-interaction chromatography and electrospray tandem mass spectrometry, *Clin. Chem.*, 57 (2011) 701-709.
- [90] J.W. Jorgenson, Electrophoresis, *Anal. Chem.*, 58 (1986) 743A-760A.
- [91] M. Albin, R. Weinberger, E. Sapp, S. Moring, Fluorescence detection in capillary electrophoresis: evaluation of derivatizing reagents and techniques, *Anal. Chem.*, 63 (1991) 417-422.
- [92] P. de Montigny, J.F. Stobaugh, R.S. Givens, R.G. Carlson, K. Srinivasachar, L.A. Sternson, T. Higuchi, Naphthalene-2,3-dicarboxyaldehyde/cyanide ion: a rationally designed fluorogenic reagent for primary amines, *Anal. Chem.*, 59 (1987) 1096-1101.
- [93] R.G. Carlson, K. Srinivasachar, R.S. Givens, B.K. Matuszewski, New derivatizing agents for amino acids and peptides: Facile synthesis of N-substituted 1-cyanobenz[f]isoindoles and their spectroscopic properties, *J. Org. Chem.*, 51 (1986) 3978-3983.
- [94] S.M. Lunte, O.S. Wong, Naphthalenedialdehyde-cyanide: a versatile fluorogenic reagent for the LC analysis of peptides and other primary amines, *LC-GC*, 7 (1989) 908-910, 912, 914, 916.

[95] S.M. Lunte, O.S. Wong, Precolumn derivatization with naphthalenedialdehyde/cyanide for fluorescence, chemiluminescence or electrochemical detection of primary amines and peptides, *Curr. Sep.*, 10 (1990) 19-25.

Chapter Three

Optimization of a Capillary Electrophoresis Separation Method for the Determination of NDA-Derivatized Methylarginines

3.1 Introduction

Nitric oxide (NO) bioavailability impacts a large number of different physiological pathways such as cellular signaling, vasodilation, and immune response. Therefore, producing adequate amounts of NO is crucial to maintaining proper biological function. As described in Chapter 2, methylarginines (MAs) are competitive inhibitors of the enzyme that produces NO. As such, when MAs are present at elevated concentrations, severe health consequences can arise, including the development of cardiovascular, renal, and respiratory diseases. Since MAs have been reported to be elevated in patients suffering from diseases where NO is depleted, these compounds could potentially serve as valuable diagnostic markers of disease onset. Given this, an analytical method capable of quantifying each MA is necessary. This method must be rapid and relatively inexpensive so that it could be used in future large-scale clinical trials.

Several previous reports have utilized liquid chromatography-tandem mass spectrometry (LC-MS/MS) for measuring MA concentrations. By monitoring specific fragmentation losses using multiple reaction monitoring mode (MRM) in the MS, selective analysis of only the compounds of interest can be achieved, even without complete chromatographic resolution [1-3]. While this technique provides benefits versus fluorescence-based methods, it has the severe limitation of cost. The mass analyzer required for MRM analysis is very expensive and requires frequent maintenance, making it cost-prohibitive for general use in most hospitals. In addition to the high cost of the instrumentation, expensive isotopically-labeled internal standards need to be utilized for calibration as well as for quantitative analysis to compensate for variability in ionization efficiency. Despite good analytical performance, these financial issues prevent LC-MS/MS from being the best choice of technique for large-scale routine analyses.

Capillary electrophoresis (CE) is capable of achieving high efficiency separations in a platform of relatively low cost. These characteristics fit the criteria mentioned above as ideal for MA determination from clinical samples. However, separating MAs by electrophoresis is a challenging endeavor. As stated previously, the rates at which analytes migrate in an electric field are based on their charges and hydrated radii. The difficulty with separating MAs by CE is due to the fact that these parameters are very similar for each MA. These arginine-based molecules all contain a guanidinium group whose pK_a is ~ 12.5 . Although pK_a values for MAs have not been published, the methyl groups on the guanidinium nitrogens add electron density to the side-chain which should stabilize the cation and, in turn, raise the pK_a slightly. Regardless of the exact values, the pK_a 's of the side-chains remain quite high. Selectively deprotonating the side-chains of the different MAs using the CE background electrolyte (BGE) would be difficult because most buffers do not have buffering capacity at such high pH. Additionally, to adjust the pH of a solution to such a high value may drastically increase the ionic strength of the solution, which can hinder electrophoretic separations by causing excessive Joule heating.

There have been multiple reports in the literature describing the use of CE in the analysis of MAs, but all have shortcomings. Many of these methods suffer from the co-migration of the MA species [4-7]. Additional limitations of these other methods stem from their choices of detection modes. The use of UV detection [5] is not ideal because of its lack of selectivity at 190 nm as well as its relatively high detection limits (compared to laser-induced fluorescence (LIF)). The studies that utilized fluorescence detection for the analysis of MAs used derivatization reagents that hindered sample throughput either by necessitating that the labeling reaction take place overnight [7] or by requiring the sample to be heated in order for derivatization to occur [6]. Neither of these approaches is ideal because of the lengthy sample

preparation times. In addition, the derivatization reagents used in previous reports are fluorescent themselves. This complicates the separation by requiring that the excess derivatization reagent in the reaction mixture be resolved from the labeled analytes of interest. The CE method in the literature that is most promising uses a tandem mass spectrometer as a detector. Despite having the best reported limits of detection for MAs [4], the cost of analysis is quite large due to the high price of a CE-MS/MS system and the need for expensive deuterated internal standards.

The purpose of this study was to develop a fast, relatively inexpensive analytical method for the determination of MAs. Run conditions were then optimized using CE-LIF in order to determine the conditions necessary to achieve baseline resolution between the four analytes of interest. Additionally, an investigation was made to identify a compound that could serve as an internal standard to improve quantitation of the method. Following optimization of the run buffer to enable a good separation between the MAs, several separation parameters such as the number of theoretical plates and peak resolution were calculated.

3.2 Materials and Methods

3.2.1 Reagents

Standards of arginine, methyllysine, arginine methyl ester, homoarginine, nitroarginine, agmatine, and canavanine were purchased from Sigma Aldrich (St. Louis, MO); asymmetric dimethylarginine (ADMA), symmetric dimethylarginine (SDMA), monomethylarginine (MMA), propylarginine (PA), ethylarginine (EA), hydroxyarginine, and nitroarginine methyl ester (L-NAME) were purchased from Enzo Life Sciences (Plymouth Meeting, PA); and hydroxynorarginine was purchased from Bachem (Torrance, CA). All standards were prepared at

10 mM concentrations in 18.2 M Ω •cm deionized water (Millipore; Billerica, MA). Samples were serially diluted to the desired concentrations prior to CE analysis. HPLC-grade dimethylsulfoxide, acetonitrile, and methanol were acquired from Fisher Scientific (Pittsburgh, PA). A stock solution of 100 mM sodium tetraborate (Sigma Aldrich) was made, and aliquots were adjusted to the indicated pH values either by the addition of 1 N HCl or the addition of 1 N and/or 10 N NaOH (Fisher Scientific). A 100 mM aqueous solution of sulfobutylether- β -cyclodextrin (SBEC) (Cydex Pharmaceuticals; Lenexa, KS) was also prepared. It should be noted that the SBEC formulation contains a range of SBE groups per cyclodextrin. The molecular weight used in the preparation of CE buffers assumed seven SBEs per molecule (this was the centroid of a relatively Gaussian distribution) even though the range varied from three to ten. To formulate the run buffers, stock solutions of borate, SBEC, and DMSO were combined and diluted to the appropriate concentrations with ultrapure water. NDA (Invitrogen; Carlsbad, CA) was dissolved in 1:1 acetonitrile: water to a final concentration of 5 mM. A 10 mM sodium cyanide (Sigma Aldrich) solution was prepared in water. Working solutions of NDA and CN⁻ were diluted in 1:1 acetonitrile: water and water, respectively.

3.2.2 Capillary Electrophoresis

A Beckman P/ACE MDQ capillary electrophoresis instrument (Brea, CA) equipped with a 65 cm (50 cm to window), 50 μ m i.d./ 360 μ m o.d. fused silica capillary (Polymicro Technologies; Phoenix, AZ) was used in the development of a method to separate the MA species. Samples were introduced into the capillary via pressure injection at 1.0 psi for 5.0 s. A 445 nm diode laser (CrystaLaser; Reno, NV) was used for sample excitation, and fluorescent emission (>490 nm) was measured with an external fluorescence detector (Picometrics;

Ramonville, France). 32 Karat software (Beckman) was utilized to control both CE operation and LIF detection.

Samples analyzed by CE were first derivatized with NDA/CN⁻ to form fluorescent cyanobenz[f]isoindole (CBI) derivatives. The derivatization procedure entailed combining equal volumes (5-20 μ L) of sample, 50 mM sodium tetraborate, 1 mM NDA, and 5 mM NaCN and allowing the mixture to react for 10 min prior to injection. Peak areas from the MAs were normalized to the peak area of the internal standard PA for quantitation. All samples were measured in triplicate unless otherwise noted.

3.3 Results and Discussion

3.3.1 Run Buffer Modifiers

Given the high degree of structural similarities between the different MAs, achieving a reasonable separation between these analytes was quite challenging. The pK_a values of the molecules are very similar which precludes a charge-based separation. Additionally, their sizes are comparable which increases the difficulty of achieving size-based separations. This problem is further accentuated after derivatization. The CBI moieties make the relative sizes of the molecules even more similar while also rendering the derivatives electrically neutral after labeling the N-terminus. Given these factors, it was not surprising that free zone electrophoresis was insufficient to separate the MAs. A sample electropherogram is shown in Figure 3.1 where complete co-migration of all the MA analogues was observed.

In an attempt to gain better resolution between MA peaks, a MEKC method was evaluated. Previous reports have demonstrated improved separations of NDA-derivatized amino

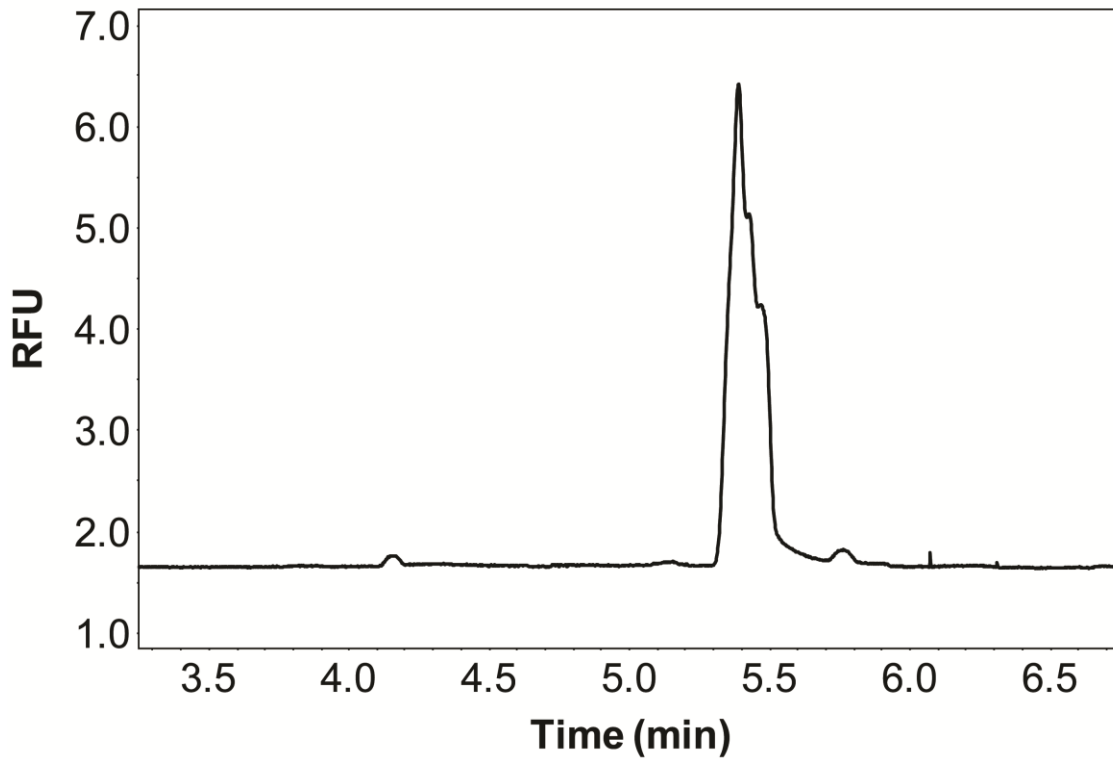


Figure 3.1 An electropherogram showing the separation of a mixture of 1 μM MAs in a 15 mM borate CE run buffer. Significant co-migration of the analytes was observed.

acids utilizing MEKC because of the different affinities of each analyte for the micelle. These papers observed unique mobilities for each sample component, and therefore, a separation of the analytes. Unfortunately, this was not the case in the analysis of MAs. Many combinations of run buffer modifiers (surfactants, organic solvents, etc.) at various concentrations were evaluated. While an improvement in resolution was observed with MEKC, significant comigration was still observed with this separations mode. The separation conditions that produced the best separation (highest peak resolution) are shown in Figure 3.2.

While MEKC did not result in a complete separation of MAs, it did prove more beneficial than free zone electrophoresis. In an attempt to further improve the separation, an ion pairing reagent was added with the rationale being that methylated side-chains on the MA analogues would have differing electrostatic interactions with the reagent. To test this hypothesis, 3-(cyclohexylamino)-1-propanesulfonic acid (CAPS) was added to the run buffer from Figure 3.2 to serve as an ion pairing reagent. The results from the experiment empirically validated the hypothesis as shown in Figure 3.3. With the optimized MEKC/ ion pair separation, Arg, MMA, and either SDMA or ADMA were separated; however, the two dimethylated analogues still co-migrated. This data confirmed that MAs have different hydrophobic interactions with the SDS micelles and different ion pairing capacities with the CAPS; however, additional buffer modification was required.

Sulfobutylether- β -cyclodextrin (SBEC) was evaluated as a buffer modifier because it integrated the previously mentioned modes of interaction that were shown to help separate MAs. SBEC (shown in Figure 3.4) is a modified cyclodextrin containing ether-linked butylsulfonate groups. Therefore, this single modifier provided electrostatic and hydrophobic interactions, while also providing hydrogen bonding sites and size-based affinity for the cyclodextrin cavity.

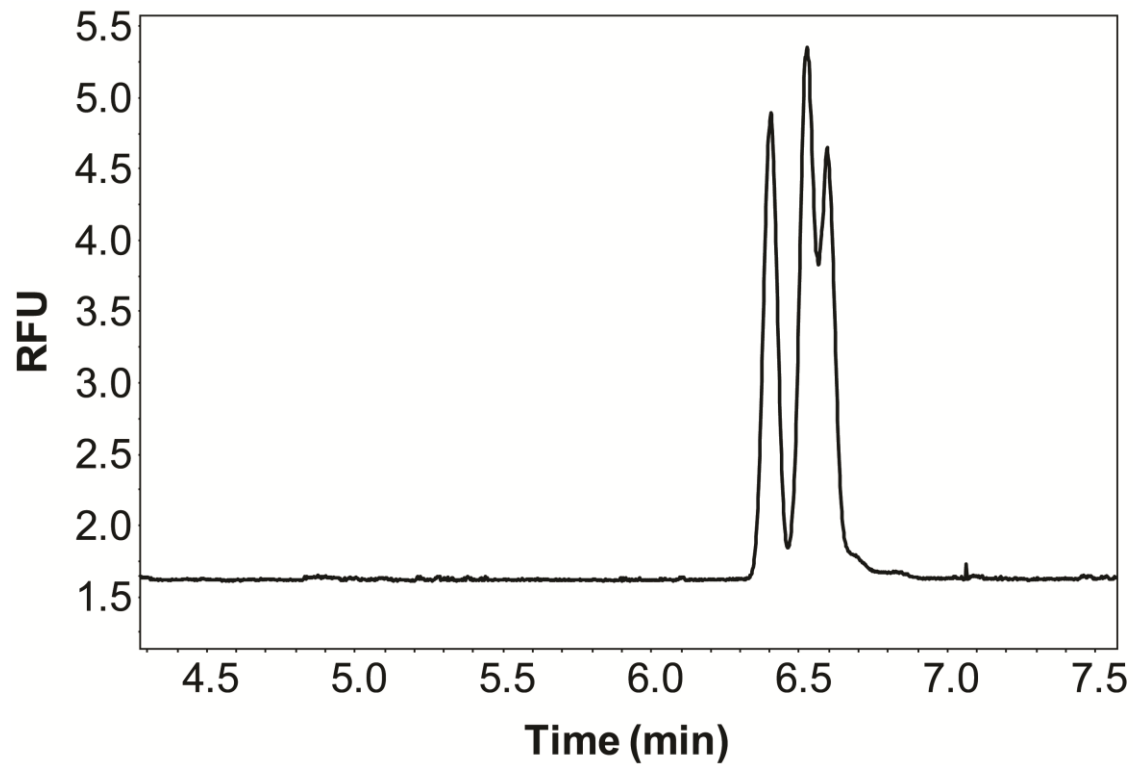


Figure 3.2 Sample electropherogram of a MEKC separation of a mixture of 1 μ M MA standards.

The run buffer consisted of 15 mM borate, 7 mM SDS, and 5% acetonitrile.

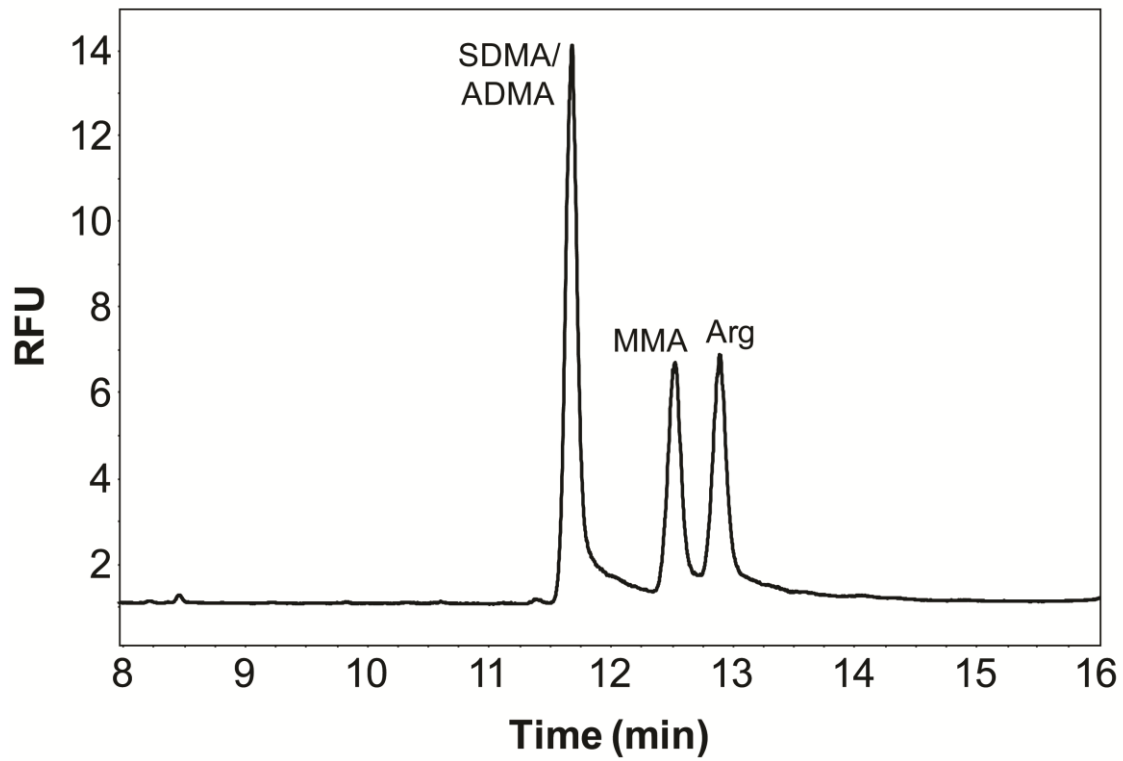


Figure 3.3 Sample electropherogram of a separation of 10 μ M MAs. The run buffer contained 30 mM borate, 5 mM SDS, and 50 mM CAPS.

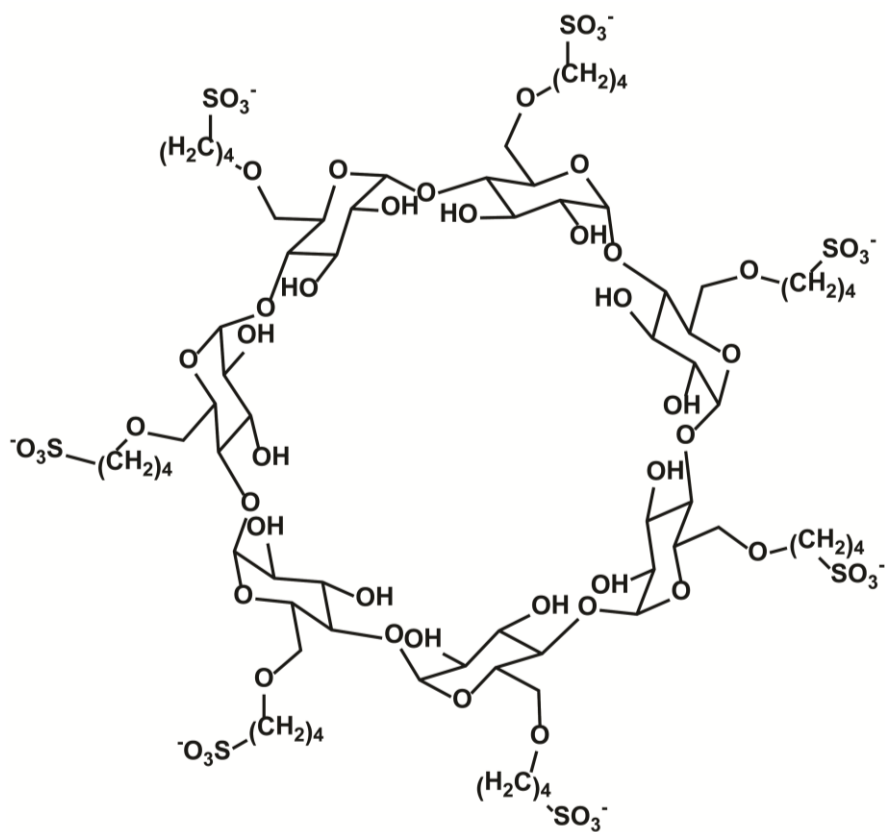


Figure 3.4 Structure of sulfobutylether-β-cyclodextrin.

Introducing this compound into a separation buffer has been shown in the past to effectively separate o-phthaldehyde-labeled biogenic amines [8]; therefore, it was investigated here as a pseudo-stationary phase. Upon addition of SBEC into a run buffer containing SDS and CAPS, a noticeable improvement in resolution was observed. After optimizing the concentrations of the various components, it was determined that the use of SBEC exclusively (without SDS or CAPS) provided the greatest resolution between MA peaks.

It is believed that SBEC facilitated the separation of NDA-labeled MAs by two mechanisms [9]. First, the CBI ring partitioned into the hydrophobic core of the cyclodextrin. Since SBEC is anionic and has a negative electrophoretic mobility, the net migration of the derivatized species was retarded as the molecule interacted with the cyclodextrin ring. In addition to the interaction with the CBI ring, the second mode of interaction was with the individual MA side-chains. The cationic guanidinium groups on the arginine residues interacted with the negatively charged sulfonate groups on the surface of the SBEC to form an ion pair. The methyl groups on MMA, ADMA, and SDMA, however, attenuated the electrostatic attraction due to steric hindrance, thereby diminishing the retention of the analyte. The extent of methylation and the subsequent inhibition of electrostatic association with the cyclodextrin correctly predicts the migration order of SDMA > ADMA > MMA > Arg. MAs were not able to be separated using unsubstituted β -cyclodextrin suggesting that the anionic nature of SBEC was crucial to achieving a good separation.

3.3.2 Separation Optimization

The concentrations of borate and SBEC as well as the run buffer pH and separation voltage were systematically varied to determine the optimal conditions for the separation of MA

standards. The concentration of SBEC was varied from 0 to 20 mM to evaluate its effect on the resolution between the analytes. It was determined that an increase in resolution was realized with increasing amounts of the anionic cyclodextrin. The MAs completely comigrated when no SBEC was included in the run buffer but complete baseline resolution was achieved at all of the other SBEC concentrations. A run buffer containing 1.5 mM SBEC was chosen for subsequent analyses because this produced the separation with the highest efficiency while also providing the shortest run times.

Sodium tetraborate is a common BGE used in CE separations. It was selected as the BGE for this analysis because of its compatibility with NDA derivatization chemistry. The borate concentration in the run buffer was varied from 5 to 50 mM in order to determine the optimal conditions for separating the analytes of interest. Higher borate concentrations provided slightly better resolution between adjacent peaks at the cost of increased analysis times. Concentrations as low as 5 mM borate still resulted in baseline resolution of the analytes. It was determined that 30 mM borate was optimal since this concentration provided the largest peak capacity in reasonably short analysis times.

The pH of the borate solution was also varied to ascertain the impact of pH on peak resolution. Run buffers consisting of 30 mM borate and 5 mM SBEC were prepared at pH 9.00, 9.25, 9.50, 9.75, and 10.00. It was determined that run buffers at higher pH produced longer migration times. This increase in migration time can be attributed to the higher ionic strength in the buffer (from the addition of the NaOH used to adjust the solution pH) which slowed the EOF. The ionization states of the MAs were not affected in the range of pH values evaluated and therefore did not influence the separation. All the compounds were completely resolved

regardless of run buffer pH. For simplicity, a pH of 9.25 was selected for subsequent analyses as that is also the optimum pH at which to derivatize the analytes of interest.

An investigation was also made into the effect of the applied separation voltages on resolution and analysis time. As expected, higher voltages led to faster analyte migration and shorter analysis times. As one of the goals of developing this method was to increase throughput, the fastest possible separation was desired. Because all species of interest remained baseline resolved at the higher field strengths, a separation voltage of 28 kV (430 V/cm) was determined to be optimal.

The optimized separation parameters were determined after performing a systematic evaluation of the analysis conditions, as described above. The final run buffer was comprised of 30 mM pH 9.25 borate and 1.5 mM SBEC, and the separation occurred at a voltage of 28 kV. Baseline resolution of all the analytes of interest was achieved with run times of less than seven minutes. An electropherogram of this separation is shown in Figure 3.5.

3.3.3 Internal Standard Identification and Peak Capacity Improvement

The incorporation of SBEC into the run buffer was crucial for providing baseline resolution between the MAs. However, before serum samples could be analyzed, the identification of an internal standard (IS) was required in order to increase quantitative precision. In order to serve as a viable IS, the compound needed to migrate prior to arginine in the separation. This requirement stems from the fact that MAs are the smallest, most positively charged species in serum and therefore migrate earliest. In serum samples, the complexity of the electropherogram after arginine is tremendous because of the other amine-containing small molecules and peptides present. Given this, any analyte that migrated in that region would be

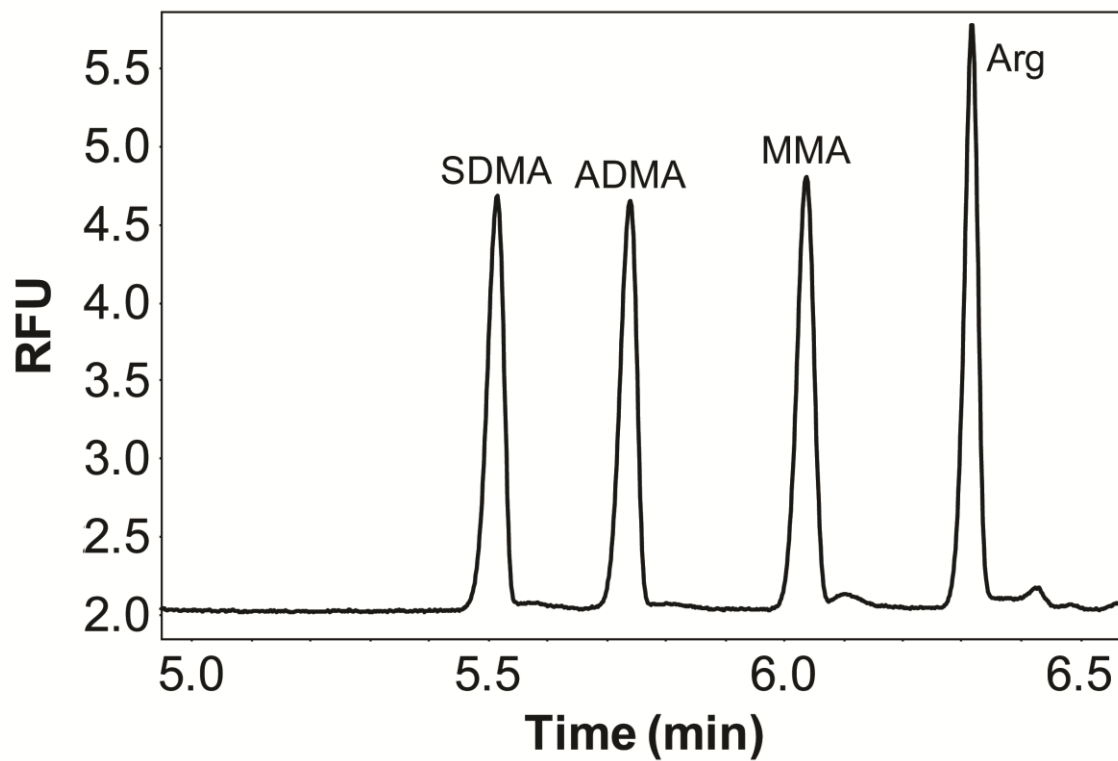


Figure 3.5 Sample electropherogram of a separation of 500 nM MAs. The run buffer contained 30 mM borate and 1.5 mM SBEC.

extremely difficult to identify and even more difficult to quantify with good precision. Therefore, the IS peak must migrate early in the separation. Several structurally analogous molecules to arginine were evaluated, but none of them proved adequate. Many species that free zone electrophoresis principles would have predicted to migrate before the MAs migrated well after them (Table 3.2). This can be attributed to their affinities for the SBEC being stronger than that of the MAs. Unfortunately, predicting the affinity turned out to be an exercise in futility since no discernible pattern emerged. The only two exogenous species that migrated in the required separation window both comigrated with MMA despite attempts made to reoptimize concentrations of run buffer components.

3.3.3.1 Dimethylsulfoxide Addition

To overcome the difficulty in selecting an IS and potentially allow either EA or PA to serve that purpose, additional peak capacity was sought. Typical run buffer modifications to achieve this goal include the addition of an organic solvent. Inclusion of an organic is quite common in the CE literature with acetonitrile or methanol typically being employed. However, neither of these compounds was found to significantly improve the separation (Table 3.1). Therefore, an exploration was made into non-traditional solvents. Acetone, 1-propanol, 2-propanol, and ethanol were incorporated into the run buffer to determine their effect on the resolution and efficiency of the separation. It was determined that there were no improvements between buffer containing these organics versus the entirely aqueous buffer; and in many cases, the resolution actually worsened due to increased peak tailing. The addition of DMSO to the run buffer, however, produced a noticeable improvement in resolution. And despite longer migration times with DMSO, which normally leads to increased longitudinal diffusion and therefore band-

Table 3.1 Effect of run buffer organic solvent on (a) the number of theoretical plates (m^{-1}) and (b) peak resolution in the separation of 500 nM MAs. The run buffer contained 30 mM borate, 1.5 mM SBEC, and 10% (v/v) of the indicated organic solvent.

a)

Solvent	SDMA	ADMA	MMA	Arg
None	9000	8400	8000	9800
DMSO	16700	14800	14800	11700
MeOH	9900	8800	9600	10500
ACN	16900	6500	7900	8200

b)

Solvent	SDMA-ADMA	ADMA-MMA	MMA-Arg
None	0.90	1.11	0.69
DMSO	0.91	1.47	1.23
MeOH	1.03	1.47	1.36
ACN	0.69	1.14	1.04

broadening, peak widths remained the same as in the unmodified buffer. Longer migration times and identical peak widths demonstrated the increased separation efficiency as evidenced by the larger number of theoretical plates. Separation parameters from run buffers containing different organics are shown in Table 3.1.

The inclusion of DMSO into a CE run buffer has not been reported before in the literature to the best of our knowledge but was found to significantly improve the separation of MAs. Given this, studies were conducted to further characterize the effect of DMSO on the separation. The migration times of several analytes were monitored under both aqueous conditions and with 5% DMSO in the run buffer. Migration times were then normalized relative to that of the arginine peak for improved precision and listed in Table 3.2. It was determined that every compound that migrated earlier than arginine migrated even earlier with DMSO in the run buffer, while every compound that migrated later than arginine migrated even later with DMSO in the run buffer (except hydroxynorarginine). Essentially, DMSO was found to effectively increase the window in which these species migrated. Following reoptimization of the run buffer composition with DMSO now included, EA and PA were able to be resolved from MMA which had comigrated under previous conditions. The newly optimized run buffer contained 15 mM borate, 10 mM SBEC, and 25% DMSO which provided unprecedented peak resolution (Figure 3.6). This now enabled PA to serve as an internal standard in the analysis of clinical samples (EA was found to comigrate with an unknown endogenous peak).

A brief investigation was made to attempt to elucidate the reason for the separation enhancement when DMSO was incorporated into the run buffer. Given the relatively high viscosity of DMSO compared to water, one hypothesis for its beneficial effects was that a higher solution viscosity provided additional drag on the analytes passing through the capillary. This

Table 3.2 Migration times (relative to arginine) of various 500 nM analytes. The run buffer contained 30 mM borate, 1.5 mM SBEC, and 5% DMSO.

Compound	$\Delta t_{m, \text{Aqueous}}$	$\Delta t_{m, \text{DMSO}}$
SDMA	-0.79	-0.88
ADMA	-0.57	-0.65
MMA	-0.27	-0.31
EA	-0.27	-0.33
Hydroxynorarginine	-0.23	0.00
Methyllysine	-0.15	-0.15
PA	-0.11	-0.13
Arg methyl ester	0.00	0.00
Hydroxyarginine	0.10	0.19
Homoarginine	0.11	0.18
Nitroarginine	0.12	0.21
L-NAME	0.16	0.21
Canavanine	0.22	0.35

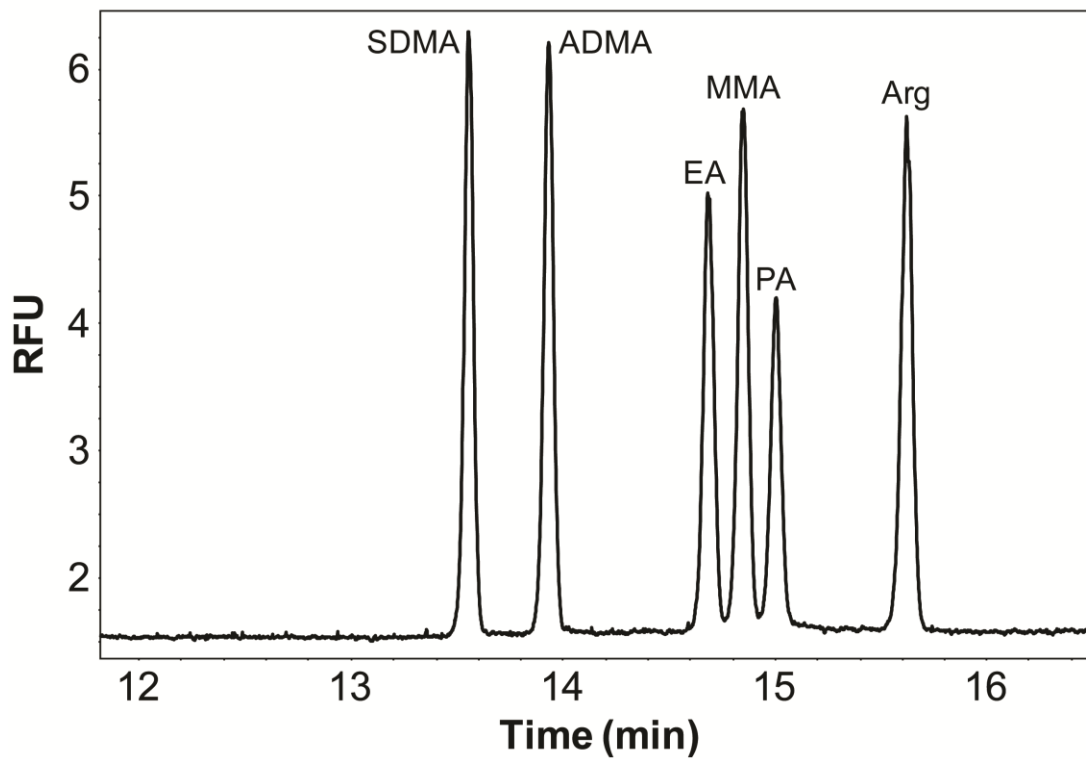


Figure 3.6 Electropherogram illustrating the separation of 500 nM MAs/EA/PA. The run buffer contained 15 mM borate, 10 mM SBEC, and 25% DMSO.

increased drag force could help enhance resolution between analytes since separation efficiency is dependent upon solution viscosity. To determine if this hypothesis was true, the kinematic viscosity of the 25% DMSO run buffer was calculated using the Refutas equation where the viscosity blending number (VBN) was determined to be 4.23. A second run buffer was then made by matching the VBN by the addition of glycerol instead of DMSO and maintaining constant borate and SBEC concentrations. The results demonstrated that the enhanced separation resolution was not strictly due to viscosity (Figure 3.7). The run buffer containing glycerol demonstrated some increased resolution between MAs and later peak migration times, but not as large as with the buffer containing DMSO. These results suggest that DMSO does not strictly enhance the separation by viscosity alone. The incorporation of DMSO must affect the equilibrium between each MA species and the SBEC molecules in a manner to provide a unique migration time for each.

3.3.4 CE-LIF Method Characterization

The separation method was characterized following the optimization of the run conditions. A sample electropherogram and the validation parameters are shown in Figure 3.6 and Table 3.3, respectively. Calibration curves were constructed for each analyte of interest from aqueous MA standards. The lines of best fit and the equations are reported in Figure 3.8. The linearity of the method was determined by constructing a calibration curve over a clinically relevant concentration range (50-1200 nM) (Figure 3.8). This method provided good linearity (≥ 0.999) and low relative standard deviations for MA standards. The average peak area deviation for each analyte was $< 5\%$ over the concentration range studied indicating a reasonable level of precision. The number of theoretical plates for each analyte was $\sim 150,000$ plates/m. The limits of

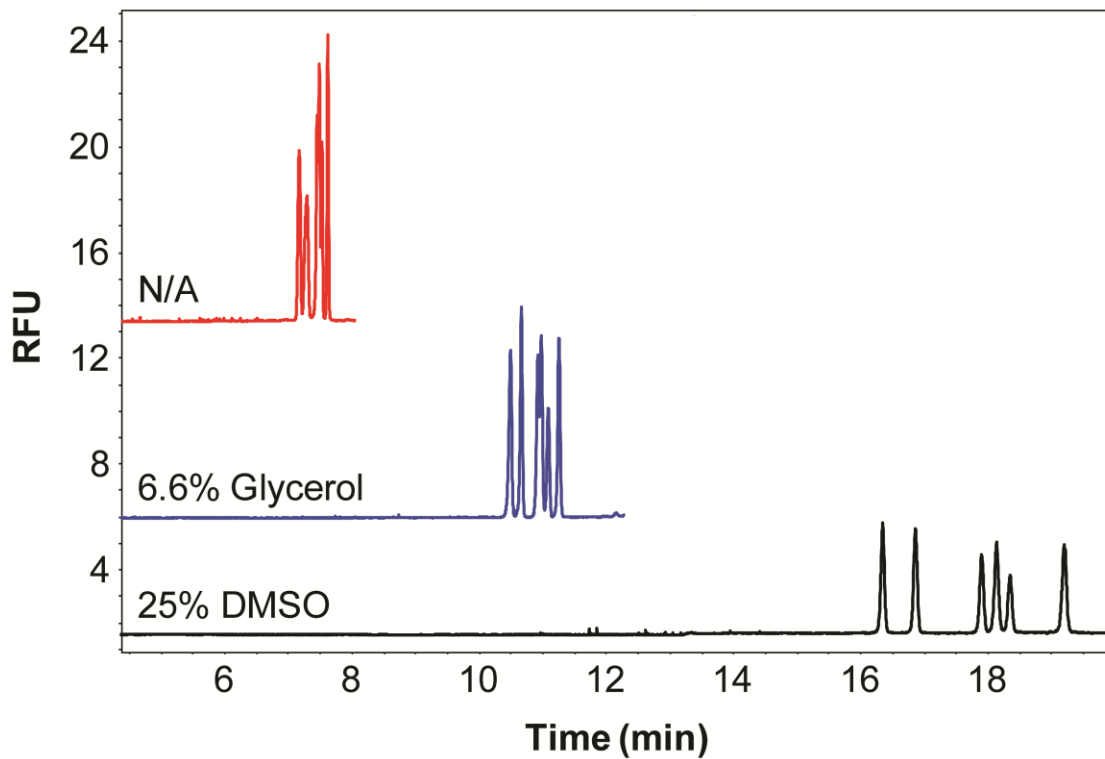
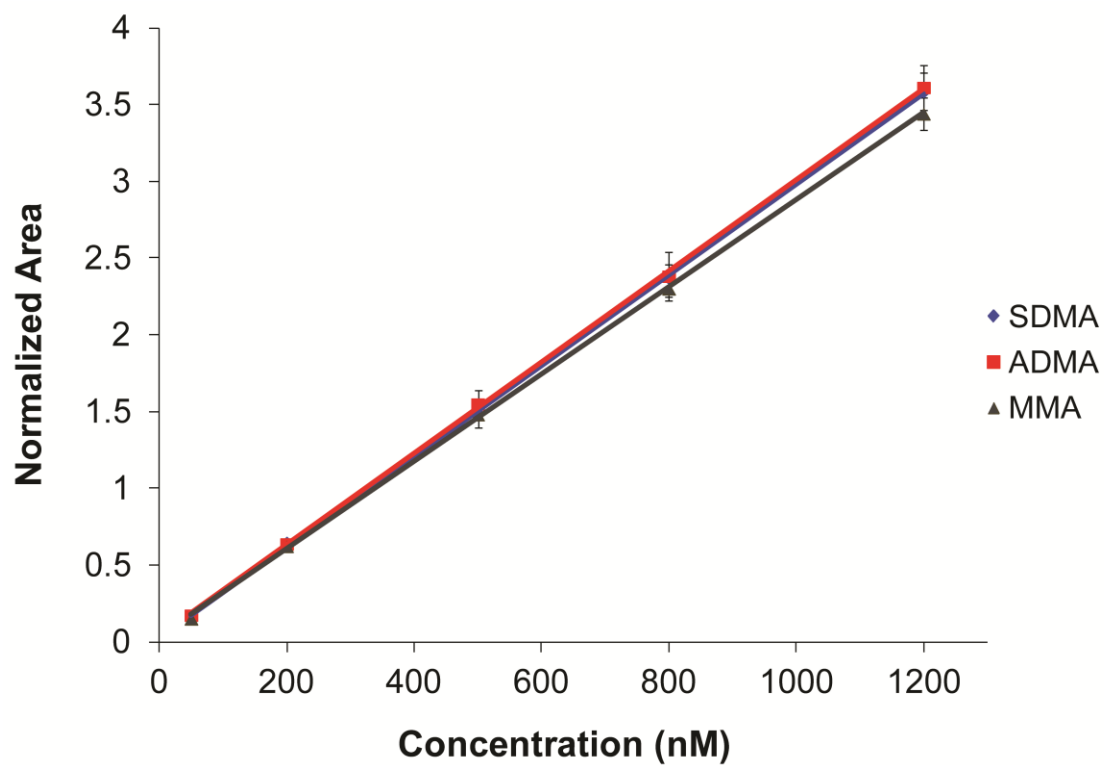


Figure 3.7 Effect of solution viscosity on separation efficiency of 500 nM MAs/EA/PA. Run buffer contained 15 mM borate, 10 mM SBEC, and the indicated additives. Run buffers modified with either DMSO or glycerol had identical kinematic viscosities.



Analyte	Slope (μM^{-1})	Y-Intercept
SDMA	0.00296	0.0221
ADMA	0.00297	0.0520
MMA	0.00284	0.0352

Figure 3.8 Calibration curve for MAs over a clinically-relevant concentration range.

Table 3.3 Validation parameters from the optimized CE-LIF method.

Compound	Number of Plates (m⁻¹)	R² *	%RSD **	LOD (nM) (S/N = 3)
SDMA	147000	0.9997	4.5	5
ADMA	127000	0.9998	4.9	5
MMA	146000	0.9998	2.6	6
PA	149000	-	-	8

*Over a concentration range between 50 and 1200 nM.

**Based on replicate peak area measurements (n=3) from each calibration standard (n=5 concentrations).

detection ($S/N=3$) were determined experimentally for each analyte of interest and found to be 5-8 nM which are all well below the expected endogenous concentrations.

The separation efficiency and detection limits of this method were good; however, the precision in analyte migration times was not (Table 3.4). Although the RSD for each analyte was only ~3%, this unfortunately corresponded to a fairly large shift in migration times. The standard deviations were ± 30 s which meant that the window in which these peaks migrated was about one minute wide. In contrast to many LC methods with a retention time variability of $<0.1\%$, the deviation of this method was quite poor. The deviation in migration times can be attributed to the dynamic conditions in which CE is operated. If adsorption of analytes onto the capillary wall occurs or if the ionic strength of the run buffer becomes depleted this will affect the migration of analytes through the capillary. However, despite the large variability in migration times of this CE-LIF method, the precision of the peak areas were high which still enabled reliable quantitation.

3.3.5 NDA Derivatization

Once a sufficient separation method was developed to resolve the different MAs (and IS) from the other components in the sample, an investigation was made into the derivatization chemistry. Although discussions on analyte labeling often times get omitted in the literature, it is a crucial aspect of the analytical method. The concentrations of derivatization reagents or reaction time can have a profound effect on the sensitivity of the method. To ensure the method under development was not being hindered by overlooking these concerns, efforts were made to optimize factors related to analyte labeling.

Table 3.4 Migration time reproducibility. Separation buffer contained 15 mM borate, 10 mM SBEC, and 25% DMSO (n=46 injections of 10-1000 nM MA standards).

Compound	Avg t_m (min)	Std Dev (min)	%RSD
SDMA	14.5	0.43	3.0
ADMA	15.0	0.46	3.1
EA	15.9	0.50	3.2
MMA	16.1	0.51	3.2
Arg	17.0	0.57	3.3

NDA is a very hydrophobic molecule that has limited solubility in aqueous solution. To aid its solubility, NDA is typically dissolved in a solution containing some percentage of organic solvent. Papers in the literature typically dissolved NDA in acetonitrile (ACN) or methanol or a mixture of those solvents with water. To determine which organic produced the most favorable results, a qualitative assessment was made to elucidate the impact of solvent composition on NDA solubility and the subsequent separation.

Considering the large amount of DMSO in the separation buffer, dissolving NDA in DMSO seemed like a logical choice to solubilize the reagent while enhancing compatibility between the sample matrix and the run buffer. However, Table 3.5 illustrates that this was not the case. Comparing fluorescent signals from MAs as a function of NDA solvent composition, it was discovered that dissolving NDA in DMSO proved problematic. The peak area deviations between multiple injections of sample containing DMSO was significantly higher than those in which NDA was dissolved in an ACN solution. Additionally, the signal from the MAs was substantially smaller with DMSO in the sample mixture than ACN. This large discrepancy in both reproducibility and fluorescent response can be attributed to the increased viscosity of DMSO. Sample injection was achieved by hydrodynamic pressure where the volume of sample introduced into the capillary is inversely proportional to the viscosity of the solution. Given the high viscosity of DMSO (compared to ACN), a smaller volume of sample would have been injected which would manifest as a lower fluorescence response. Similarly, any discrepancies in injection time or pressure would be accentuated with a high viscosity sample since the relative volume difference would be greater and would therefore increase the %RSD over multiple injections.

Table 3.5 Effect of NDA solvent (1:1 water: solvent) on analyte peak area RSDs and relative fluorescence responses. 500 nM standards were derivatized with 1 mM NDA, 5 mM NaCN, and 50 mM borate.

Analyte	%RSD ACN	%RSD DMSO	ACN/DMSO Response
SDMA	3.3	19	2.0
ADMA	1.6	17	2.0
EA	4.6	18	2.0
MMA	1.6	20	2.0
Arg	2.9	18	1.9

Evaluation of more commonly utilized solvents showed that no significant differences existed between methanol and ACN when in 1:1 or 1:2 ratios with water. Each solvent mixture was sufficiently hydrophobic to solubilize NDA without impacting the separation. The use of an exclusively aqueous solvent produced no noticeable difference in the separation; however, a substantial effort was required to dissolve the solid NDA in water. Aqueous solubility of NDA was found to be ~2 mM. The most interesting observation was found when NDA was dissolved in 100% ACN. While the NDA rapidly dissolved into solution, this solvent composition produced a noticeable effect on the separation. Figure 3.9 demonstrates that when NDA was dissolved in pure ACN, each analyte peak began to split into two. Even though the final concentration of ACN in the derivatization mixture was 25% and the sample plug only constituted a small percentage of the total capillary volume, this volume of organic was sufficient to impact the separation. This suggests that a partitioning phenomenon occurred in the capillary between the run buffer and the ACN causing the analyte plug to spread out into two bands. Because this was quite detrimental to the separation and caused a significant loss of resolution, this solvent composition was not used further. It was ultimately determined that a 1:1 ACN:H₂O mixture yielded the most consistent separations and was selected as the solvent moving forward.

Once an appropriate solvent was identified for NDA dissolution, optimization of the amount of NDA and CN⁻ in the derivatization mixture was required. Although there are numerous reports utilizing NDA/CN⁻ in the literature to derivatize analytes, no discussion is made regarding the amounts introduced into the sample mixture. While the exact ratios vary from paper-to-paper, a seemingly arbitrary 1:2 ratio of NDA:CN⁻ appears to be most commonly employed. Therefore, the first factor evaluated was the ratio of NDA to CN⁻ used in sample

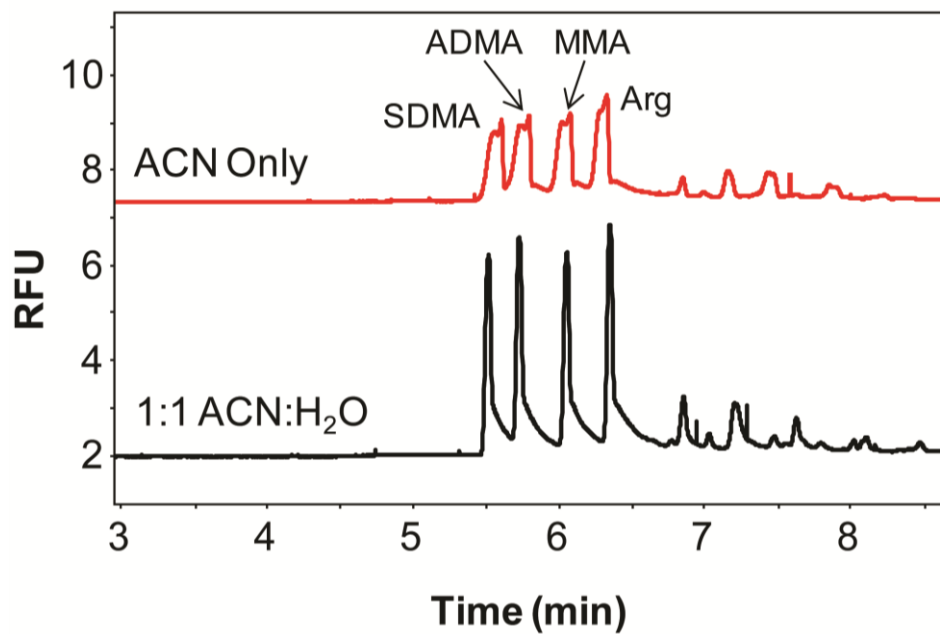


Figure 3.9 Effect of NDA solvent on the CE separation. Final NDA solvent concentration was 25% v/v. 500 nM standards were derivatized with 1 mM NDA and 5 mM NaCN.

derivatization. Figure 3.10 illustrates that increasing the concentration of CN^- (while holding the NDA concentration constant) results in an increase in the fluorescence response of the analytes. However, this improved response tapers off once the ratio reaches a certain threshold ($\sim 1:5$). Based on the absolute peak areas, a NDA: CN^- ratio of 1:5 was determined to be optimal to provide the most intense response while minimizing the chemical noise.

An evaluation was also made to optimize the time necessary to enable the derivatization reaction to go to completion and produce the highest fluorescent responses from the analytes of interest. All samples were prepared in an identical manner and allowed to sit until the indicated derivatization time, at which point sample was injected into the CE. It was determined from this study that more derivatized products were able to form as longer reaction times were reached (Figure 3.11a). However, a maximum was reached after which no additional increase in signal was observed. The plateau beginning at ~ 10 min indicates that all analytes in the sample were labeled by that time with no additional benefits observed by allowing the mixture to react for extra time (*i.e.* 15 and 20 min). Interestingly, though, normalized responses were unaffected by the derivation time (Figure 3.11b). This finding suggests that derivatization rates are the same for each MA and that the relative response between MAs is constant. This is a beneficial property because any experimental imprecision in the amount of time the mixture is allowed to react is mitigated since normalized responses are the same regardless of derivatization time. It was ultimately determined that 10 min was the optimum reaction time. This time provided the highest sensitivity while still enabling the greatest sample throughput.

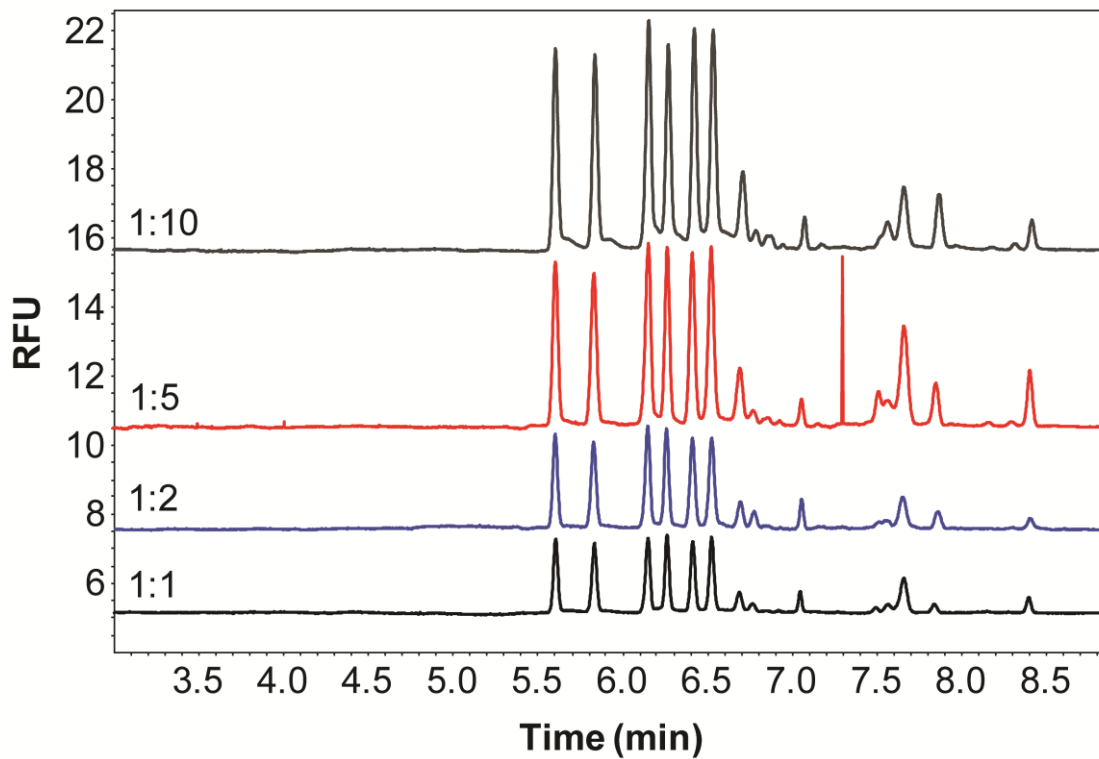


Figure 3.10 Effect of NDA:CN⁻ ratio on peak height. 500 nM standards were derivatized with 1 mM NDA and the corresponding amount of CN⁻. Peak identities were as follows: (1) SDMA, (2) ADMA, (3) MMA, (4) methyllysine, (5) arginine, (6) homoarginine, and (7) canavanine.

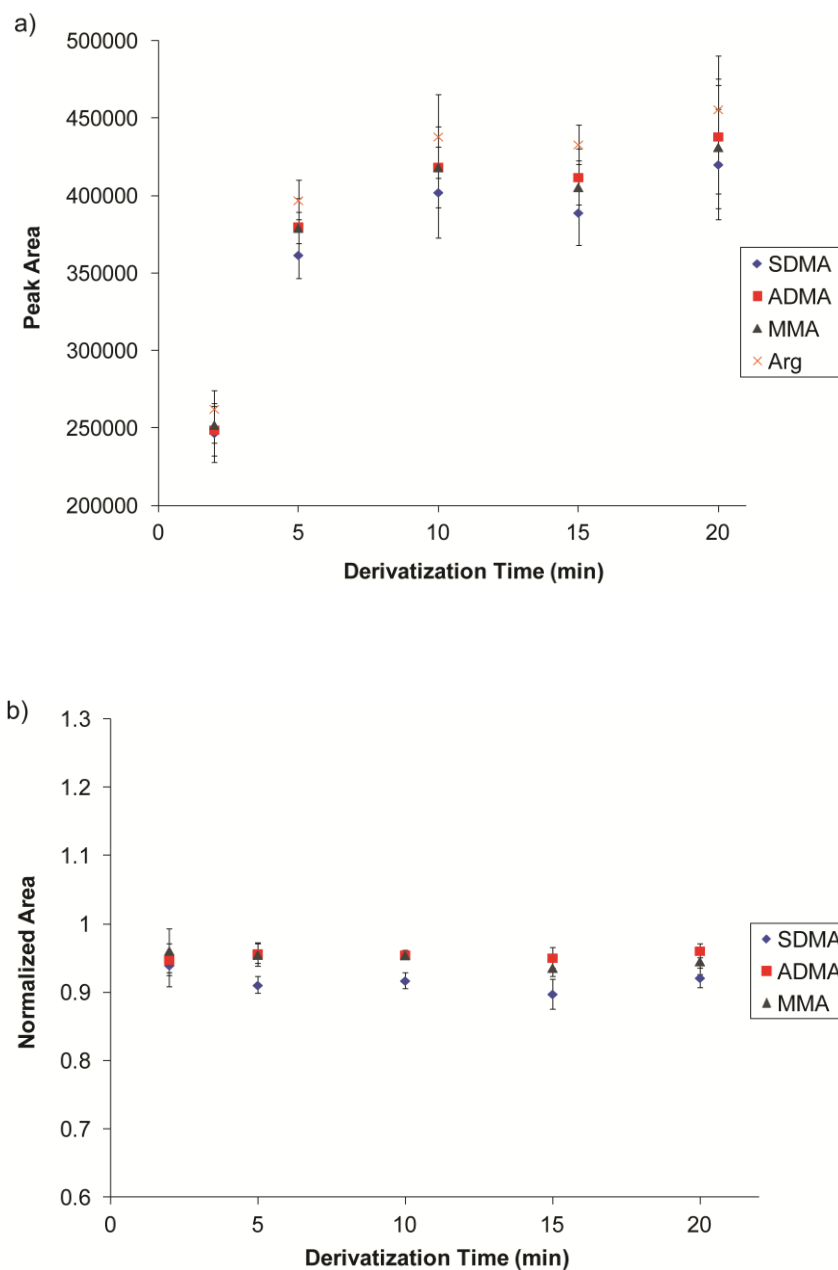


Figure 3.11 Fluorescence responses of 500 nM MA standards derivatized with 1 mM NDA, 5 mM NaCN, and 50 mM borate as a function of derivatization time. Raw peak areas (a) and areas normalized to arginine (b) are shown. Separation buffer contained 30 mM borate and 1.5 mM SBEC.

3.3.6 Other Separation Considerations

While analyzing serum-based samples, it was observed that noise in the electropherograms increased as the number of runs increased (Figure 3.12a). To diminish the harmful impact of this noise on the precision of peak integration in the later runs, additional rinse cycles were included in between runs. Although more time spent rinsing the capillary reduced the number of samples that could be run per day, the gain in precision would be worth the time delays. However, the inclusion of the rinses between runs did not influence the baseline noise, as it continued to increase with each additional run (Figure 3.12b). The factor that was found to have the most profound effect on preventing the noise from increasing was the replacement of the run buffer. When run buffer vials were changed between runs, the noise increase never onset (Figure 3.12c). This trend was found to continue for several runs even without rinsing the capillary in between.

An often overlooked factor that was found to have a substantial impact on the quality of the separation was the geometry of the capillary inlet. This problem is difficult to diagnose even when one is looking for it because the difference between a perfectly flat capillary end and one at a slight angle is hardly noticeable with the eye. Figure 3.13 illustrates how identical samples being separated in the same capillary before and after squaring off the capillary end can produce distinctly different looking electropherograms. With a flat inlet, the sample plug was able to migrate in a condensed band which produced a nice symmetric peak shape. However, the presence of either a chip in the capillary inlet or an end cut at a slight angle resulted in a distorted plug shape and a peak that had a substantial tail to it. By being attentive to the physical capillary and exercising diligence when setting up the system, the separation resolution can be significantly improved without manipulating a single chemical variable.

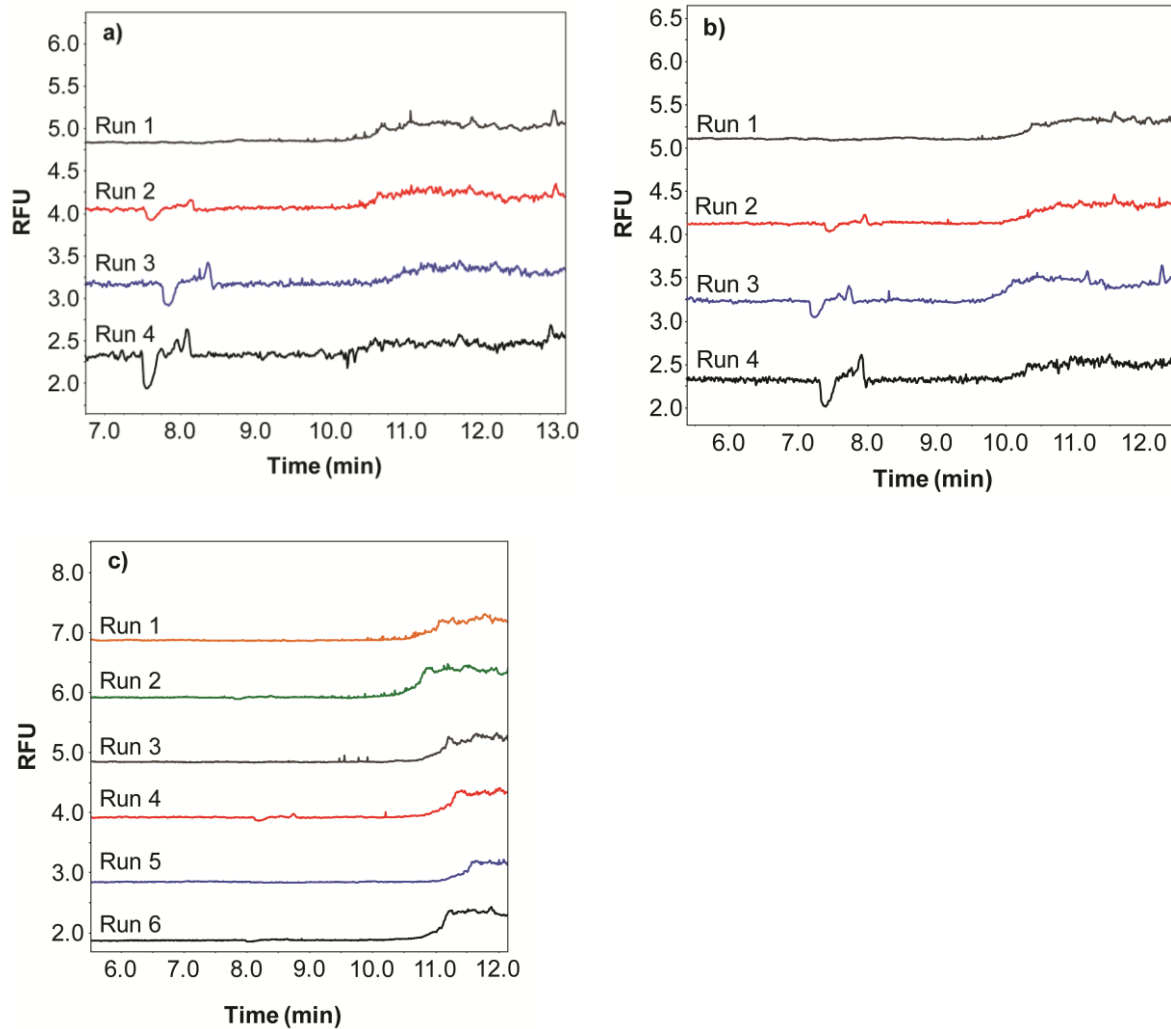


Figure 3.12 Impact of run buffer usage on baseline noise in the analysis of serum samples. (a) Single run buffer vial without rinsing in between runs; (b) Single run buffer vial with rinsing in between every run; (c) Multiple run buffer vials replaced every other run without rinsing in between.

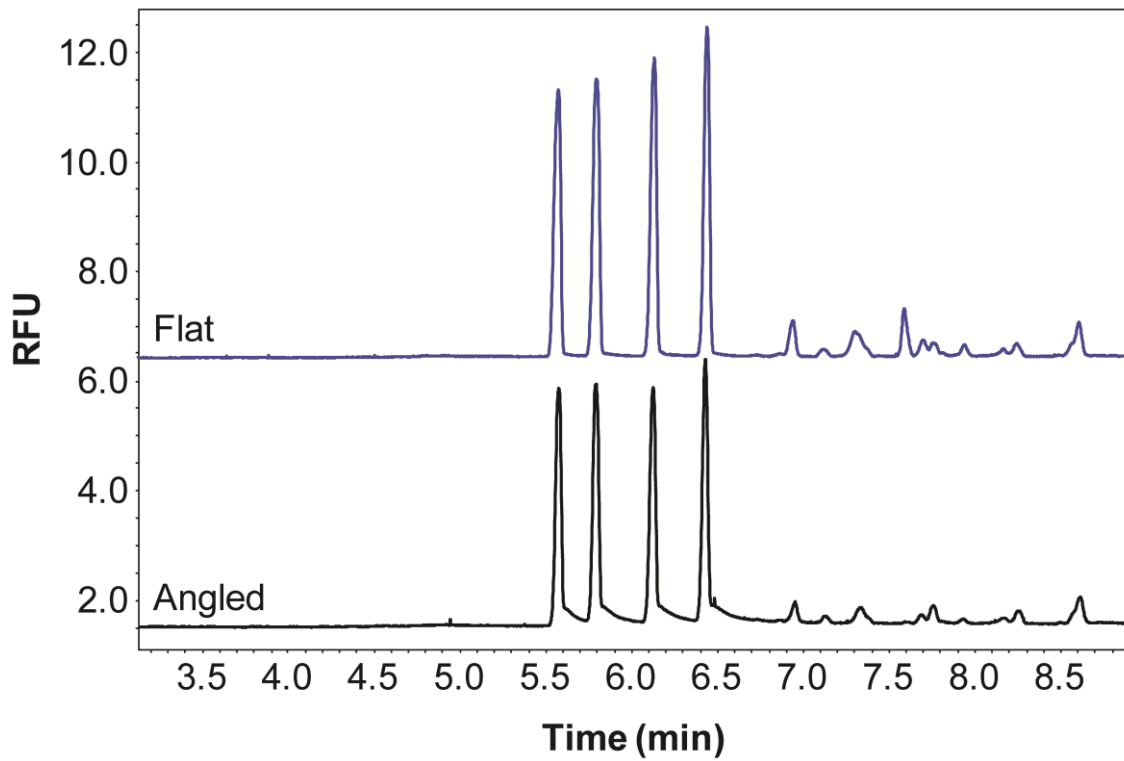


Figure 3.13 The effect of the capillary inlet geometry on the quality of the separation.

3.4 Conclusions

A capillary electrophoresis separation method was developed for the determination of MAs. A run buffer containing 15 mM pH 9.25 borate, 10 mM SBEC, and 25% DMSO, and a separation voltage of 28 kV (430 V/cm) were determined to be optimal run parameters. Baseline resolution was achieved between NDA-derivatized SDMA, ADMA, MMA, PA, and arginine in ~15 min. Detection limits for those analytes were ~5 nM using this CE-LIF method. With a highly efficient separation developed, this method could now be applied to the analysis of more interesting biological samples since the peak capacity is high enough to resolve MA peaks from other sample components.

3.5 References

- [1] M. Zotti, S. Schiavone, F. Tricarico, M. Colaianna, O. D'Apolito, G. Paglia, G. Corso, L. Trabace, Determination of dimethylarginine levels in rats using HILIC-MS/MS: An in vivo microdialysis study, *J. Sep. Sci.*, 31 (2008) 2511-2515.
- [2] K. Vishwanathan, R.L. Tackett, J.T. Stewart, M.G. Bartlett, Determination of arginine and methylated arginines in human plasma by liquid chromatography-tandem mass spectrometry, *J. Chromatogr. B*, 748 (2000) 157-166.
- [3] J. Martens-Lobenhoffer, S.M. Bode-Boger, Fast and efficient determination of arginine, symmetric dimethylarginine, and asymmetric dimethylarginine in biological fluids by hydrophilic-interaction liquid chromatography-electrospray tandem mass spectrometry, *Clin. Chem.*, 52 (2006) 488-493.
- [4] C. Desiderio, D.V. Rossetti, I. Messina, B. Giardina, M. Castagnola, Analysis of arginine and methylated metabolites in human plasma by field amplified sample injection capillary electrophoresis tandem mass spectrometry, *Electrophoresis*, 31 (2010) 1894-1902.
- [5] A. Zinellu, S. Sotgia, B. Scanu, M. Formato, L. Deiana, C. Carru, Assessment of protein-incorporated arginine methylation in biological specimens by CZE UV-detection, *Electrophoresis*, 28 (2007) 4452-4458.
- [6] G. Trapp, K. Sydow, M.T. Dulay, T. Chou, J.P. Cooke, R.N. Zare, Capillary electrophoretic and micellar electrokinetic separations of asymmetric dimethyl-L-arginine and structurally related amino acids: Quantitation in human plasma, *J. Sep. Sci.*, 27 (2004) 1483-1490.
- [7] E. Causse, N. Siri, J.F. Arnal, C. Bayle, P. Malatray, P. Valdiguie, R. Salvayre, F. Couderc, Determination of asymmetrical dimethylarginine by capillary electrophoresis-laser-induced fluorescence, *J. Chromatogr., B: Biomed. Sci. Appl.*, 741 (2000) 77-83.

- [8] K.B. Male, J.H. Luong, Derivatization, stabilization and detection of biogenic amines by cyclodextrin-modified capillary electrophoresis-laser-induced fluorescence detection, *J. Chromatogr. A*, 926 (2001) 309-317.
- [9] V. Zia, R.A. Rajewski, V.J. Stella, Effect of cyclodextrin charge on complexation of neutral and charged substrates: comparison of sulfobutyl ether- β -cyclodextrin to hydroxypropyl β -cyclodextrin, *Pharm. Res.*, 18 (2001) 667-673.

Chapter Four

Development of a Heat-Assisted Extraction Sample Preparation Method for the Determination of Methylarginines in Serum

4.1 Introduction

As stated in previous chapters, methylarginines (MAs) inhibit nitric oxide synthase and compete with the enzyme substrate arginine for cellular uptake. For these reasons, elevated concentrations of MAs *in vivo* diminish endogenous production of nitric oxide (NO). A reduced bioavailability of NO has been associated with various pathological conditions, including the development of cardiovascular diseases (CVDs) [1, 2]. Not surprisingly, elevated concentrations of MAs have been found in the blood of patients suffering from a number of CVDs including various forms of heart disease [3-9] and stroke [10, 11]. Because of the effect that MAs have on NO production and the onset of CVD, a rapid and inexpensive method to measure their concentrations in blood as a means of diagnosing CVD would be highly valuable.

Biological matrices, such as blood serum, often prove to be major obstacles when developing analytical methods because of their extreme complexity. Matrix effects can substantially diminish a measured signal for a variety of reasons, including incompatible pH or solvent composition [12]. This reduction in sensitivity could make the detection of low abundance endogenous compounds, such as MAs, difficult. To circumvent these issues, sample preparation steps must be integrated into the analytical method to isolate the small molecules of interest in a solution that is compatible with the analysis technique [13]. Often, a necessary first step is to remove macromolecules (*e.g.* proteins) from the sample so they do not interfere with the analysis [14]. Conventional protein precipitation methods include the addition of an organic solvent to the sample or altering the pH of the sample. A subsequent centrifugation step then effectively isolates small molecules in the supernatant. Following this preparation, the analytes of interest are no longer in a macromolecule-rich environment; however, they are still in a potentially problematic matrix. The sample solution is now diluted and either contains an organic

solvent or is at an extreme pH. These factors may present a challenge for subsequent quantitative analysis. Additional sample preparation steps are often undertaken to evaporate the organic solvent or remove interferents using solid-phase extraction (SPE), but all these methods further complicate the analysis, increasing the total analysis time and introducing additional potential sources of error.

Thermal coagulation of serum is an attractive alternative method for removing macromolecules from solution due to the simplicity of the method. Rapidly heating serum provides excess energy into the system which can break the non-covalent forces crucial for maintaining protein tertiary structure. As a gel forms during the heating process, small molecules become entrapped in the pores of the cross-linked protein framework [15]. These molecules can later be removed from the gel by performing a solid-liquid extraction. Heating methods to congeal serum have been reported in the distant past, albeit sparingly, to measure small molecules including urate [16], glucose [17], and creatinine [18]. Limitations to the reported procedures, however, were that the samples still experienced appreciable dilution and required additional heating steps, which increased the time required for preparation.

Previous reports in the literature concerned with measuring MAs from blood samples employed either LC or CE coupled to spectroscopic or mass spectrometric detection [19, 20]. Regardless of analysis technique, SPE has still been the method of choice for sample preparation even though it is time-consuming and can therefore limit sample throughput [21]. The goal of this work was to create a rapid and inexpensive method to extract small molecules from serum into a simple matrix that could be analyzed directly to quantify endogenous MA concentrations by CE-LIF. A heat-assisted extraction method is described here that provides a means of rapidly isolating small molecules in a solvent compatible with the analysis method without requiring

further sample clean-up. This is especially beneficial for fluorescence detection schemes that require analyte derivatization prior to analysis because analytes can be extracted directly into a solution compatible with derivatization. Additionally, the lack of dilution afforded by this method obviates preconcentration and allows samples to be analyzed immediately.

4.2 Materials and Methods

4.2.1 Reagents

Standards of monomethylarginine (MMA), asymmetric dimethylarginine (ADMA), symmetric dimethylarginine (SDMA), and propylarginine (PA) were acquired from Enzo Life Sciences (Farmingdale, NY). Sodium tetraborate and sodium cyanide were purchased from Sigma Aldrich (St. Louis, MO). Naphthalene-2,3-dicarboxaldehyde (NDA) was purchased from Invitrogen (Carlsbad, CA). Sulfobutylether- β -cyclodextrin (SBEC) was acquired from Cydex Pharmaceuticals (Lenexa, KS). HPLC-grade dimethylsulfoxide, acetonitrile, methanol, and ammonium hydroxide were purchased from Fisher Scientific (Pittsburgh, PA). All solutions were made in 18.2 M Ω •cm deionized water (Millipore; Billerica, MA) unless otherwise noted. Pooled serum samples from anonymous donors were obtained from Lawrence Memorial Hospital (Lawrence, KS).

4.2.2 Capillary Electrophoresis

The CE-LIF method employed to separate MAs was described in the previous chapter. A Beckman P/ACE MDQ capillary electrophoresis instrument (Brea, CA) with a 50 μ m i.d. capillary segment (Polymicro Technologies; Phoenix, AZ) 65 cm in length (50 cm to window)

was utilized in this study. Samples were injected hydrodynamically at 1.0 psi for 5.0 s, and separations were carried out at an applied field strength of 430 V/cm. Fluorescent emission (>490 nm) was measured with an external fluorescence detector (Picometrics; Ramonville, France) following excitation with a 445 nm diode laser (CrystaLaser; Reno, NV). Both CE operation and LIF detection were controlled with 32 Karat software (Beckman). The run buffer consisted of 15 mM sodium tetraborate, 10 mM SBEC, and 25% (v/v) DMSO.

Samples analyzed by CE were first derivatized with NDA/CN⁻. NDA was dissolved in 1:1 acetonitrile:water; all other solutions were prepared in deionized water. The derivatization procedure entailed combining equal volumes of sample, 50 mM sodium tetraborate, NDA, and 5 mM NaCN and allowing the mixture to react for 10 min prior to injection. The initial NDA concentration was 1 mM when derivatizing standards and 5 mM when derivatizing serum samples. These NDA concentrations provided the maximal signal while preserving the best signal-to-noise (see 4.3.1). Propylarginine was used as an internal standard for each analysis. Fluorescence signals from both standards and serum samples were normalized to the peak area of PA for quantitation. All standards/samples were measured in triplicate unless otherwise noted.

4.2.3 Heat-Assisted Extraction Procedure

To prepare the serum samples, 100 μ L aliquots of pooled serum were transferred into 2 mL polypropylene microcentrifuge tubes (Fisher Scientific) to which 5 μ L of 10 μ M PA was added. The tubes were immersed in a beaker of boiling water (100 °C) for 1.5 min. During the heating process, the liquid serum quickly congealed to form a solid gel. Once the serum gel was formed, 100 μ L of water was added to each vial and vortexed for ~20 s to dislodge the clot from the bottom of the vial and break it into smaller pieces; however, complete homogenization was

not achieved. Samples were then centrifuged to sediment the aggregated proteins, and the supernatants were decanted into separate tubes for subsequent analysis. The volume recovered following the extraction was slightly greater than the initial volume of water added to the vial. An illustration depicting the overall sample preparation scheme is shown in Figure 4.1a.

4.2.4 Solid-Phase Extraction Procedure

For the SPE procedure, 100 μL aliquots of pooled serum and 5 μL of 10 μM PA were first transferred into microcentrifuge tubes. Proteins were then precipitated by adding 200 μL methanol to each vial. Samples were centrifuged to pellet the precipitated proteins, and the supernatant was decanted. This sample was then subjected to SPE without further pretreatment.

HyperSep Retain CX strong cation exchange (SCX) SPE cartridges (Thermo Scientific; Waltham, MA) were utilized to isolate MAs present in the serum samples. SPE was performed based on a modified procedure from the manufacturer. Our procedure included an initial wash step to desorb an interfering compound that was found to leach out of the stationary phase. This was performed by first hydrating the SPE resin with 5% NH_4OH in 1:1 methanol:water followed by equilibration with 1:1 methanol:water. After binding and rinsing the serum supernatant, analytes were eluted in 1 mL of 10% NH_4OH in 1:1 methanol:water. Samples were evaporated to dryness using a Savant SpeedVac SC110 centrifugal evaporator (Thermo Scientific) and resuspended in 100 μL of water. A schematic illustrating the steps required for SPE is shown in Figure 4.1b.

4.3 Results and Discussion

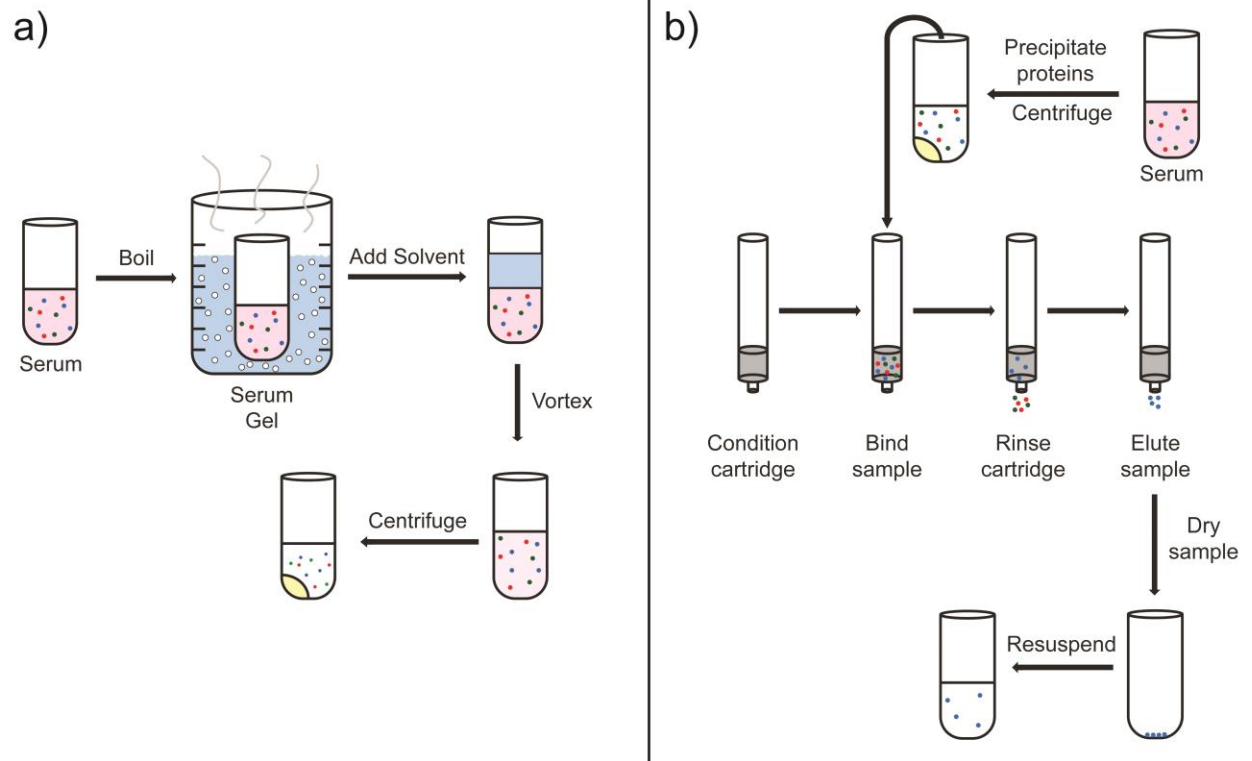


Figure 4.1 Schematic of the (a) heat-assisted extraction and (b) solid phase extraction sample preparation methods used to extract MAs from serum.

4.3.1 NDA Derivatization

An important factor to consider in the analysis of blood-derived samples is the amount of derivatization reagents used to label the analytes in the sample. If NDA/CN⁻ are limiting reagents, the sensitivity of the analysis will be diminished since not all analytes will have been tagged. To avoid this scenario and improve the sensitivity of the method, control experiments were performed to determine the amount of NDA and CN⁻ needed to completely label MAs and also whether limiting amounts of NDA/CN⁻ would affect quantitation.

Standards of 500 nM MAs were derivatized to determine the optimal amount of NDA/CN⁻ required to completely derivatize the analytes. The NDA:CN⁻ ratio was fixed at 1:5 for the experiment based on the optimization results described in Chapter 3. It was found that the absolute fluorescence response was dependent upon the concentrations of reagents used for derivatization. The data in Figure 4.2 indicate that a maximum signal was obtained at 1 mM NDA and moving to higher NDA concentrations provided no additional benefit. However, following normalization to the PA peak, all responses were identical. This indicates that even if NDA was a limiting reagent, quantitation should not suffer since the relative responses for each analyte were the same. The same data is shown in Table 4.1.

Although it was found that 1 mM and 5 mM NDA produced similar peak areas for the MAs, a discrepancy was observed between the two electropherograms. As can be seen in Figure 4.3, the 1 mM trace had lower noise than the 5 mM trace. This observation is interesting because it demonstrates that a high excess of derivatization reagents in the sample mixture can produce deleterious effects on the separation. NDA and CN⁻ appear to react with each other at high concentrations to form a weakly fluorescent product as evidenced by a stair-step-like increase in the baseline. This step coincides with a substantial increase in baseline noise and persists

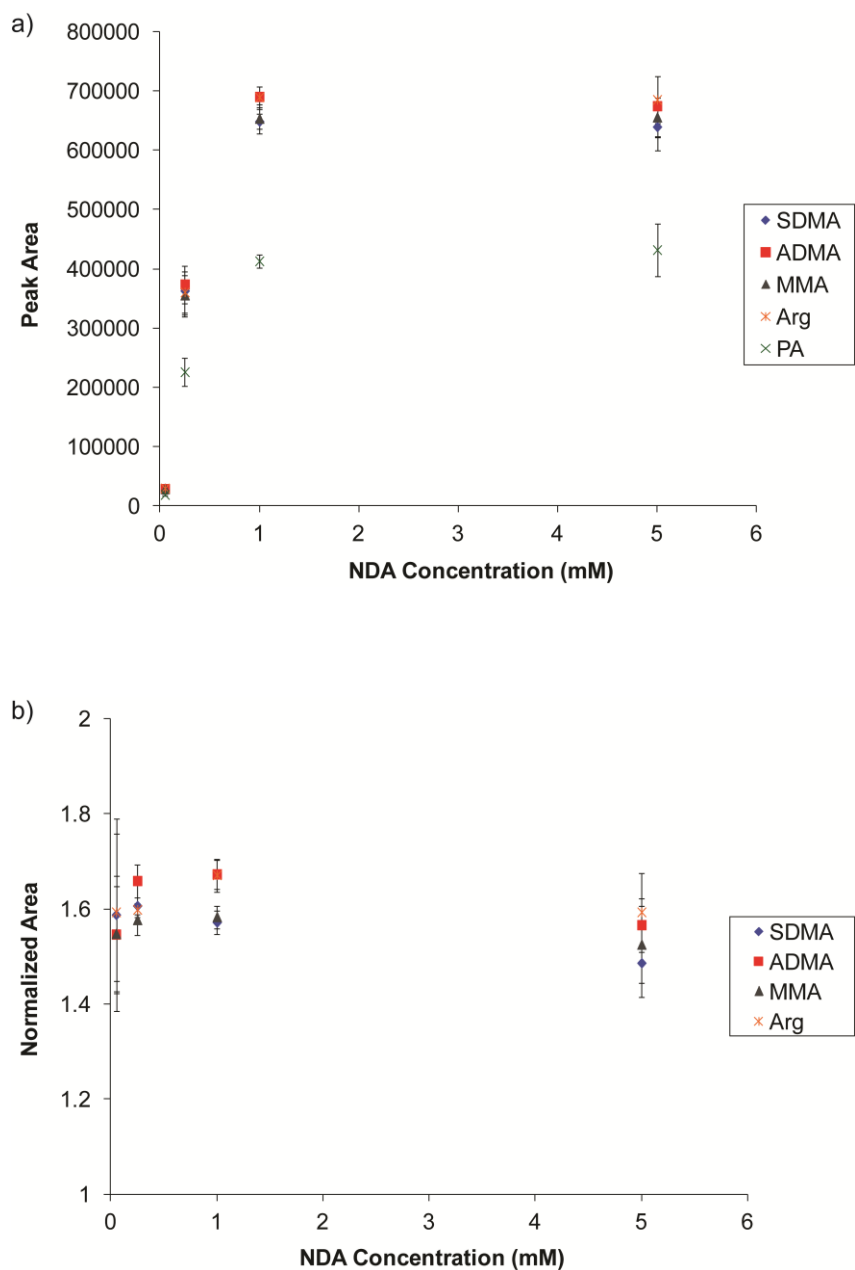


Figure 4.2 Effect of NDA concentration on the fluorescent response of 500 nM MAs/PA. The NDA:CN⁻ ratio was held constant at 1:5. Raw peak areas (left) and areas normalized to PA (right) are shown. Separation buffer contained 15 mM borate, 10 mM SBEC, and 25% DMSO.

Table 4.1. Tabular effect of NDA/CN⁻ concentration on fluorescence response. The NDA:CN⁻ ratio was 1:5.

Fold Excess NDA	SDMA % Response	ADMA % Response	MMA % Response	PA % Response	Arg % Response
20	4.5	4.2	4.3	4.3	4.3
100	57	55	54	52	53
400	101	102	100	96	101
2000	100	100	100	100	100

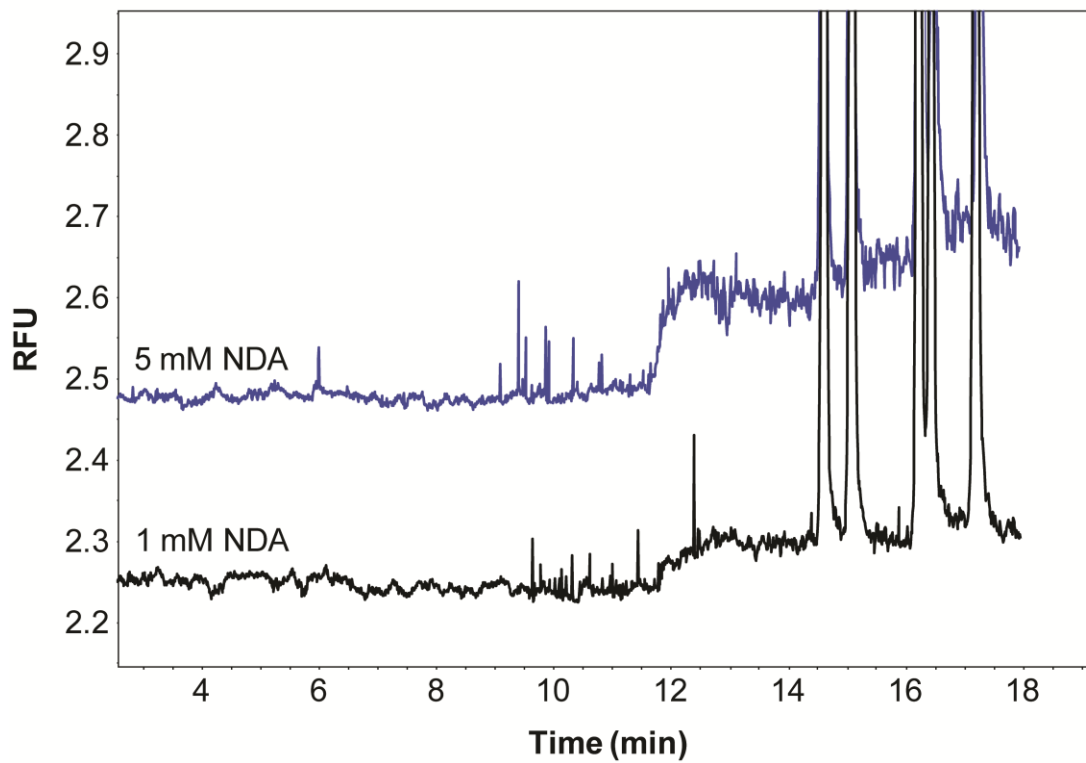


Figure 4.3 Effect of derivatization reagent concentration on chemical noise in the separation.

The NDA:CN⁻ ratio was preserved at 1:5.

throughout the remainder of the separation. While it is possible that a labeling of an impurity in the derivatization mixture could be the cause of this observed phenomenon, it is more likely that the gross excess amounts of NDA and CN^- are forming a side-product and migrating as a very broad, relatively short peak. It is unlikely that the step was from a void peak because that appears to migrate earlier in the separation (Figure 3.12a). Regardless of the source of this noise, it would be most prudent to prevent this noise entirely to enhance precision during peak integration. Therefore, a NDA concentration of 1 mM was selected for the analysis of standards because it provided the maximal response while preserving the best signal-to-noise

In the analysis of serum-derived samples, a diminished response was observed in serum samples derivatized with 1 mM NDA. Increasing the NDA concentration to 5 mM provided more intense peaks without increasing noise. No additional improvements in signal were observed at higher NDA concentrations, so 5 mM was chosen for future experiments analyzing serum. Additionally, the 1:5 ratio of NDA: CN^- optimal for derivatizing standards was no longer ideal for the analysis of serum because of the presence of additional components in the sample. The electropherograms in Figure 4.4 illustrate how a rising baseline was observed at a high NDA: CN^- ratio. This presented a challenge for quantitation because of increased imprecision due to the unstable baseline. However, at lower NDA: CN^- ratios, this phenomenon was no longer observed. Therefore, a 1:1 ratio of NDA: CN^- was selected to minimize chemical noise and allow more precise quantitation.

4.3.2 Capillary Electrophoresis Characterization

Calibration curves were constructed for each analyte of interest from aqueous MA standards. The lines of best fit are shown in Figure 4.5 and the equations are reported in the table

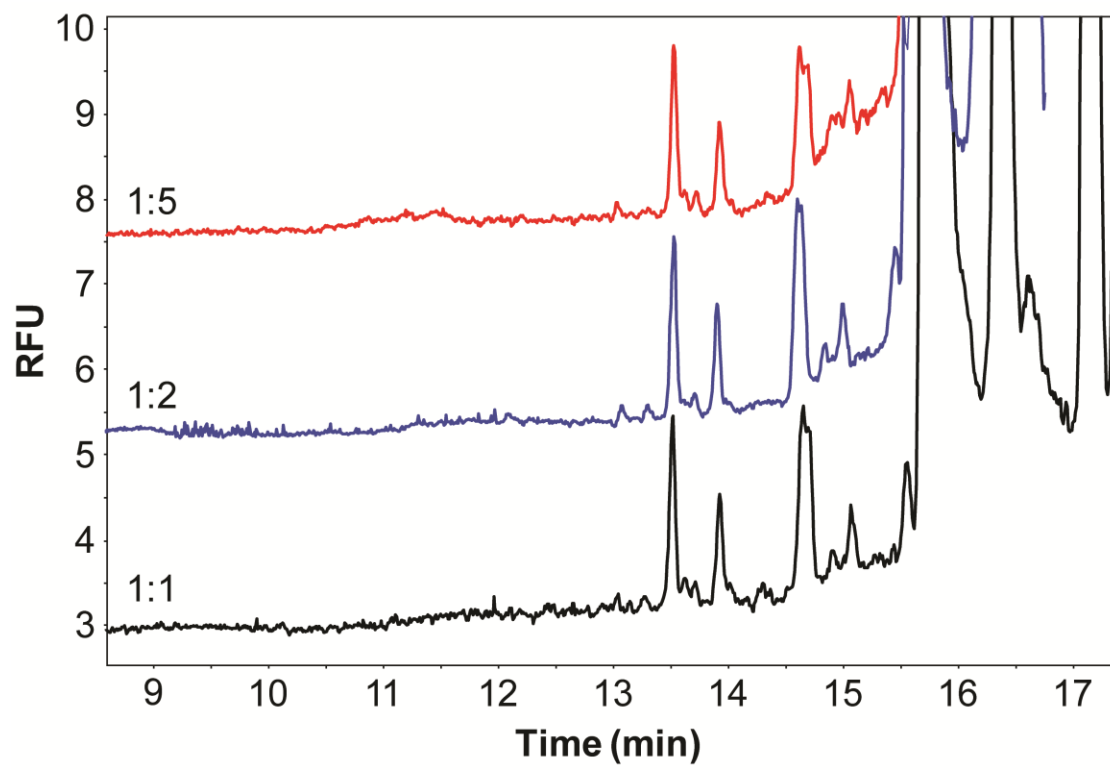


Figure 4.4 Effect of NDA:CN⁻ ratio on the CE separation of serum samples. The NDA concentration for each run was 5 mM.

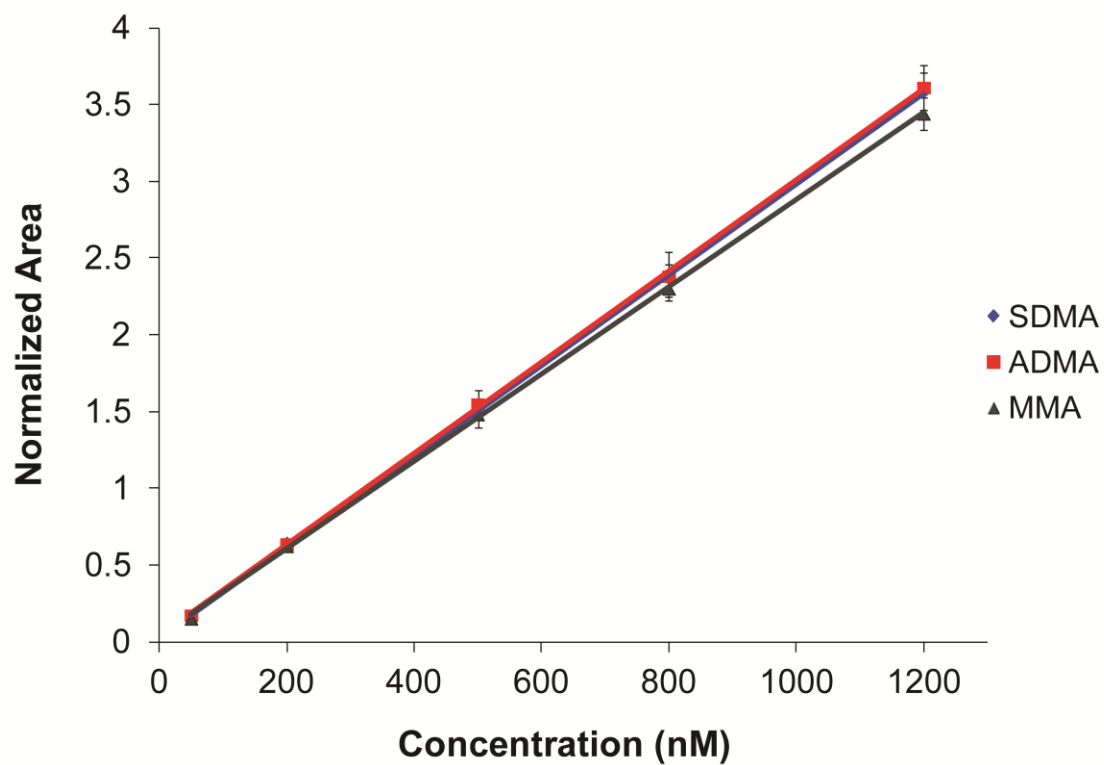
below. The separation parameters for each analyte of interest are shown in Table 4.2. The precision with regards to peak area was quite high with this method. Additionally, the calibration curve showed strong linearity demonstrating the good analytical merits of this method.

4.3.3 Solid-Phase Extraction Characterization

The SPE recoveries for the compounds of interest were determined prior to the analysis of serum samples. Aqueous standards were first combined with methanol and then underwent SPE (n = 3 cartridges for each concentration). The lines of best fit are displayed in Figure 4.6, while the line equations are shown in the adjoining table. The separation parameters from the SPE calibration curve for each analyte of interest are shown in Table 4.3 along with the SPE recoveries from the cartridges.

Similar recoveries of ~90% were observed for standards of SDMA, ADMA, and MMA; however, PA exhibited a much lower recovery (52%) than did the MAs (Table 4.3). Additionally, the imprecision in recovery between cartridges was high and could prove quite detrimental to the analysis. To account for the discrepancies in recovery and inter-cartridge variability, calibration standards were subjected to the SPE procedure to generate a second calibration curve. This curve helped to ensure accurate quantitation for serum samples that underwent SPE. While the recoveries of the standards were reasonably high for the MAs, the linearity and precision of the method were poor. The predominant reason for this originated from high inter-cartridge variability, which increased the imprecision of the method.

Determining the SPE recoveries for each MA was not as trivial as expected. During initial experiments, the recoveries were found to be ~150% relative to the non-extracted standards. The results indicated that matter was somehow created during sample preparation



Analyte	Slope (μM^{-1})	Y-Intercept
SDMA	0.00296	0.0221
ADMA	0.00297	0.0520
MMA	0.00284	0.0352

Figure 4.5 Calibration curve used for determining MA concentrations from the heated serum samples.

Table 4.2 Validation parameters from the optimized CE-LIF method.

Compound	R² *	%RSD **
SDMA	0.9997	4.5
ADMA	0.9988	4.9
MMA	0.9998	2.6
PA	-	-

*Over a concentration range between 50 and 1200 nM.

**Based on replicate peak area measurements (n=3) from each calibration standard (n=5 concentrations).

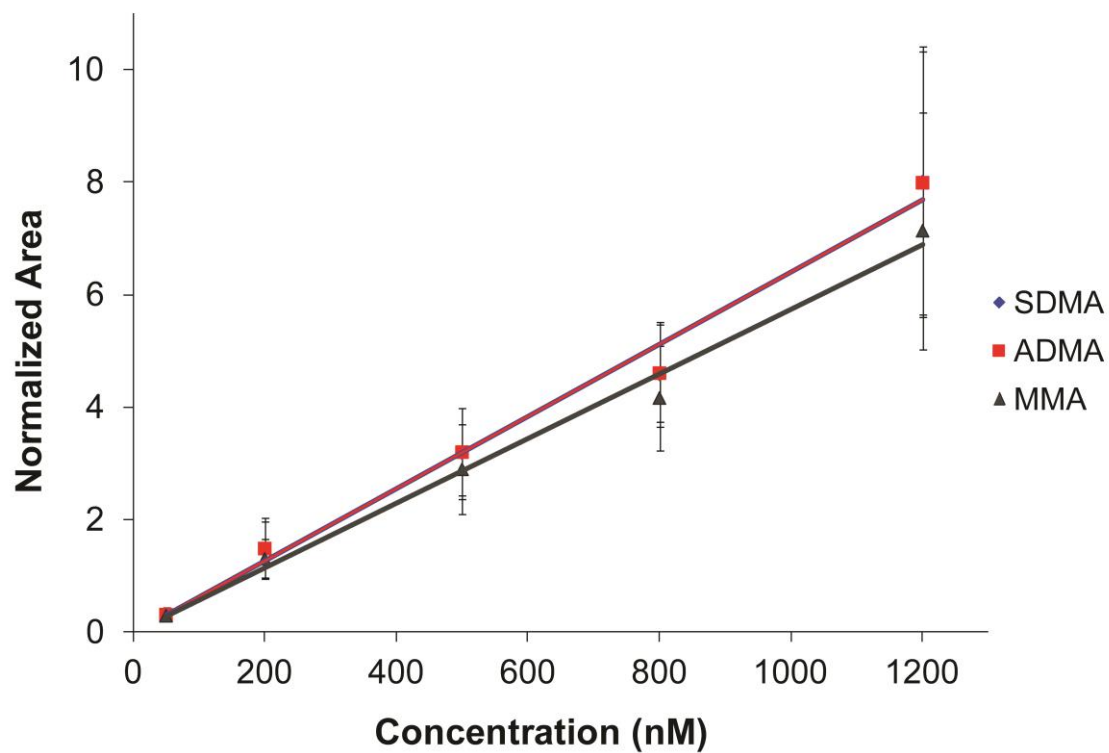


Figure 4.6 Calibration curve used for determining MA concentrations from samples that underwent SPE.

Table 4.3 Analytical parameters of standards prepared by SPE (n=3 cartridges). Recoveries were determined by dividing the response from the SPE standards by the responses from non-extracted standards of the same concentration.

Compound	Recovery (%)	R²	%RSD
SDMA	90 ± 36	0.9881	28
ADMA	91 ± 40	0.9887	30
MMA	89 ± 29	0.9905	27
PA	52 ± 26	-	-

which obviously does not make physical sense. Therefore, a series of controls were prepared to determine the source of this discrepancy. Aqueous standards were prepared without any further sample preparation (unextracted); following the standard SPE protocol (SPE); evaporating aqueous standards to dryness and resuspending in the original volume of water (heat control); and adding 1 mL elution solvent (10% NH_4OH in 1:1 methanol:water) to the aqueous standards, evaporating those to dryness, and reconstituting them in the initial volume of the aqueous standards (elution control).

Following preparation, the samples were analyzed by CE-LIF to determine the responses. The results demonstrated that the unextracted standards had substantially lower responses than not only samples that underwent SPE (which was consistent with previous observations) but also the other controls (Figure 4.7). Unexpectedly, simply evaporating the water from the standards and resuspending the dried analytes in the initial volume resulted in larger measured signals. It is unclear how removing and reconstituting the analytes would cause a change in peak area since the concentrations should have remained constant. Heat-induced sample degradation emanating from the evaporation step would have resulted in lower recoveries, not higher ones. This strange discrepancy was even further enhanced when standards were mixed with the elution solution. The elution control produced larger MA peaks than any other sample even though all resuspended analytes should have been present at the same concentrations. CE stacking effects from residual salts should not explain this phenomenon since increases were also observed from the salt-less heat control samples. The combination of heating off the solvent along with any residual ions left from the elution solvent somehow increased the observed response from the MAs. Therefore, to determine an accurate recovery for the MAs, the responses from the SPE'd

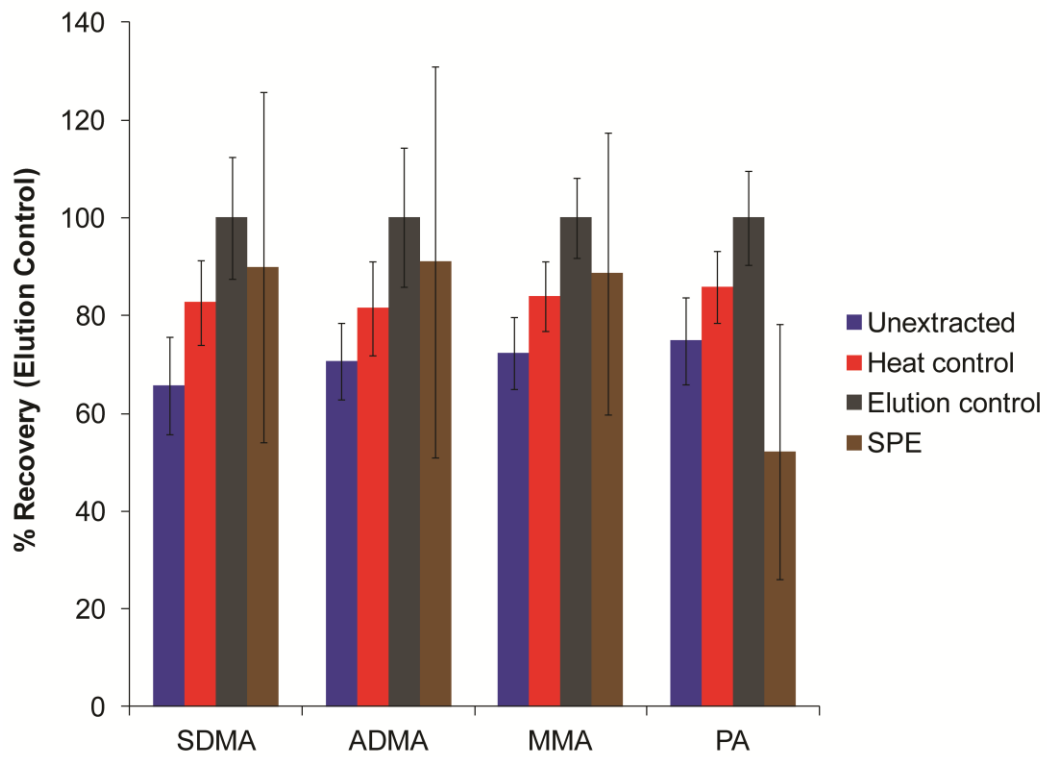


Figure 4.7 MA recoveries from different control samples relative to that of the elution control.

standards were normalized to those from the elution control. Those values were reported in Table 4.3.

4.3.4 Sample Preparation Considerations

Solid-phase extraction is a sample preparation technique that has been widely used for decades. Despite its prevalence, however, SPE suffers from many drawbacks. In the case of common SCX SPE procedures used for MA determination, analytes are isolated in an eluent containing a high percentage of ammonia and methanol [22, 23]. This is problematic when utilizing amine-based derivatization chemistry because ammonia reacts with NDA/CN⁻ and methanol interferes with the derivatization reaction [24]. Both of these factors decreased the sensitivity of the analysis. Additionally, the SPE procedure required desorbing the analytes in an elution volume an order of magnitude higher than the volume of the initial sample to ensure that maximum recovery was obtained. This presents a challenge when analyzing MAs present endogenously at nanomolar concentrations because any appreciable dilution may reduce the concentrations below the detection limits of the method. To circumvent dilution and to remove the ammonia and methanol from the sample, an evaporation step needed to be performed prior to derivatization. This added significantly to the total time of the preparation method.

Heat-induced coagulation of serum is a simple alternative sample preparation method for serum samples providing that the small molecules of interest are stable at high temperatures and can survive the initial heating process. Following heating, the intact molecules can be readily extracted from the gel into an external solvent. By putting forethought into the experimental set-up, no dilution is necessary during the extraction step. Additionally, choosing an appropriate extraction solvent will allow the resulting sample matrix to be compatible with the subsequent

derivatization procedure. This will allow samples to be analyzed directly without requiring the solvent to first be evaporated.

4.3.5 Heat-Assisted Extraction Optimization

The application of extreme heat to a serum sample can cause protein denaturation and subsequent aggregation. When interested in measuring small molecules, maintaining the native conformations of the proteins in the sample is of little concern. However, the stability of the small molecules of interest is crucial for the implementation of this procedure. Therefore, compounds that are liable to heat-induced degradation or oxidation would be poor candidates for this sample preparation procedure. To ensure that MAs are thermally stable, 500 nM MA standards were placed in boiling water for 2 min, and then derivatized and analyzed via CE-LIF. It was determined that the heating procedure did not affect the integrity of the molecules since no loss was observed between the heated and non-heated samples (Figure 4.8). An insignificant increase in analyte recovery was observed in the heated standards, which was most likely caused by slight losses in solvent volume due to evaporation (Figure 4.8a). Normalization of the data demonstrated identical recoveries for heated and non-heated samples which confirmed that MAs were stable throughout the heating process (Figure 4.8b).

The heating time required to generate protein aggregation was also evaluated. It was determined that 30 s was insufficient to induce complete formation of a gel as evidenced by the serum still appearing slightly “runny” and a large broad peak spanning through the electropherogram (Figure 4.9). This peak was most likely comprised of proteins and peptides that were not given sufficient time to become entangled in the protein gel. As such, they were able to leach out into the extraction solvent and complicate the separation. Extending the heating

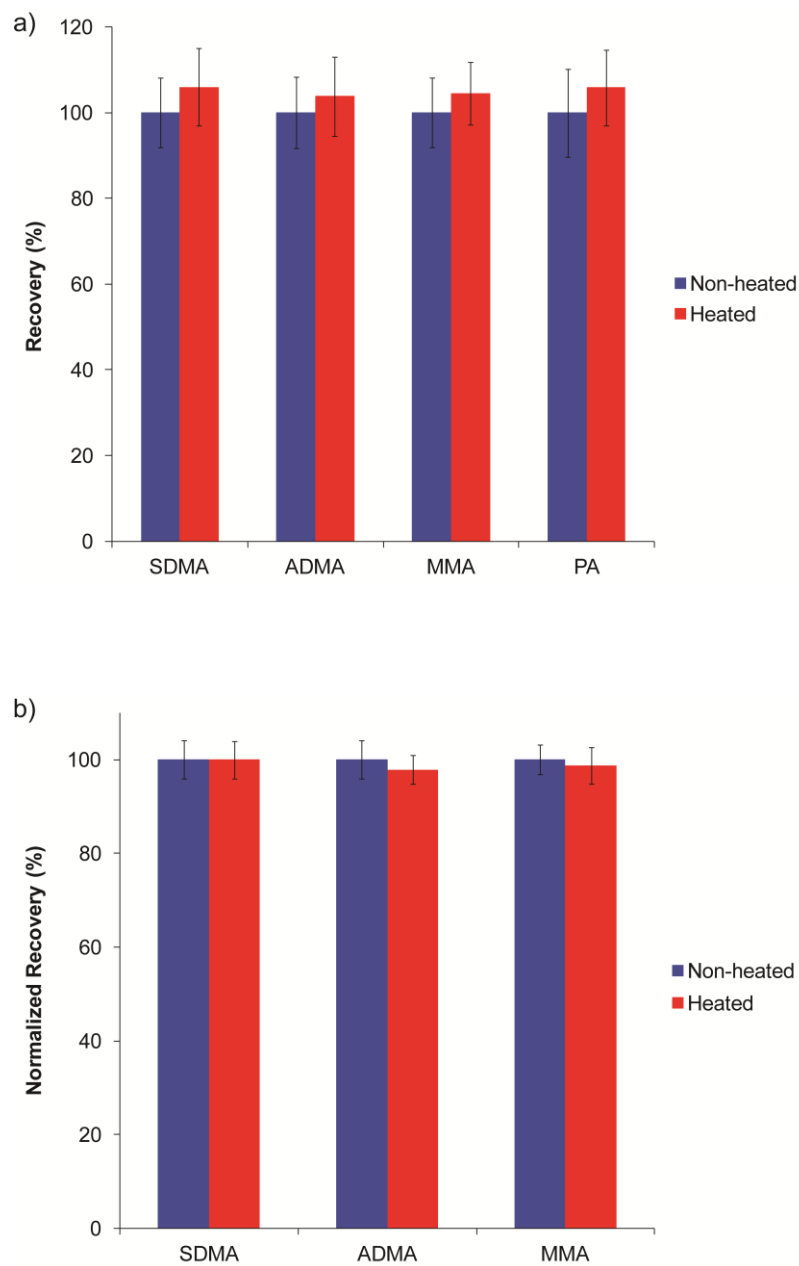


Figure 4.8 Stability of the MAs in extreme heat conditions. 500 nM standards heated for 2 min (n=3) were compared with non-heated standards. Quantitation was performed using CE-LIF. Raw recoveries of the heated and non-heated samples are shown in (a) while the normalized recoveries are compared in (b).

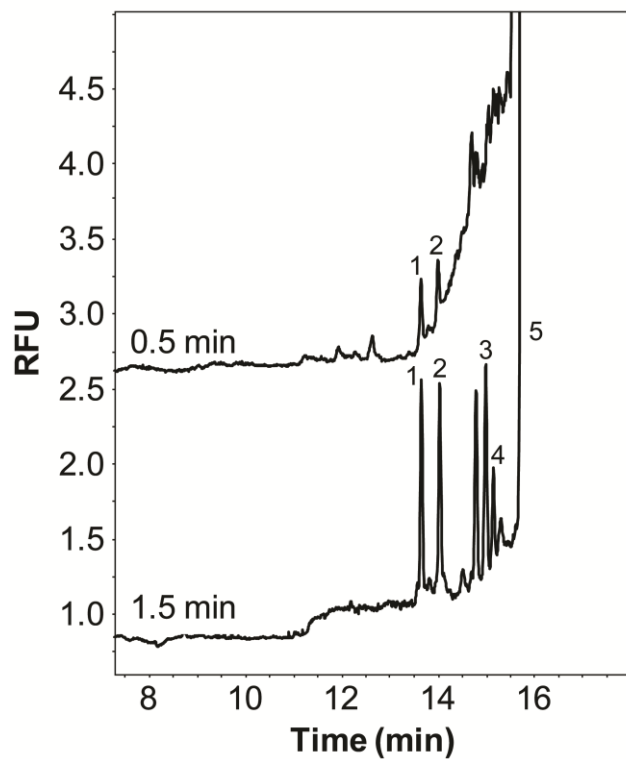


Figure 4.9 Electropherograms demonstrating the impact of heating times on the formation and stability of serum gel. Vials of serum were immersed in boiling water for either 0.5 min (bottom) or 1.5 min (top). Peaks are (1) SDMA, (2) ADMA, (3) MMA, (4) PA, and (5) Arg.

time to 1 min, however, alleviated this problem. There was no difference between samples heated between 1 and 4 min, so 1.5 min was chosen as a middle point for further experiments.

After the serum was heated and congealed, water was added over the gel and briefly vortexed to extricate the coagulum from the bottom of the container. The time the water was incubated with the serum gel (at room temperature) was optimized to maximize the amount of MAs extracted into solution. (Recovery was determined by first normalizing the peak areas of PA in serum samples to those in unextracted standards to determine the fraction recovered. The peak areas of the other MAs from each run were then normalized to the average MA peak areas and multiplied by the recovered fraction of PA to determine their recoveries.) Results from this experiment showed that there were no significant increases in MA recoveries for extractions over a 1 h period and that all MAs were extracted at similar rates (Figure 4.10). Since a steady-state recovery (within error) was reached within 5 min, this duration was used in further experiments to expedite the analysis. It should be noted that a 15 min centrifugation step was performed to sediment the proteins from solution after the incubation period. This step increased the time that the extraction solvent remained in contact with the solid, and was not accounted for in Figure 4.10.

The recovery of MAs from the serum gel ranged between 52 and 58% using the method described above. Because of this, the incorporation of an internal standard was crucial to obtaining accurate results. Since a suitable internal standard was identified (*i.e.* PA), this method was acceptable as is. However, to increase the extraction efficiency, a heated extraction could have been performed to help resolubilize the analytes of interest [17]. Previous methods have reported that complete recovery could be achieved by adding water to the coagulated serum and extracting the mixture at 37 °C for 30–60 min or at room temperature overnight [25-27]. In the

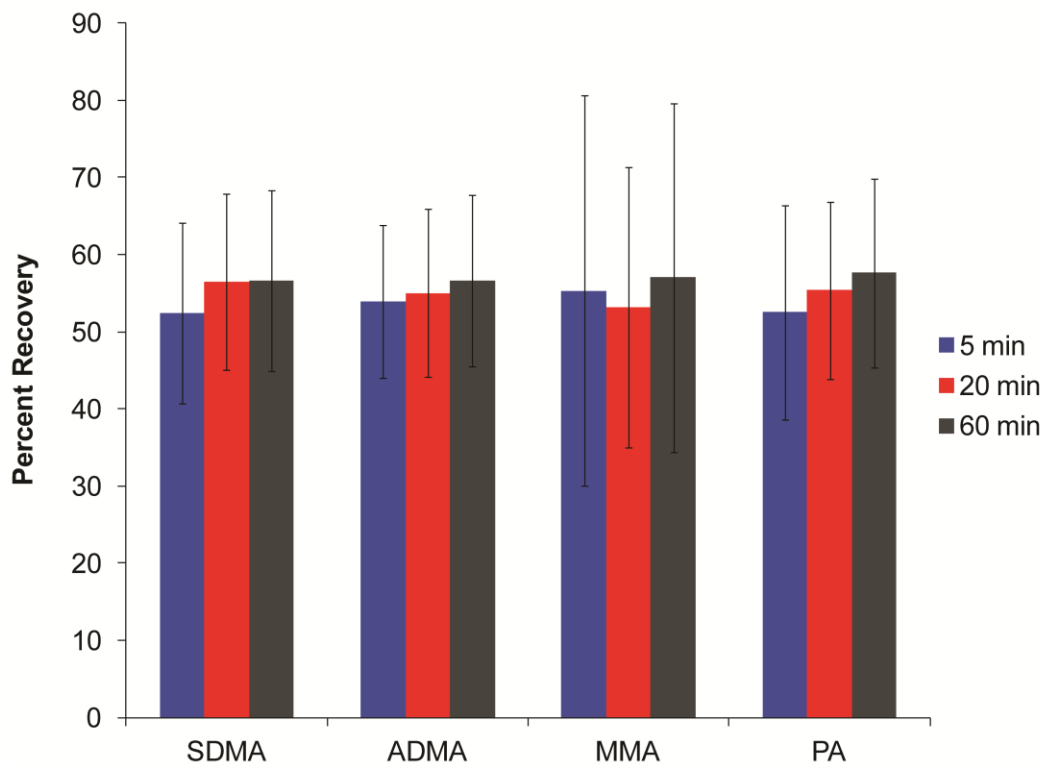


Figure 4.10 Evaluation of extraction times on PA recovery. Congealed serum was incubated with water for the indicated time (n=3 for each point) and then analyzed via CE-LIF.

interest of minimizing the complexity of the analysis and the total analysis time, this was not performed in our method.

In an effort to improve the recovery of MAs from the serum gel without complicating the extraction procedure, an experiment was conducted to determine if an increase in the surface area-to-volume ratio would aid recovery. Serum aliquots of 100 μL , 50 μL , and 25 μL from a single lot were dispensed into separate vials into which 5 μL , 2.5 μL , and 1.25 μL of 10 μM PA was added, respectively (each sample was prepared in triplicate), to hold the ratio of serum to water constant for each sample. Samples were heated for 1.5 min and then extracted into a volume of water identical to the original volume of serum for a no-net-dilution extraction. Following a 5 min incubation period with the extraction solvent and subsequent centrifugation, the supernatants were analyzed by CE-LIF in duplicate. It was determined from this experiment that the original serum volume impacted the recovery of MAs. Figure 4.11 illustrates that the average recovered concentration for each MA species was higher for the smaller volume samples. This can be attributed to larger solvent-accessible surface area. Thinner serum clots better allowed the extraction solvent to penetrate into the gel and resolubilize the analytes trapped within the protein framework. Smaller initial serum volumes (25 μL) enabled recoveries of ~90% as opposed to the ~60% recovery observed with larger serum volumes (100 μL).

An investigation was also performed into whether the blood matrix impacted the heat-prep method. All experiments to this point were performed with serum which is a less complex matrix compared to plasma which contains additional proteins. To determine if a difference in MA quantitation would be observed between the two matrices, whole blood drawn from a single individual was split into two fractions: one aliquot was spun down to plasma, while the other was converted to serum. Each sample underwent heat-assisted extraction followed by CE-LIF

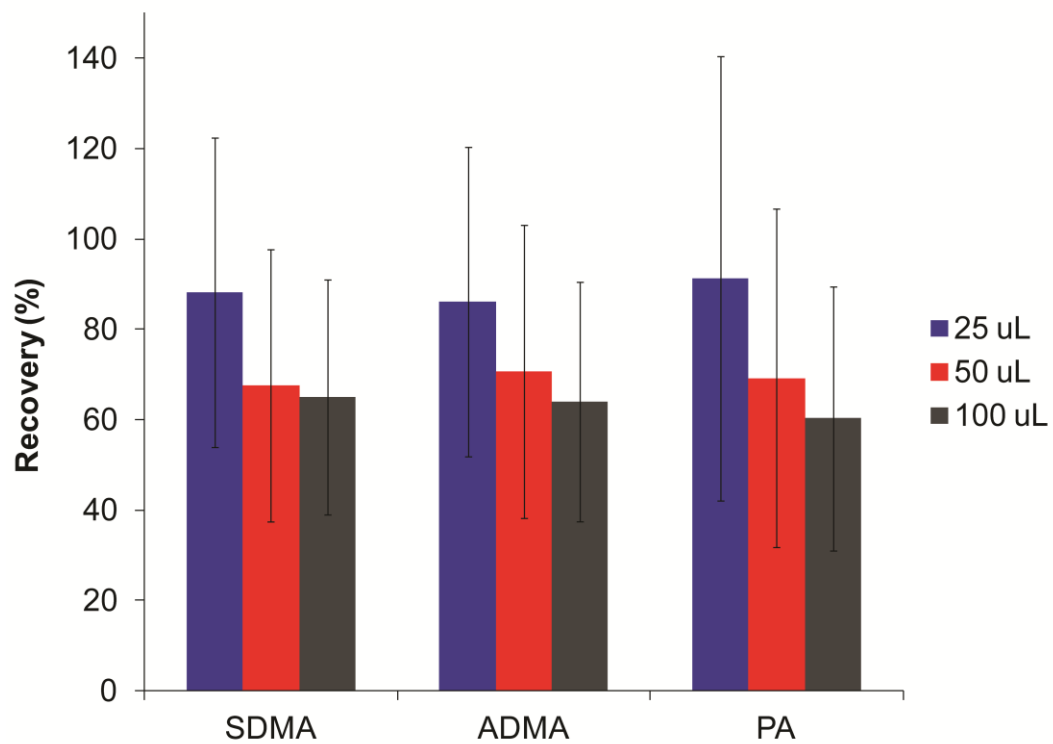


Figure 4.11 Effects of initial serum volume on extraction recoveries of MAs from serum gel.

analysis (each matrix was prepared in triplicate). Table 4.4 lists the concentrations of MAs in each matrix. The results indicated that no significant difference existed between matrices. This finding was expected since the additional proteins from the plasma should have denatured and incorporated into the gel framework without impacting the extraction of small molecules from the gel.

4.3.6 Sample Preparation Method Comparison

Extracted serum samples derived from both the SPE and heating procedures were compared to determine the differences in their pH values and conductivities. The pH values (colorpHast strips, EM Reagents, Cherry Hill, NJ) showed that both samples were slightly basic regardless of the extraction procedure (Table 4.5). The pH from the heated sample matched well with a previously reported value acquired using a thermal coagulation method that attributed the basic pH to a release of CO₂ during the heating process [26]. The conductivity of each sample was also measured. For comparison purposes, the conductivity values from the extracted serum samples were normalized to that of the 50 mM borate used in the NDA derivatization reaction. Table 4.5 shows that serum that underwent the heating method had a conductivity similar to that of borate while the SPE sample was over an order of magnitude less conductive. This result is not surprising because samples bound to the SPE stationary phase should have had all of the residual ions from the serum rinsed to waste before the analytes of interest were desorbed from the resin. In the heating procedure, however, the salts in the serum gel were able to readily redissolve into the extraction solvent. While the conductivities of the heat-prepared samples were substantially higher, they were on par with that of the borate used for derivatization and were not found to hinder the CE analysis.

Table 4.4 Comparison of the effect of blood sample matrix on MA quantitation.

Analyte	Serum (nM)	Plasma (nM)
SDMA	414 ± 41	393 ± 53
ADMA	342 ± 28	354 ± 60
MMA	64 ± 36	57 ± 19

Table 4.5 Comparison of the conductivity and pH of extracted serum samples as compared to the borate used for derivatization.

Sample	Normalized conductivity	pH
50 mM borate	1.0	9.2
Heated serum	1.1	8.4
SPE serum	0.07	7.6

The migration times of the analytes of interest are shown in Table 4.6. Although the more conductive serum-derived samples had slight increases in analyte migration times than those of the standards, the differences were insignificant. Additionally, no loss of resolution was observed between samples and standards. These findings indicate that the sample matrix did not have an appreciable effect on the CE separation.

A substantial savings in both sample preparation time and the cost of analysis was also realized with the heating method compared to SPE. The heating procedure could be performed in ~30 min with the majority of the time allotted for the centrifugation cycle and the time spent waiting for the water bath to come to a boil. This was in stark contrast to the SPE procedure where the time required to prepare the necessary solutions, perform SPE, and then evaporate the samples to dryness was ~4 h. The time difference was even further accentuated when one considers that in the SPE protocol, standards also had to undergo SPE to permit accurate quantitation of unknowns. Additionally, a significant financial savings was obtained by forgoing SPE entirely since the need for cartridges and solvents was obviated. The production of chemical solvent waste generated during SPE was also eliminated by implementing the heating procedure in its place.

4.3.7 Determination of Serum MAs

Following the optimization of the heating procedure, the method was applied to the determination of MAs in serum. A single lot of pooled serum was divided into two fractions to undergo either SPE or heat-assisted extraction. To maintain consistency between sample preparation methods, this study utilized 100 μL of serum per sample since this higher volume was more amenable for SPE. Sample electropherograms from samples prepared by each method

Table 4.6 Migration times of the MAs following sample preparation. Migration times from serum samples were taken from the electropherograms used to produce Table 4.2 (n = 6 for each preparation method), while those from standards came from the non-extracted calibration curve (n = 15).

Analyte	Standards t_m (min)	SPE-prepped t_m (min)	Heat-prepped t_m (min)
SDMA	13.7 ± 0.2	14.0 ± 0.4	14.2 ± 0.3
ADMA	14.1 ± 0.2	14.4 ± 0.5	14.6 ± 0.3
MMA	15.1 ± 0.2	15.5 ± 0.5	15.7 ± 0.3
PA	15.3 ± 0.2	15.6 ± 0.5	15.9 ± 0.3

are shown in Figure 4.12. Concentrations of SDMA, ADMA, and MMA from samples that underwent the heating procedure were quantified using the calibration curve from the non-extracted standards (Figure 4.5). Similarly, the endogenous MA concentrations from samples that were prepared with SPE were determined from the calibration curve constructed from standards subjected to SPE themselves (Figure 4.6). The calculated values from the two methods are reported in Table 4.7. A comparison shows that the mean concentrations were similar in the two sample preparation methods even though the absolute peak areas were higher in SPE-prepped samples than in heat-prepped samples. This discrepancy arose from the differences in recoveries between the two methods. The SPE recoveries for MAs were ~90% (Table 4.3) while the recoveries from heat-prepped samples were only ~55% (Figure 4.10). The calibration curves compensated for this, and following normalization of the peak areas, no significant differences in MA concentrations were determined between the two sample preparation methods. It should also be noted that the precision of the heat-assisted extraction method was better than that from the more conventionally accepted SPE method as evidenced by lower relative standard deviations for each analyte of interest.

The MA concentrations determined in this experiment are within the range of those reported in the literature. Average endogenous concentrations compiled from a number of reports found that SDMA, ADMA, and MMA were present at 480 nM [3, 4, 6, 11, 23, 28-33], 605 nM [3-6, 8, 10, 11, 23, 28-36], and 142 nM [3, 8, 31], respectively, while the concentration ranges were 370–750 nM, 340–1030 nM, and 70–195 nM for each analyte, respectively. The large concentration ranges were most likely due to a combination of the different clinical populations used in each study and inherent patient-to-patient variability. The MA concentrations found in

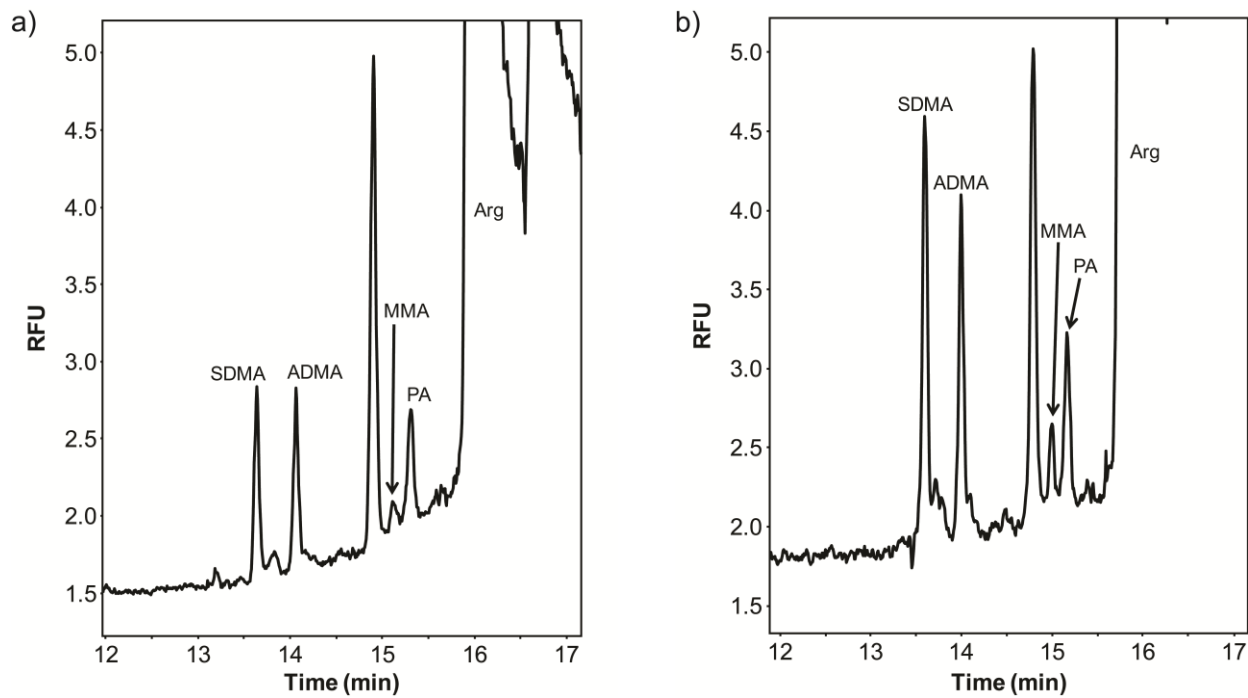


Figure 4.12 Representative electropherograms of serum samples prepared by the (a) SPE or (b) heating procedures.

Table 4.7 Endogenous serum concentrations of MAs. MAs from a single lot of pooled serum were isolated by either the heating or SPE sample preparation methods (n = 3 samples for each method). Each sample was analyzed by CE-LIF in duplicate.

Compound	Heat (nM)	SPE (nM)
SDMA	436 ± 46	385 ± 64
ADMA	374 ± 49	307 ± 42
MMA	53 ± 16	71 ± 43

this study were all below the average inter-study values, but still fell mostly within the reported ranges.

4.4 Conclusions

Matrix effects can have a substantial impact on the quality of an analytical measurement. To diminish their influence, sample preparation steps must be undertaken, which can be major obstacles to sample throughput. As a result, this study was conducted to develop a rapid and low-cost method to extract small molecules from serum samples by means of a heat-assisted extraction procedure. This procedure was found to effectively isolate small molecules in an aqueous solution compatible with the derivatization reaction with no-net-dilution. This allowed low abundance biomarkers of CVD to be extracted much more quickly and inexpensively than with a commonly employed SPE method. Serum concentrations of MAs determined by the two methods were in good agreement with each other and with previously reported values in the literature after analysis by CE-LIF.

4.5 References

- [1] P. Vallance, J. Leiper, Cardiovascular Biology of the Asymmetric Dimethylarginine: Dimethylarginine Dimethylaminohydrolase Pathway, *Arterioscler. Thromb. Vasc. Biol.*, 24 (2004) 1023-1030.
- [2] E. Culotta, D.E. Koshland, Jr., NO news is good news, *Science*, 258 (1992) 1862-1865.
- [3] Z. Wang, W.H.W. Tang, L. Cho, D.M. Brennan, S.L. Hazen, Targeted Metabolomic Evaluation of Arginine Methylation and Cardiovascular Risks: potential mechanisms beyond nitric oxide synthase inhibition, *Arterioscler. Thromb. Vasc. Biol.*, 29 (2009) 1383-1391.
- [4] Z. Ajtay, F. Scalera, A. Cziraki, I. Horvath, L. Papp, E. Sulyok, C. Szabo, J. Martens-Lobenhoffer, F. Awiszus, S.M. Bode-Boeger, Stent placement in patients with coronary heart disease decreases plasma levels of the endogenous nitric oxide synthase inhibitor ADMA, *Int. J. Mol. Med.*, 23 (2009) 651-657.
- [5] T.K. Krempl, R. Maas, K. Sydow, T. Meinertz, R.H. Boeger, J. Kaehler, Elevation of asymmetric dimethylarginine in patients with unstable angina and recurrent cardiovascular events, *Eur. Heart J.*, 26 (2005) 1846-1851.
- [6] M. Zeller, C. Korandji, J.-C. Guillard, P. Sicard, C. Vergely, L. Lorgis, J.-C. Beer, L. Duvillard, A.-C. Lagrost, D. Moreau, P. Gambert, Y. Cottin, L. Rochette, Impact of Asymmetric Dimethylarginine on Mortality After Acute Myocardial Infarction, *Arterioscler. Thromb. Vasc. Biol.*, 28 (2008) 954-960.
- [7] H. Miyazaki, H. Matsuoka, J.P. Cooke, M. Usui, S. Ueda, S. Okuda, T. Imaizumi, Endogenous nitric oxide synthase inhibitor: a novel marker of atherosclerosis, *Circulation*, 99 (1999) 1141-1146.

- [8] J.A. Chirinos, R. David, J.A. Bralley, H. Zea-Diaz, E. Munoz-Atahualpa, F. Corrales-Medina, C. Cuba-Bustinza, J. Chirinos-Pacheco, J. Medina-Lezama, Endogenous Nitric Oxide Synthase Inhibitors, Arterial Hemodynamics, and Subclinical Vascular Disease, Hypertension, 52 (2008) 1051-1059.
- [9] C. Dueckelmann, F. Mittermayer, D.G. Haider, J. Altenberger, J. Eichinger, M. Wolzt, Asymmetric dimethylarginine enhances cardiovascular risk prediction in patients with chronic heart failure, Arterioscler. Thromb. Vasc. Biol., 27 (2007) 2037-2042.
- [10] J.H. Yoo, S.C. Lee, Elevated levels of plasma homocyst(e)ine and asymmetric dimethylarginine in elderly patients with stroke, Atherosclerosis, 158 (2001) 425-430.
- [11] T. Leong, D. Zylberstein, I. Graham, L. Lissner, D. Ward, J. Fogarty, C. Bengtsson, C. Bjorkelund, D. Thelle, Asymmetric Dimethylarginine Independently Predicts Fatal and Nonfatal Myocardial Infarction and Stroke in Women, Arterioscler. Thromb. Vasc. Biol., 28 (2008) 961-967.
- [12] Z.K. Shihabi, Effects of sample matrix on capillary electrophoretic analysis, Handbook of Capillary Electrophoresis (2nd Edition), CRC, 1997, pp. 454-477.
- [13] M.L. Chiu, W. Lawi, S.T. Snyder, P.K. Wong, J.C. Liao, V. Gau, Matrix effects-a challenge toward automation of molecular analysis, JALA, 15 (2010) 233-242.
- [14] S. Tulipani, R. Llorach, M. Urpi-Sarda, C. Andres-Lacueva, Comparative Analysis of Sample Preparation Methods To Handle the Complexity of the Blood Fluid Metabolome: When Less Is More, Anal. Chem., (2012).
- [15] C. Huggins, A.S. Cleveland, E.V. Jensen, Thermal coagulation of serum in diagnosis, J. Am. Med. Assoc., 143 (1950) 11-15.

- [16] M. London, J.H. Marymont, Jr., Analyses on heat-coagulated blood and serum. I. Determination of uric acid, *Clin. Chem.*, 10 (1964) 298-305.
- [17] J.H. Marymont, Jr., M. London, Analysis on heat-coagulated blood and serum. V. Determination of glucose, *Clin. Chem.*, 10 (1964) 942-949.
- [18] M. London, I.A. Freiburger, J.H. Marymont, Jr., Analyses on heat-coagulated blood and serum. Determination of creatinine, *Clin. Chem.*, 13 (1967) 970-975.
- [19] E. Schwedhelm, Quantification of ADMA: analytical approaches, *Vasc. Med.*, 10 Suppl 1 (2005) S89-95.
- [20] J. Martens-Lobenhoffer, S.M. Bode-Boeger, Chromatographic-mass spectrometric methods for the quantification of L-arginine and its methylated metabolites in biological fluids, *J. Chromatogr., B: Anal. Technol. Biomed. Life Sci.*, 851 (2007) 30-41.
- [21] T. Teerlink, HPLC analysis of ADMA and other methylated L-arginine analogs in biological fluids, *J. Chromatogr., B: Anal. Technol. Biomed. Life Sci.*, 851 (2007) 21-29.
- [22] P. Vallance, A. Leone, A. Calver, J. Collier, S. Moncada, Accumulation of an endogenous inhibitor of nitric oxide synthesis in chronic renal failure, *Lancet*, 339 (1992) 572-575.
- [23] T. Teerlink, R.J. Nijveldt, S. de Jong, P.A.M. van Leeuwen, Determination of arginine, asymmetric dimethylarginine, and symmetric dimethylarginine in human plasma and other biological samples by high-performance liquid chromatography, *Anal. Biochem.*, 303 (2002) 131-137.
- [24] B.K. Matuszewski, R.S. Givens, K. Srinivasachar, R.G. Carlson, T. Higuchi, N-substituted 1-cyanobenz[f]isoindole: evaluation of fluorescence efficiencies of a new fluorogenic label for primary amines and amino acids, *Anal. Chem.*, 59 (1987) 1102-1105.

- [25] J.H. Marymont, M. London, Analyses performed with heat-coagulated blood and serum. II. The determination of urea nitrogen, *Am. J. Clin. Pathol.*, 39 (1963) 342-348.
- [26] J.H. Marymont, Jr., M. London, Analysis on heat-coagulated blood and serum. IV. Direct determination of uric acid by ultraviolet absorption, *Clin. Chem.*, 10 (1964) 937-941.
- [27] J. Benotti, S. Pino, H. Gardyna, Separation of protein-bound iodine and nonprotein iodine by serum coagulation, *Clin. Chem.*, 12 (1966) 37-39.
- [28] R.H. Boger, S.M. Bode-Boger, A. Szuba, P.S. Tsao, J.R. Chan, O. Tangphao, T.F. Blaschke, J.P. Cooke, Asymmetric dimethylarginine (ADMA): a novel risk factor for endothelial dysfunction. Its role in hypercholesterolemia, *Circulation*, 98 (1998) 1842-1847.
- [29] P. Valtonen, J. Karppi, K. Nyyssoenen, V.-P. Valkonen, T. Halonen, K. Punnonen, Comparison of HPLC method and commercial ELISA assay for asymmetric dimethylarginine (ADMA) determination in human serum, *J. Chromatogr., B: Anal. Technol. Biomed. Life Sci.*, 828 (2005) 97-102.
- [30] J. Martens-Lobenhoffer, S.M. Bode-Boeger, Fast and efficient determination of arginine, symmetric dimethylarginine, and asymmetric dimethylarginine in biological fluids by hydrophilic-interaction liquid chromatography-electrospray tandem mass spectrometry, *Clin. Chem.*, 52 (2006) 488-493.
- [31] G. Weaving, B.F. Rocks, M.P. Bailey, M.A. Titheradge, Arginine and methylated arginines in human plasma and urine measured by tandem mass spectrometry without the need for chromatography or sample derivatization, *J. Chromatogr., B: Anal. Technol. Biomed. Life Sci.*, 874 (2008) 27-32.
- [32] M. Marra, A.R. Bonfigli, R. Testa, I. Testa, A. Gambini, G. Coppa, High-performance liquid chromatographic assay of asymmetric dimethylarginine, symmetric dimethylarginine,

and arginine in human plasma by derivatization with naphthalene-2,3-dicarboxaldehyde, *Anal. Biochem.*, 318 (2003) 13-17.

[33] E. Schwedhelm, R. Maas, J. Tan-Andresen, F. Schulze, U. Riederer, R.H. Boeger, High-throughput liquid chromatographic-tandem mass spectrometric determination of arginine and dimethylated arginine derivatives in human and mouse plasma, *J. Chromatogr., B: Anal. Technol. Biomed. Life Sci.*, 851 (2007) 211-219.

[34] R. Schnabel, S. Blankenberg, E. Lubos, K.J. Lackner, H.J. Rupprecht, C. Espinola-Klein, N. Jachmann, F. Post, D. Peetz, C. Bickel, F. Cambien, L. Tiret, T. Muenzel, Asymmetric Dimethylarginine and the Risk of Cardiovascular Events and Death in Patients With Coronary Artery Disease. Results from the AtheroGene Study, *Circ. Res.*, 97 (2005) e53-e59.

[35] G. Trapp, K. Sydow, M.T. Dulay, T. Chou, J.P. Cooke, R.N. Zare, Capillary electrophoretic and micellar electrokinetic separations of asymmetric dimethyl-L-arginine and structurally related amino acids: Quantitation in human plasma, *J. Sep. Sci.*, 27 (2004) 1483-1490.

[36] E. Causse, N. Siri, J.F. Arnal, C. Bayle, P. Malatray, P. Valdiguie, R. Salvayre, F. Couderc, Determination of asymmetrical dimethylarginine by capillary electrophoresis-laser-induced fluorescence, *J. Chromatogr., B: Biomed. Sci. Appl.*, 741 (2000) 77-83.

Chapter Five

Determination of Methylarginines in Clinical Samples

5.1 Introduction

Adequate nitric oxide (NO) production is crucial to maintaining proper function of numerous physiological processes in the pulmonary, cardiovascular, neuronal, and immune systems. It is believed that the onset of various pathologies, especially those pertaining to the endothelium, is due at least in part to a reduction in NO bioavailability. Without sufficient NO, endothelial function is disrupted and could stimulate disease development. One potential cause of diminished NO production is the presence of high concentrations of methylarginines (MAs). MAs inhibit NO synthesis and have been shown to be present at elevated amounts in patients with various pathologies. Given this, systemic concentrations of MAs could serve as diagnostic markers for NO-related diseases of the endothelium.

Two classes of disease that originate from impaired endothelial function are cardiovascular diseases (CVDs) and respiratory disorders. Although the symptoms of those disease states and the exact mechanisms of onset are quite different, a common origin of each of them is a diminished bioavailability of NO. Since MAs are key regulators of endogenous NO production, they may prove to be key biomarkers for preventive diagnostics for both disease classes. By determining how MA concentrations vary between healthy and diseased patients, potential diagnostic thresholds could be established.

In order to determine the role MAs play in disease onset and potentially utilize these biomarkers as a means of monitoring disease progression, an assay capable of measuring these species first had to be developed. To that end, analytical methods were optimized to prepare serum samples and measure endogenous MA concentrations using capillary electrophoresis (CE) (Chapters 3 and 4). These methods were then applied to the analysis of patient-generated samples. The preliminary results derived from those analyses are reported in this chapter.

Specifically, concentrations of MAs in clinical samples were determined and the arginine methylation index (ArgMI) calculated. These values were then compared to clinical outcomes in an effort to determine whether either value could serve as accurate diagnostic markers for patients with heart disease or infants suffering respiratory distress.

5.2 Materials and Methods

5.2.1 Reagents

Standards of monomethylarginine (MMA), asymmetric dimethylarginine (ADMA), symmetric dimethylarginine (SDMA), and propylarginine (PA) were purchased from Enzo Life Sciences (Farmingdale, NY). Sodium tetraborate and sodium cyanide were obtained from Sigma Aldrich (St. Louis, MO). Naphthalene-2,3-dicarboxaldehyde (NDA) was procured from Invitrogen (Carlsbad, CA). Sulfobutylether- β -cyclodextrin (SBEC) was acquired from Cydex Pharmaceuticals (Lenexa, KS). HPLC-grade dimethylsulfoxide, acetonitrile, and formic acid were purchased from Fisher Scientific (Pittsburgh, PA). All solutions were prepared with 18.2 M Ω •cm deionized water (Millipore, Billerica, MA). Serum samples from individual patients suspected of having heart disease were acquired from Lawrence Memorial Hospital (Lawrence, KS). Scavenged plasma samples from infants were acquired from Children's Mercy Hospital (Kansas City, MO).

5.2.2 Patient Populations

The cardiovascular disease population consisted of 17 patients who were recommended to undergo coronary angiography due to suspected heart disease. On the day of the angiograms,

patients underwent catheterization as part of the standard angiography procedure. Those who consented to participate in the study had a few milliliters of extra blood drawn from their catheters which was spun down to serum. Samples were stored at $-80\text{ }^{\circ}\text{C}$ until they were ready to be transferred to KU for analysis. Angiogram results were disclosed to KU following analysis of samples so that average concentrations from patients diagnosed with or without disease could be compiled.

The patients enrolled in the respiratory distress portion of the project were newborns in the neonatal intensive care unit (NICU). Plasma was collected from five infants of different ages. No infant identification criteria could be disclosed so it is unknown whether the patients in the study were experiencing respiratory distress. All that was given was the age of the infants and the fact that they were ill enough to be housed in the NICU. Plasma samples were stored at $-80\text{ }^{\circ}\text{C}$ and then shipped to KU for analysis.

5.2.3 Heat-Assisted Extraction Procedure

To prepare the heart disease patient serum samples, $100\text{ }\mu\text{L}$ aliquots of pooled serum were transferred into 2 mL polypropylene microcentrifuge tubes (Fisher Scientific) to which $5\text{ }\mu\text{L}$ of $10\text{ }\mu\text{M}$ PA was added. For the infant samples, $25\text{ }\mu\text{L}$ of plasma was mixed with $1.25\text{ }\mu\text{L}$ of $10\text{ }\mu\text{M}$ PA. All tubes were immersed in boiling water ($100\text{ }^{\circ}\text{C}$) for 1.5 min . During the heating process, the liquid serum quickly congealed to form a solid gel. Once the serum gel was formed, water was added to each vial at a volume identical to the initial serum volume (*i.e.* $100\text{ }\mu\text{L}$ for heart disease samples and $25\text{ }\mu\text{L}$ for infant samples) for extraction and then vortexed for $\sim 20\text{ s}$. Samples were then centrifuged to sediment the aggregated proteins, and the supernatants were decanted into separate tubes for subsequent analyses. The reason for the discrepancy in sample

volume between adults and infants was strictly due to chronological method development. The adult samples were analyzed first, during which time the procedure called for 100 μL of serum. Subsequent sample preparation optimization determined that 25 μL of serum was more ideal, so infant samples were prepared using this lower sample volume. All serum/ plasma samples were prepared in triplicate.

5.2.4 Capillary Electrophoresis

A Beckman P/ACE MDQ CE instrument (Brea, CA) with a 50 μm i.d. capillary (Polymicro Technologies; Phoenix, AZ) 65 cm in length (50 cm to window) was utilized in this study. The run buffer consisted of 15 mM sodium tetraborate and 10 mM SBEC. Run buffer for the analysis of CVD samples also contained 25% (v/v) DMSO. The run buffer for the analysis of infant samples contained 28% (v/v) DMSO (see 5.3.1). Samples were injected hydrodynamically at 1.0 psi for 5.0 s, and separations were carried out at an applied field strength of 430 V/cm for CVD samples and 460 V/cm for infant samples. A 445 nm diode laser (CrystaLaser; Reno, NV) was used to stimulate fluorescent emission which was measured with an external laser-induced fluorescence (LIF) detector (Picometrics; Ramonville, France). 32 Karat software (Beckman) was used to operate both CE operation and LIF detection.

Samples analyzed by CE were first derivatized with NDA/CN⁻. NDA was dissolved in 1:1 acetonitrile:water; all other solutions were prepared in deionized water. The derivatization procedure entailed combining equal volumes of sample, 50 mM sodium tetraborate, NDA, and 5 mM NaCN and allowing the mixture to react for 10 min prior to injection. The initial NDA concentration was 1 mM when derivatizing standards and 5 mM when derivatizing blood samples. Peak areas from both standards and serum samples were normalized to the area of the

internal standard PA for quantitation. All standards were measured in triplicate. Serum samples from heart disease patients were analyzed by CE-LIF once each, while infant samples were analyzed in duplicate.

5.2.5 Liquid Chromatography-Tandem Mass Spectrometry (LC-MS/MS)

A LC-MS/MS study was performed to identify unknown components in serum samples. Following heat-assisted extraction, samples were analyzed by liquid chromatography (Waters; Milford, MA) coupled to a LTQ linear ion trap mass spectrometer (Thermo Scientific; San Jose, CA). A sample volume of 5 μL was injected onto a self-packed 500 μm x 10 cm column containing 5 μm C18 particles with 300 \AA pores (Restek; Bellefonte, PA). Mobile phase A contained 99.9% water/ 0.1% formic acid, and mobile phase B was comprised of 99.9% acetonitrile/ 0.1% formic acid. A linear gradient was applied starting at 3% B and increasing to 80% B over 20 min, followed by a 10 min re-equilibration period. The flow rate was 50 $\mu\text{L}/\text{min}$. Serum samples were diluted with mobile phase A 1:99 prior to analysis.

After sample injection, a 2 min delay was implemented prior to MS data acquisition to allow salts in the sample to be diverted to waste. Following this diversion period, eluent from the LC column was introduced into the mass spectrometer by electrospray ionization (ESI). A spray voltage of 3.0 kV and 15 psi of nitrogen nebulizing gas were applied to achieve ESI while holding the capillary temperature at 250 $^{\circ}\text{C}$. All analytes were detected in positive ion mode. Collision-induced dissociation was performed to acquire tandem MS data. All data acquisition and analysis was performed using Xcaliber 2.1 software (Thermo).

5.3 Results and Discussion

5.3.1 CE Separation Optimization

An efficient CE method was developed for the separation of MAs that provided baseline resolution between the analytes of interest (described in Chapter 3). This method was capable of quantifying unknown MA concentrations in serum; however, the reproducibility of the separation was somewhat variable. Although no problems were observed in most instances, in a few of the analyses, the resolution between peaks from MMA and an unknown endogenous analyte was diminished to the point where quantitation of MMA was precluded (Figure 5.1). This problem arose in the analysis of samples obtained from CVD patients. To prevent this issue from affecting the newborn respiratory study, additional buffer modifications were evaluated prior to analyzing those samples.

While other additives, such as hydroxypropyl- β -cyclodextrin, were added to the run buffer in an attempt to improve resolution, it was ultimately determined that the best solution to the comigration problem discussed above was simply adjusting the DMSO content. Baseline resolution between MMA and the unknown compound was achieved by increasing the amount of DMSO in the run buffer from the previous optimum of 25% to 28%. While the resolution between MMA and PA was slightly worse under this set of conditions, it actually allowed for more precise peak integration. These conditions were found to split the unknown component in serum samples into two distinct peaks. Increasing the percentage of DMSO in the run buffer caused one of them to migrate earlier in the electropherogram, while the other now migrated out after PA (Figure 5.2). Under these new conditions, the MA peaks of interest were no longer obscured by the interfering compounds, allowing for more precise quantitation. Because

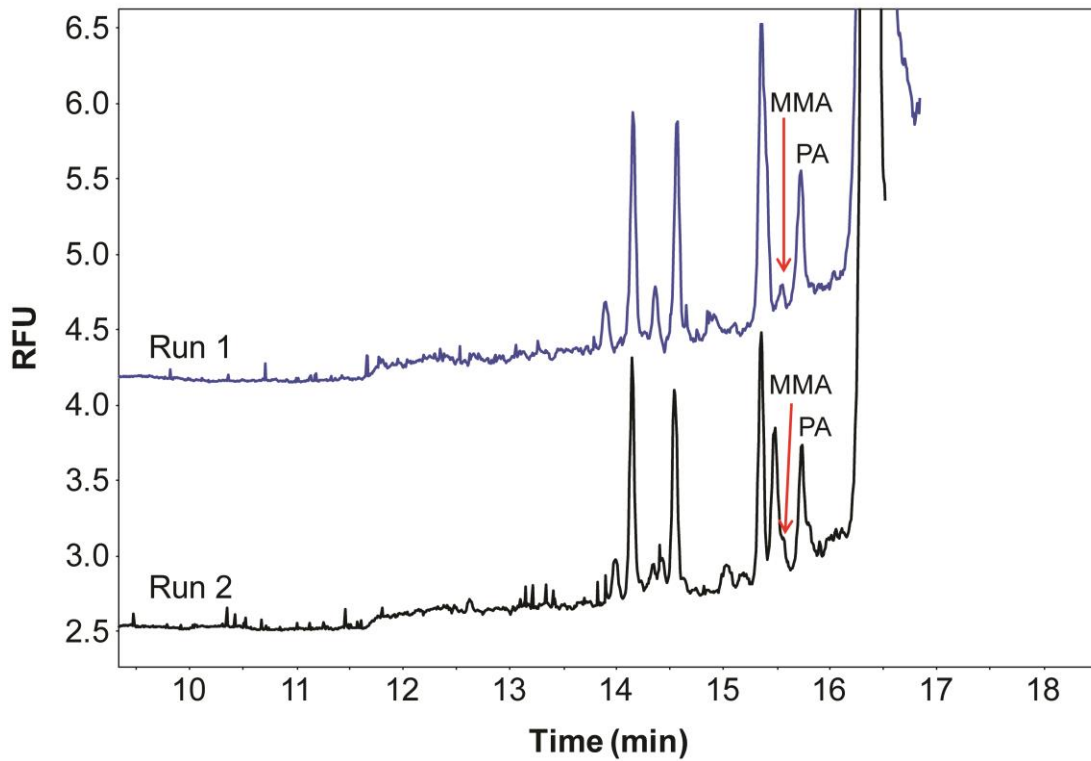


Figure 5.1 Sequential CE analyses of the same serum sample. The MMA peak is either well-resolved from (Run 1) or obscured by (Run 2) unknown interfering species.

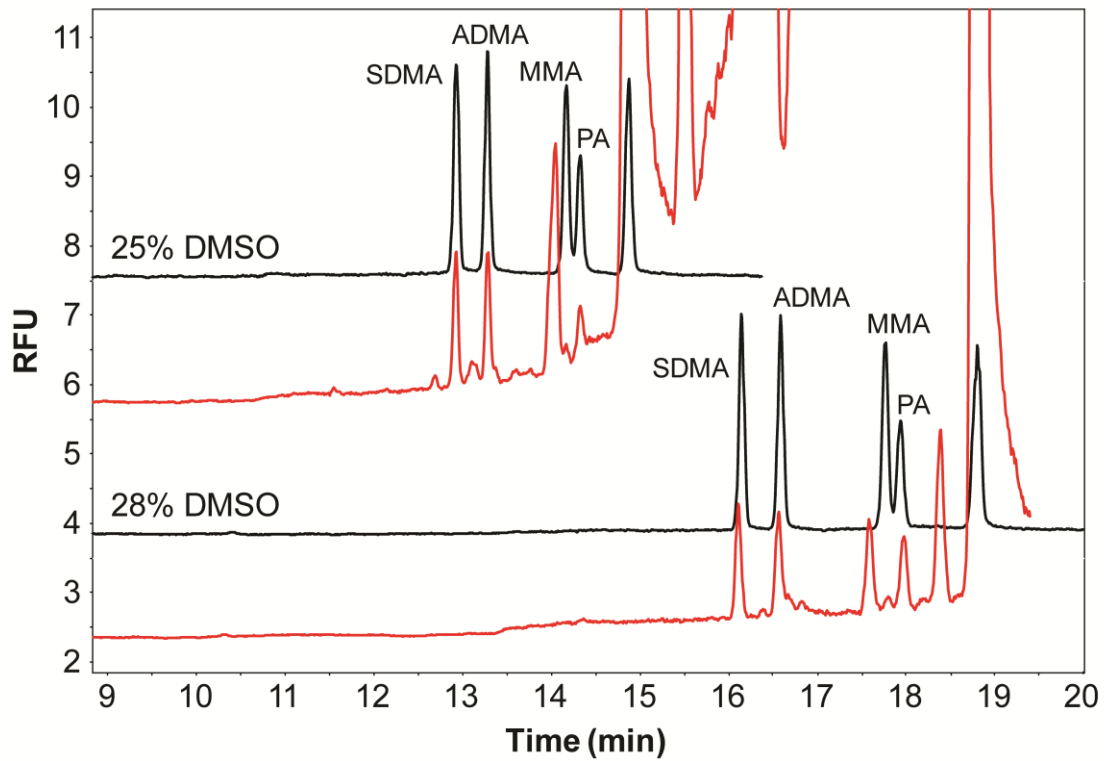


Figure 5.2 CE separation of standards (black) and serum samples (red) with 25% and 28% DMSO in the run buffer. Two unknown peaks resolve from the MMA peak when DMSO is increased to 28%.

migration times increased as a result of the additional DMSO, the separation voltage was increased to 460 V/cm. This was found to maintain similar analysis times without diminishing peak resolution.

5.3.2 Analysis of Cardiovascular Disease Serum Samples

A small-scale clinical study was undertaken to determine the impact of MA concentrations on the extent of CVD progression. Previous literature has demonstrated a correlation between MA concentrations and the severity of heart disease. A similar study was designed herein to measure MAs using the faster and less expensive methods described in Chapters 3 and 4.

5.3.2.1 Determination of Clinical Methylarginine Concentrations

Samples obtained from Lawrence Memorial Hospital were subjected to the optimized heat extraction and CE-LIF methods for blind analysis. Concentrations of the MA species in the serum samples were quantified. Following analysis, LMH provided yes/no responses as to whether each individual patient was diagnosed with coronary artery disease (CAD) following angiography. Patients were sorted into classes based on the diagnoses and the MA concentrations averaged within each class (Figure 5.3). It was determined that there was no difference in MA amounts between patients with and without heart disease. Although the average concentrations were higher among those patients with CAD, the differences were insignificant.

The conclusions drawn from this preliminary research were that there was no significant difference between patients with and without CAD. These findings are contrary to what has been previously published. However, a problem with the current study was in the number of patient

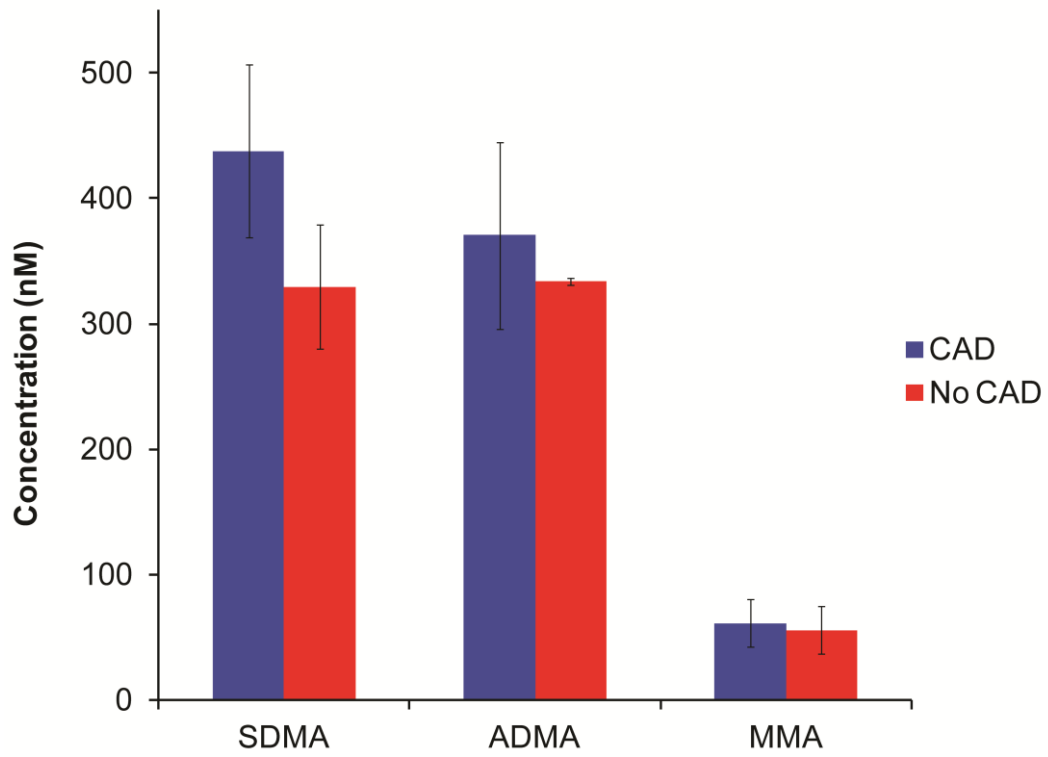


Figure 5.3 Average MA concentrations in patients diagnosed with and without coronary artery disease.

samples available for analysis. While other reports enrolled hundreds of patients, this data set was substantially smaller. Samples were collected from only 17 patients. This impacted the statistical analysis of the data and also led to higher deviations. This effect was especially pronounced in the samples from patients without CAD because that data set was comprised of a mere two people. Having such few data points in the average precludes any relevant statistical analyses from being performed. Additionally, if either/both of the people had atypical MA concentrations then the average would be significantly affected. As a result of the limited clinical population, all conclusions from this study must be taken as preliminary findings and not meaningful clinical observations.

5.3.2.2 Arginine Methylation Index

Although the patient population in this study was inadequate, MA concentration data was still available (5.3.2.1) from which a preliminary determination could be made regarding the prognostic ability of the ArgMI. The concentrations of ADMA, SDMA, and MMA were manipulated to obtain index values from each patient ($\text{ArgMI} = (\text{SDMA} + \text{ADMA}) / \text{MMA}$) [1]. These values were then averaged by diagnostic class and plotted in Figure 5.4. The data demonstrated that no significant difference existed between classes, which suggests that the ArgMI does not serve as a beneficial index for preemptively diagnosing patients with CAD. These findings conflict with a previous report in the literature that found the ArgMI to be a good predictor of CAD [1]. Furthermore, the ArgMI values reported in that paper for patients with and without CAD were 28.6 and 22.5, respectively. Our results found those values to be 13.2 and 11.9, respectively. It is unclear why the values for both the diseased and control populations in our study were so much lower. Again, a larger patient population would help to obtain more

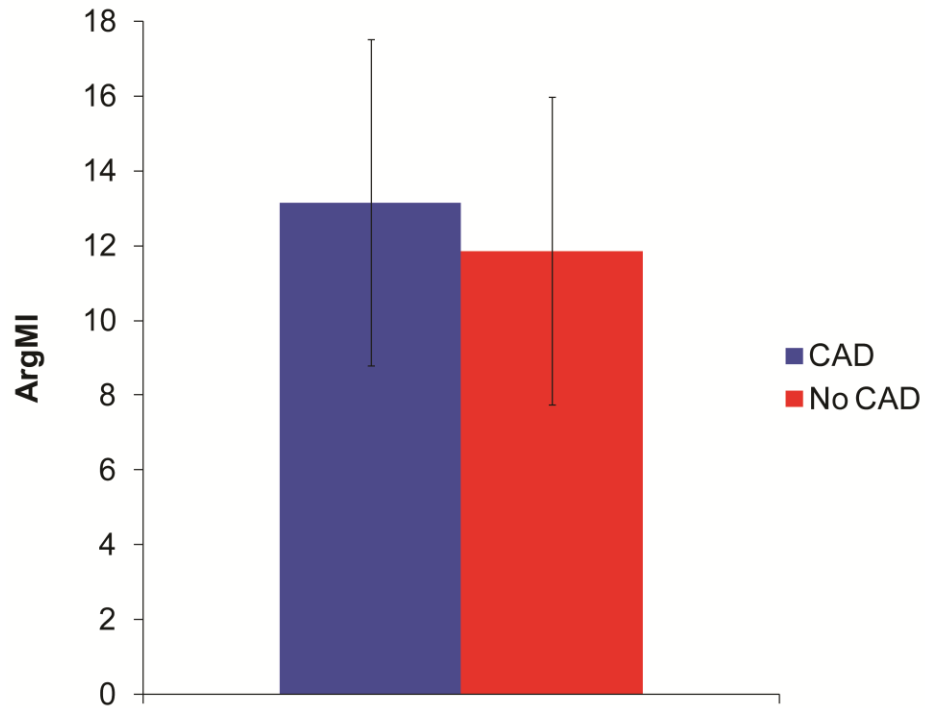


Figure 5.4 Average arginine methylation index values between patients with and without coronary artery disease.

accurate clinical population averages with less associated error. However, given the restrictions of time and resources available for this project, these initial results are all that could be obtained and must be taken with a grain of salt.

5.3.2.3 Interfering Species

During the analysis of a few of the patient samples, a rather broad, large peak was observed in the middle of the electropherogram. This peak was wide enough to comigrate with MMA to the point where it could not be quantified while also somewhat obscuring PA. This unfortunately prevented MMA concentrations from those patients from being included in the data set for the whole patient population. It also may have reduced the quantitative precision of the normalized peaks by interfering with PA. Although this peak was only present in a relatively small percentage of samples, an investigation was made to determine its source with the hope of eliminating it in samples collected in the future.

The interfering peak in question can be seen in Figure 5.5 between the ADMA and PA peaks. The large peak width suggests that the analyte is present at relatively high concentrations; however, it is interesting to note that the peak height is relatively small. This suggests that this compound was not effectively derivatized or else the peak height would have been substantially larger. Also, considering that the compound was present at a seemingly high concentration in a few patients but not present at all in other patients suggests that either these few patients were incredibly ill or the peak is an artifact of sampling.

To determine the identity of this peak, LC-MS/MS was implemented to determine the molecular weight of the analyte. Two samples were analyzed using this method that were found by CE to contain this peak along with two samples that were found not to have this peak. The

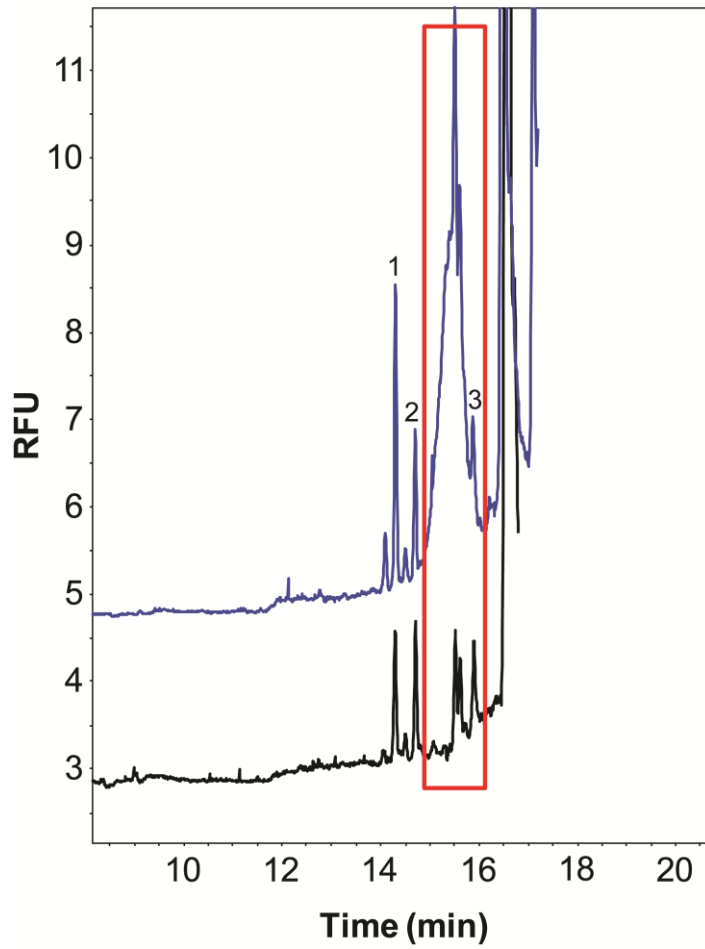


Figure 5.5 Sample electropherograms from patient samples with (top) and without (bottom) the presence of an unknown interfering species.

total ion chromatogram (TIC) between the samples showed a clear distinction between the two sets of samples. Samples that were initially found to contain this peak had two very large peaks in the TIC that were not present in the other samples. Deconvolution of the data found that the isotopic distributions from both peaks were identical with parent masses of 1549.7 Da. Figure 5.6 shows the extracted ion chromatograms (XICs) for this isolated mass which illustrates the prominence of this analyte in the samples from patients that had this unidentified peak present.

The presence of dual isobaric peaks suggests that they may be enantiomeric peptides with some degree of chromatographic resolution between them. To identify the composition of the peaks, the mass was inputted into a protein sequence database (UniProt) to determine the most probable peptide sequence capable of producing the specific parent mass. It was found that a peptide sequence from albumin matched the mass and isotopic distribution of the parent ion; however, the relative intensities of the isotopic peaks between the experimental and theoretical values were quite different. Figure 5.7 shows how the experimental data had a much less intense isotopic distribution profile than would be expected in a peptide of that size. This observation suggested that the molecule of interest may not be a peptide but rather an unusually monoisotopic small molecule.

A search was then performed in a small molecule/ metabolite database (METLIN) where a high probability candidate was found. The drug iodixanol had not only had the desired mass, but its isotopic distribution matched very well as well (Figure 5.8). This compound contains six iodines per molecule which accounts for the abnormally small isotopic intensity of a molecule that size since iodine has only one stable naturally occurring isotope. Tandem MS studies were then performed on the patient-generated serum samples which further confirmed the identity of the interfering molecule as iodixanol based on its fragmentation pattern.

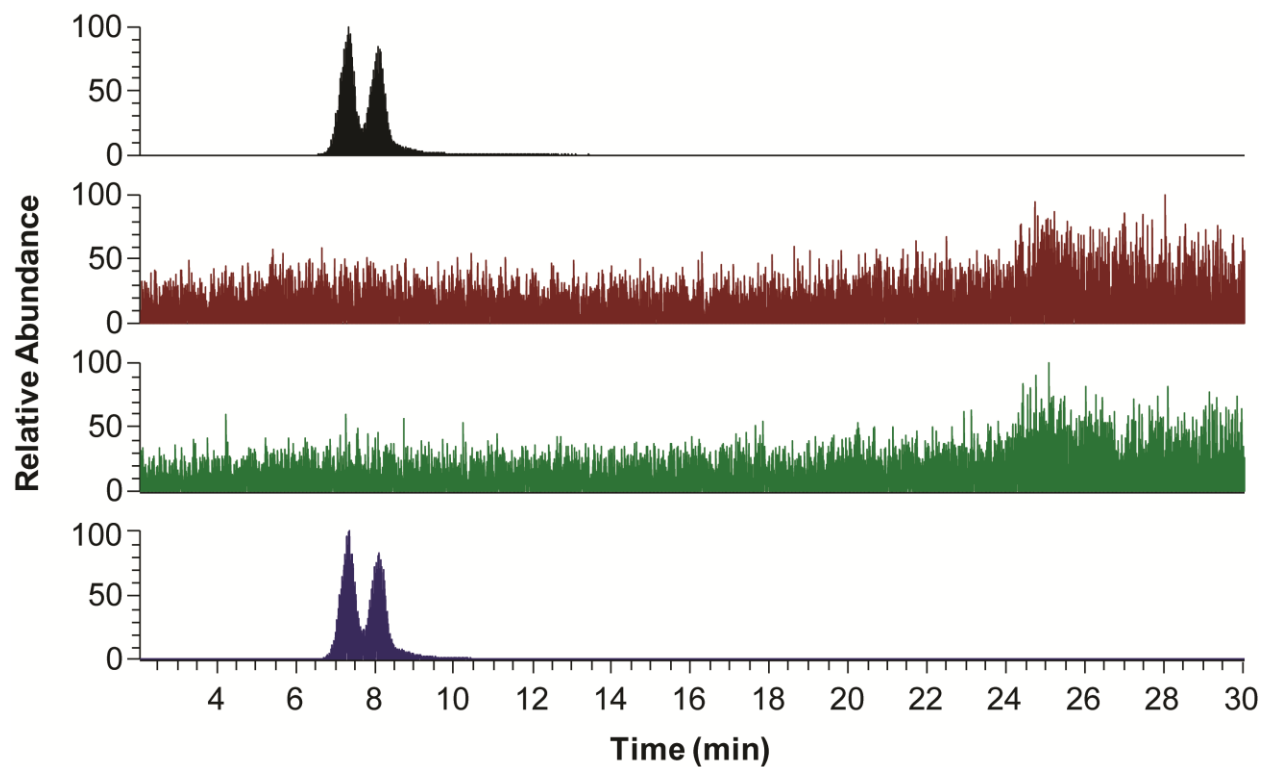


Figure 5.6 Extracted ion chromatograms (m/z 1550.7) from patients with (top and bottom) and without (middle) the interfering peak present in their CE electropherograms.

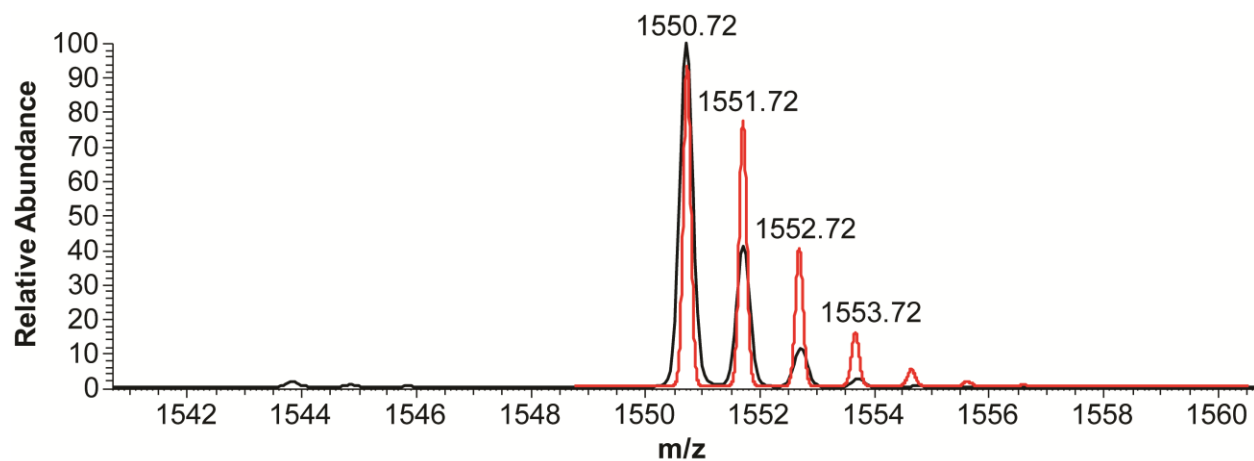


Figure 5.7 Comparison of the experimentally determined isotopic distribution of the unknown peak (black) and the theoretical distribution of a peptide from digested albumin (red). Poor overlap between the experimental and theoretical isotopic intensities was observed.

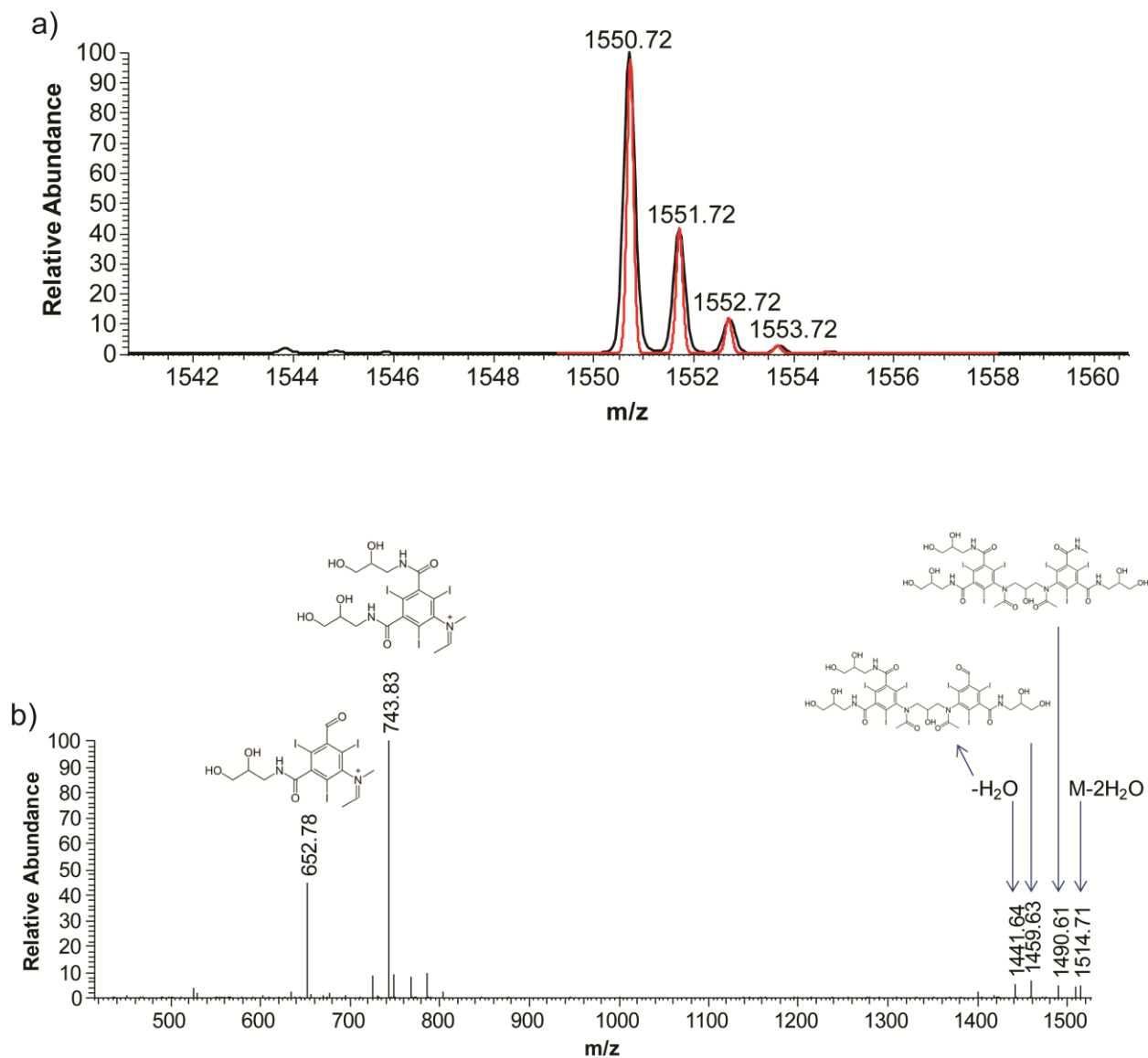


Figure 5.8 (a) Comparison of the experimentally determined isotopic distribution of the unknown peak (black) and the theoretical isotopic distribution of the drug iodixanol (red). Good overlap between the experimental and theoretical isotopic intensities is observed. (b) Tandem mass spectrometry was performed to confirm the identity of the iodixanol in a clinical sample.

The identity of the interfering species in some of the patient samples was determined by mass spectrometry to be iodixanol. Upon investigation into the applications of the drug, it was discovered that iodixanol is utilized as a contrast agent during coronary angiography. The drug is administered to a patient prior to the procedure at a concentration of ca. 0.61 g/mL iodixanol (the exact concentration and injection volume varies depending on the patient). Assuming a volume of distribution of 5 L, this equates to an approximate systemic concentration of drug of 7.9 mM. The very high concentration of iodixanol in the body confirms the suspicion that this is the interfering peak in the CE data. The drug does not contain a primary amine and therefore does not get derivatized by NDA/CN⁻. However, the high amount in the sample may be sufficient to produce a different background fluorescence and manifest as a broad peak in the electropherogram. The observation that only a few of the clinical samples contained this peak suggests that most patients had blood collected prior to initiation of the procedure while a few had it drawn after the contrast agent had already been administered. Therefore, for future sample collection, blood must be drawn before beginning the procedure to avoid corrupting CE results.

5.3.3 Analysis of Respiratory Disease Plasma Samples

Newborns housed in the NICU remain under close observation because of the severe health issues that they face. These infants suffer from various pathologies that can be quite serious since their immune systems and organs may not yet be fully mature. Ventilatory support is frequently administered to aid their breathing, and in the case of those with hypoxic respiratory failure, NO can also be given.

Because of NO's ability to dilate blood vessels and improve blood oxygenation, inhaled nitric oxide (iNO) therapy has been used to treat pulmonary disorders [2-6]; however, there have

only been a few clinical studies designed to evaluate the efficacy of iNO therapy in infants. One such trial monitored the total NO metabolites (NO_x) and correlated those levels to preterm infant survival without the onset of bronchopulmonary dysplasia (BPD). It was shown that infants with the lowest initial concentrations of NO_x experienced dramatically improved outcomes after receiving iNO. Infants with higher amounts of NO_x prior to iNO administration demonstrated no significant benefit after receiving the treatment [7]. This supports the hypothesis that insufficient endogenous production of NO causes hypoxia or BPD. Unfortunately, there is no way to directly measure nitric oxide synthase activity in the lung tissue of live patients to determine if they are good candidates for iNO therapy. Therefore, alternative analytical approaches must be established to predict the efficacy of iNO.

Since MAs regulate NO synthesis, they could potentially be used as markers to indicate the amount of NO present. Therefore, by monitoring these compounds, predictions could be made to determine which individual patients would respond favorably to iNO prior to initiation of the treatment. However, before determining the MA concentrations that could be used as diagnostic thresholds for patient screening, baseline levels first had to be established. An initial small-scale study was performed to measure the endogenous concentrations of MAs from ill infants in the NICU. Concentrations were determined at multiple ages to establish whether the levels fluctuated after birth.

5.3.3.1 Clinical Methylarginine Concentrations

An investigation was performed to determine the concentrations of MAs in the plasma of critically ill infants. Due to the small volumes that can be collected from these babies, there was insufficient volume to convert plasma to serum. However, since it was determined in Chapter 4

that plasma and serum contained the same MA concentrations, this should not have affected the outcome of this study. The results showed that newborns had very high amounts of MAs (Figure 5.9a), particularly during the first month of life. These high concentrations were consistent with the few existing reports in the literature measuring MAs in newborns [8-10]. Significant differences were observed (based on a two-tailed t-test) between the different ages, especially with SDMA which first increased in concentration, and then diminished. ADMA and MMA maintained similar concentrations initially but then exhibited a significant concentration reduction as the infants aged. Initial ADMA and SDMA concentrations were $>1 \mu\text{M}$ for the first 1+ month of life which was substantially higher than adults suffering from CVD (as determined in section 5.3.2.1) (Figure 5.9b). As the infants aged, however, the MA concentrations decreased significantly. Once infants reached 6 months of age, their MA concentrations were similar to the values observed in adults.

There are several potential causes for the high MA concentrations observed in newborns. The hemoglobin in fetal blood has a higher affinity for oxygen than does the blood of its mother. This ensures that the developing child obtains sufficient oxygen in the womb. However, if the amount of oxygen is too high, it is possible that the body would try to increase vasoconstriction to prevent hyperoxia. One potential manner of accomplishing this *in vivo* would be to upregulate production of MAs. This hypothesis suggests that MAs would remain elevated after birth until the newborn's hemoglobin matures and the partial pressure of oxygen reaches "normal" levels.

Another potential cause of the elevated MA concentrations stems from improper expression of proteins and enzymes in the newborn. Homeostasis of the NO pathway is carefully regulated to ensure adequate vasodilation levels are achieved. However, if normal homeostasis cannot be established and the enzymes involved (*e.g.* dimethylarginine dimethylaminohydrolase

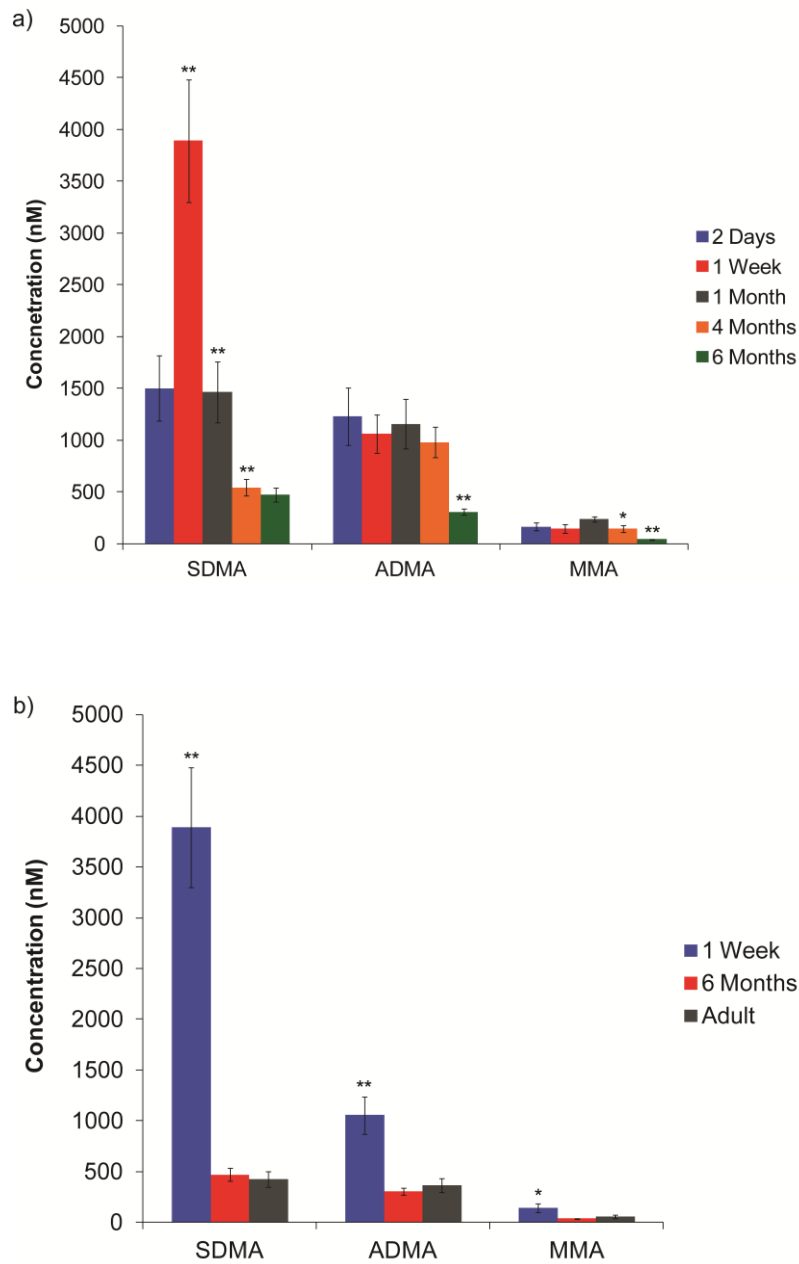


Figure 5.9 (a) Concentrations of MAs in the plasma of newborns. Scavenged plasma was pooled by age group. Samples were prepared in triplicate and analyzed by CE-LIF in duplicate. (b) Comparison of the concentrations of MAs between newborns and adults.

* $p < 0.05$; ** $p < 0.001$

(DDAH) or protein arginine methyltransferase (PRMT)) are mis-expressed then a rise in MA concentrations is plausible. Studies have been conducted investigating the expression DDAH in a porcine model as a means of understanding enzyme distribution and activity as it pertains to MAs. It was shown that DDAH expression and activity increases before birth and then declines thereafter [11]. This would suggest that ADMA and MMA concentrations begin high and then taper off within a few days after birth. While our data do show a decline in the amounts of MAs, a few months are required before they reach adult baseline levels, not a few days. This discrepancy could reflect a difference in NO pathways between pigs and humans or could be attributed to the health of the infants. The same study demonstrated that DDAH activity was severely reduced when piglets were made hypertensive, which would result in increased ADMA and MMA concentrations.

The substantially higher SDMA concentration observed at “1 Week” (Figure 5.9a) versus any of the other analytes or time points is quite puzzling. The predominance of this peak could possibly be explained by the relative activities of the enzymes mentioned above. If PRMT-II was over-expressed in comparison to PRMT-I, this would explain why SDMA concentrations were so much larger than those of ADMA. Alternatively, this significant concentration difference could be explained by analyte clearance. DDAH metabolizes ADMA and MMA, but does not affect SDMA. SDMA is cleared exclusively by the kidney. Therefore, if the sample was collected from newborns suffering from renal disease or from those whose kidneys were not fully developed, then plasma accumulation of SDMA would be expected. Providing that those same newborns produced adequate DDAH, ADMA and MMA concentrations would have remained normal.

Other potential reasons for observing elevated MA concentrations in newborn plasma could stem from an artifact of sample collection. All newborn-derived samples had evidence of hemolysis as evidenced by the red color of the plasma (in contrast to the normal dull yellow color). Reports have shown that red blood cells (RBCs) contain a clinically relevant amount of MAs [12, 13]. If the RBCs in the samples lysed, they could have increased the observed MA concentrations and biased the results. This seems like a plausible explanation (at least in part) to the increased MA levels observed in newborns. Since the RBCs of infants tend to be more fragile than those from adults, they have a greater propensity to lyse. Therefore, the pressure drop between the patient and the vacutainer may have been great enough to cause cell lysis during sample collection, which could account for the seemingly abnormally high MA concentrations.

5.3.3.2 Arginine Methylation Index

The Arginine Methylation Index has been demonstrated to be an accurate predictor of mortality in adults suffering from CVD [1]. Given its good acumen to forecast health problems, an investigation was made into its ability to predict whether a newborn would show clinical improvement. The concentration data (5.3.3.1) was manipulated to calculate the ArgMI values for infants of various ages (Figure 5.10). The data show that the time point at which these infants were most at-risk was at one week of age. The ArgMI value was significantly higher for the “1 Week” sample than for any other time point. It is unclear at this point if this finding is relevant since the ArgMI has only been demonstrated to have meaning in CVD. If infants are most susceptible to NO-related pathologies at one week old, this finding might prove insightful. However, given that the index is higher at six months old than one or four months old, it seems like this index has no use prognostic value since the infants should have stabilized by that age.

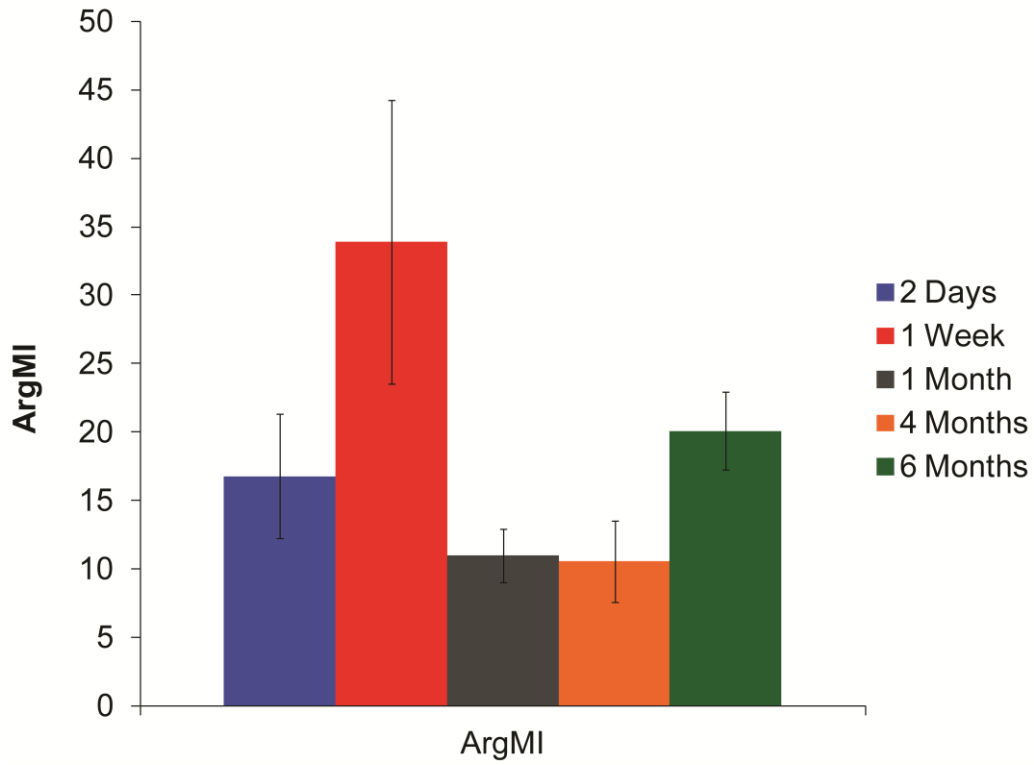


Figure 5.10 Arginine methylation index of newborns by age group.

5.4 Conclusions

Data from this chapter demonstrate the application of the optimized methods to the analysis of clinical samples. A small-scale study was performed to discover the utility of MAs to serve as diagnostic biomarkers of coronary artery disease. The outcome of these experiments showed that while MA concentrations were elevated in patients with CAD, the differences were not significant. Additionally, it was determined that the ArgMI did not prove useful in predicting CAD given the very similar values between patients with and without heart disease.

The MA assay was also applied to the analysis of samples collected from newborns in the NICU. The results from this study indicated that these infants had extremely high MA concentrations even when compared to adults with CAD. The elevated concentrations in the newborns indicate that they may suffer from NO-related pathologies, which may be the reason for their hospitalization. However, at six months of age, it was shown that the MA concentrations diminished to those found in adults.

5.5 References

- [1] Z. Wang, W.H.W. Tang, L. Cho, D.M. Brennan, S.L. Hazen, Targeted Metabolomic Evaluation of Arginine Methylation and Cardiovascular Risks: potential mechanisms beyond nitric oxide synthase inhibition, *Arterioscler. Thromb. Vasc. Biol.*, 29 (2009) 1383-1391.
- [2] R.H. Steinhorn, Neonatal pulmonary hypertension, *Pediatr. Crit. Care Med.*, 11 (2010) S79-84.
- [3] A. Bin-Nun, M.D. Schreiber, Role of iNO in the modulation of pulmonary vascular resistance, *J. Perinatol.*, 28 (2008) S84-92.
- [4] B.C. Creagh-Brown, M.J. Griffiths, T.W. Evans, Bench-to-bedside review: Inhaled nitric oxide therapy in adults, *Crit. Care*, 13 (2009) 221.
- [5] R.F. Soll, Inhaled nitric oxide in the neonate, *J. Perinatol.*, 29 (2009) S63-67.
- [6] R.H. Steinhorn, Nitric oxide and beyond: New insights and therapies for pulmonary hypertension, *J. Perinatol.*, 28 (2008) S67-71.
- [7] M.A. Posencheg, A.J. Gow, W.E. Truog, R.A. Ballard, A. Cnaan, S.G. Golombek, P.L. Ballard, Inhaled nitric oxide in premature infants: effect on tracheal aspirate and plasma nitric oxide metabolites, *J. Perinatol.*, 30 (2010) 275-280.
- [8] I.M. Di Gangi, L. Chiandetti, A. Gucciardi, V. Moret, M. Naturale, G. Giordano, Simultaneous quantitative determination of NG,NG-dimethyl-L-arginine or asymmetric dimethylarginine and related pathway's metabolites in biological fluids by ultrahigh-performance liquid chromatography/electrospray ionization-tandem mass spectrometry, *Anal. Chim. Acta*, 677 (2010) 140-148.

- [9] G. Vida, E. Sulyok, T. Ertl, J. Martens-Lobenhoffer, S.M. Bode-Boeger, Birth by cesarean section is associated with elevated neonatal plasma levels of dimethylarginines, *Pediatr. Int.*, 54 (2012) 476-479.
- [10] M.A. Bordigato, D. Piva, I.M. Di Gangi, G. Giordano, L. Chiandetti, M. Filippone, Asymmetric dimethylarginine in ELBW newborns exposed to chorioamnionitis, *Early Hum. Dev.*, 87 (2011) 143-145.
- [11] F.I. Arrigoni, P. Vallance, S.G. Haworth, J.M. Leiper, Metabolism of asymmetric dimethylarginines is regulated in the lung developmentally and with pulmonary hypertension induced by hypobaric hypoxia, *Circulation*, 107 (2003) 1195-1201.
- [12] M. Davids, A.J. van Hell, M. Visser, R.J. Nijveldt, P.A.M. van Leeuwen, T. Teerlink, Role of the human erythrocyte in generation and storage of asymmetric dimethylarginine, *Am. J. Physiol. Heart Circ. Physiol.*, 302 (2012) H1762-1770.
- [13] S.S. Billecke, L.A. Kitzmiller, J.J. Northrup, S.E. Whitesall, M. Kimoto, A.V. Hinz, L.G. D'Alecy, Contribution of whole blood to the control of plasma asymmetrical dimethylarginine, *Am. J. Physiol.*, 291 (2006) H1788-H1796.

Chapter Six

Development of a Microchip Electrophoresis Point-of-Care Device for the Determination of Methylarginines

6.1 Introduction

There has been a push over the last 10-20 years towards the miniaturization of analytical systems [1]. Instruments that enable rapid measurements to be made using smaller sample volumes and that generate less reagent waste are quite attractive for numerous reasons. The high throughput achieved by these systems would enable many clinical samples to be analyzed rapidly to allow a fast turn-around of information to the presiding doctor [2]. This so-called bench-to-bedside system would allow patients to be diagnosed more quickly and therefore expedite the initiation of a therapeutic regimen. Substantial cost savings can be also be realized with this technology by utilizing fewer reagents and obviating the shipment of clinical samples to a central laboratory for analysis. Additionally many of these systems have been developed to be inexpensive and, in many cases, disposable [3]. The goal of such point-of-care (POC) devices is to have a relatively autonomous system that would enable samples to be directly analyzed on-site.

As mentioned in previous chapters, MAs have the potential to be informative biomarkers of various pathologies including cardiovascular and respiratory diseases. However, in order to achieve widespread utility in clinical diagnosis, the analysis system would have to shift from a complex bench-top instrument to a simple stand-alone unit. This entails miniaturizing the system, reducing its total cost, and simplifying the procedure such that the analysis can be performed by people without advanced training. A first step to begin to meet these criteria is to reduce the size of the analytical set-up. A key benefit of capillary electrophoresis (CE) is that it miniaturizes nicely into a microfluidic platform without a loss in separation efficiency [4]. Given that, a method employing microchip electrophoresis (MCE) to separate and quantify MAs would be highly valuable towards the development of a POC detection system. The short analysis times

afforded by MCE provide higher sample throughput than other analytical techniques, which will be necessary for future clinical studies addressing MAs.

Multiple detection modes can be coupled to a MCE separation. Both electrochemical detection (EC) and laser-induced fluorescence (LIF) detection schemes have been employed for MCE analyses [5, 6]. An ongoing project in the Lunte group is the development of a miniaturized MCE-EC system that incorporates a microchip, potentiostat, and high voltage power supply into a single integrated unit with the total size comparable to a small shoe box. Because significant effort has already been made advancing this technology, using that equipment for POC MA measurements seemed logical. However, initial progress in our lab has also been made towards the development of a miniature LIF system. LIF detection provides unparalleled sensitivity for CE and MCE analyses so this may be a more ideal detection method [3, 7]. The goal of this chapter was to determine whether MCE coupled to EC or LIF could provide a reasonable separation of the MAs as an initial step towards the development of a point-of-care system.

6.2 Methods and Materials

6.2.1 Reagents

Arginine, citrulline, sodium tetraborate, mercaptoethanesulfonic acid (MESA), 2-mercaptoethanol (2-ME), mercaptosuccinic acid, chlorobenzenethiol, fluorothiophenol, sodium azide, N-acetylcysteine, and penicillamine were purchased from Sigma Aldrich (St. Louis, MO). Monomethylarginine (MMA), asymmetric dimethylarginine (ADMA), and symmetric dimethylarginine (SDMA) were procured from Enzo Life Sciences (Farmingdale, NY).

Naphthalene-2,3-dicarboxaldehyde (NDA) was purchased from Invitrogen (Carlsbad, CA). Sulfobutylether- β -cyclodextrin (SBEC) was acquired from Cydex Pharmaceuticals (Lenexa, KS). HPLC-grade acetonitrile and potassium cyanide were purchased from Fisher Scientific (Pittsburgh, PA). All solutions were prepared in 18.2 M Ω •cm deionized water (Millipore; Billerica, MA).

All analytes were derivatized with NDA for both EC and LIF analyses. A 5 mM solution of NDA was prepared in 1:1 acetonitrile:water. All nucleophiles were dissolved in water at 10 mM concentrations. For EC experiments, the derivatization reaction was carried out by adding sample, NDA, and then finally a nucleophile into a reservoir filled with 20 mM borate. All reagents were mixed in equal volumes. The point when the final reagent in the derivatization mixture was added (*i.e.* the nucleophile) was considered time zero ($t = 0$) for the reaction. For MCE-LIF studies, CN⁻ was used exclusively as the nucleophile. All labeling reagents were combined into a single vial and allowed to react for ≥ 10 min prior to the first injection.

6.2.2 Microchip Fabrication

6.2.2.1 PDMS Microchips

Microchip devices comprised of polydimethylsiloxane (PDMS) have been commonly implemented for electrophoretic separations for over a decade [8, 9]. The popularity of this material stems from its simple fabrication and low cost. These traits allow PDMS chips to be discarded after an experiment and readily replaced. Chip designs can also be varied relatively inexpensively which allows experimentation with slight channel modifications to determine an optimal configuration for a given experiment. While the advantages of PDMS revolve around the

mass production and low cost aspects of the material, significant drawbacks exist, especially with regards to electrophoretic separations. The surface of PDMS changes over time in an unpredictable manner and is also prone to analyte adsorption [10]. This causes an inconsistent EOF, which can have a substantial impact on the efficiency of the separation. Unlike glass surfaces which can be conditioned to regenerate the surface charge, PDMS does not revert back to its native state as easily. In general, once a PDMS device fails, it must be replaced.

To fabricate PDMS microchips, standard soft lithographic procedures were followed. A master was first made containing the channel designs of interest. First, a clean silicon wafer (Silicon Inc.; Boise, ID) was coated with a 15 μm thick layer of SU8-10 negative photoresist (MicroChem; Newton, MA). Once the photoresist was coated onto the wafer and briefly heated to help adhesion, it was transferred to a mask aligner (ABM; Scotts Valley, CA). During this process, a photomask (Infinite Graphics; Minneapolis, MN) containing the design of interest was placed over the wafer and brought into conformal hard contact. The UV flood source in the mask aligner was then activated, exposing the wafer/photomask for 16 s to crosslink the photoresist. Following exposure, the photomask was removed, and the silicon wafer submerged in SU8 developer (MicroChem) to remove the uncrosslinked photoresist. The end result of this process was a wafer containing raised features from the photomask. A final bake step was then performed to ensure strong adhesion of the hardened photoresist to the wafer.

After the silicon master was made, PDMS chips could easily be reproduced from the master mold. Sylgard 184 PDMS elastomer base and curing agent (Ellsworth Adhesives; Germantown, WI) were weighed out and mixed in a given ratio depending on the desired structural properties of the PDMS. A ratio of 7:1 produces a more rigid piece of PDMS while a 20:1 ratio produces very tacky, flexible PDMS. The ratio used is dependent upon the application,

but in general, a 10:1 ratio is preferable and was used in most of the experiments described here. Once the base and curing agent were thoroughly mixed, they were placed in a vacuum desiccator to remove any air entrapped in the viscous fluid. Next, the degassed PDMS was poured onto the master where it was allowed to slowly cover the entirety of the wafer and then placed in an oven (~80 °C) for 1-2 hours. Once fully cured, the solid PDMS was carefully peeled off from the master, and reservoirs were created using a biopsy punch (Ted Pella Inc.; Redding, CA). The final dimensions of the fluidic channels used in this study were 15 μm x 40 μm . A schematic illustrating the fabrication of PDMS channels is shown in Figure 6.1.

The substrate containing the electrode was fabricated following a similar procedure to the one described above using an appropriate photomask. However, after a PDMS channel was created, a carbon fiber (Avco Specialty Materials; Lowell, MA) 33 μm in diameter was inserted into the channel. The end of the fiber was put into electrical contact with a copper wire using silver colloidal paste (Ted Pella Inc.). Upon fabricating this electrode substrate, the fluidic channel layer was aligned over the electrode and then reversibly sealed by pressing the two PDMS pieces into contact. An end-channel electrode alignment was employed where the electrode was placed 5-10 μm from the exit of the separation channel [11]. Two forms of electrophoresis were conducted in the experiments described in this chapter: microchip electrophoresis and electrokinetic flow injection analysis (EFIA). The schematics for both designs are shown in Figure 6.2.

6.2.2.2 Glass Microchips

From a separations standpoint, glass is an ideal material from which to fabricate microchips. The surface properties of glass are very similar to that of fused silica, which is the

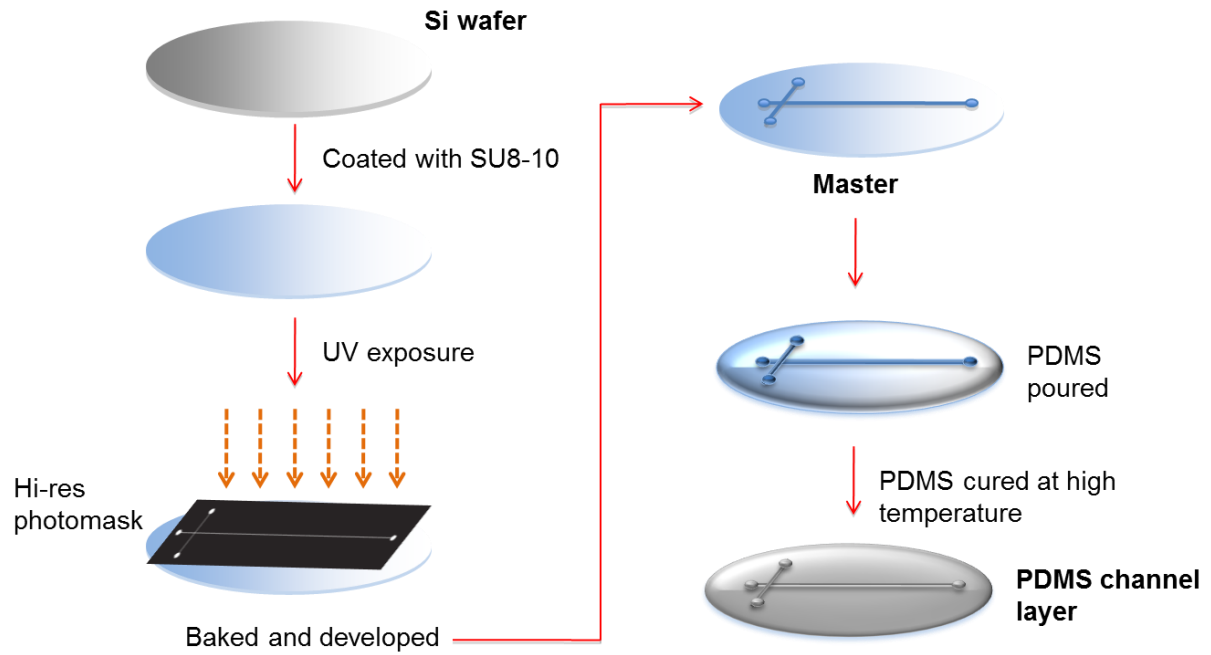


Figure 6.1 Schematic for the fabrication of PDMS microchips. Figure courtesy of Pradyot Nandi.

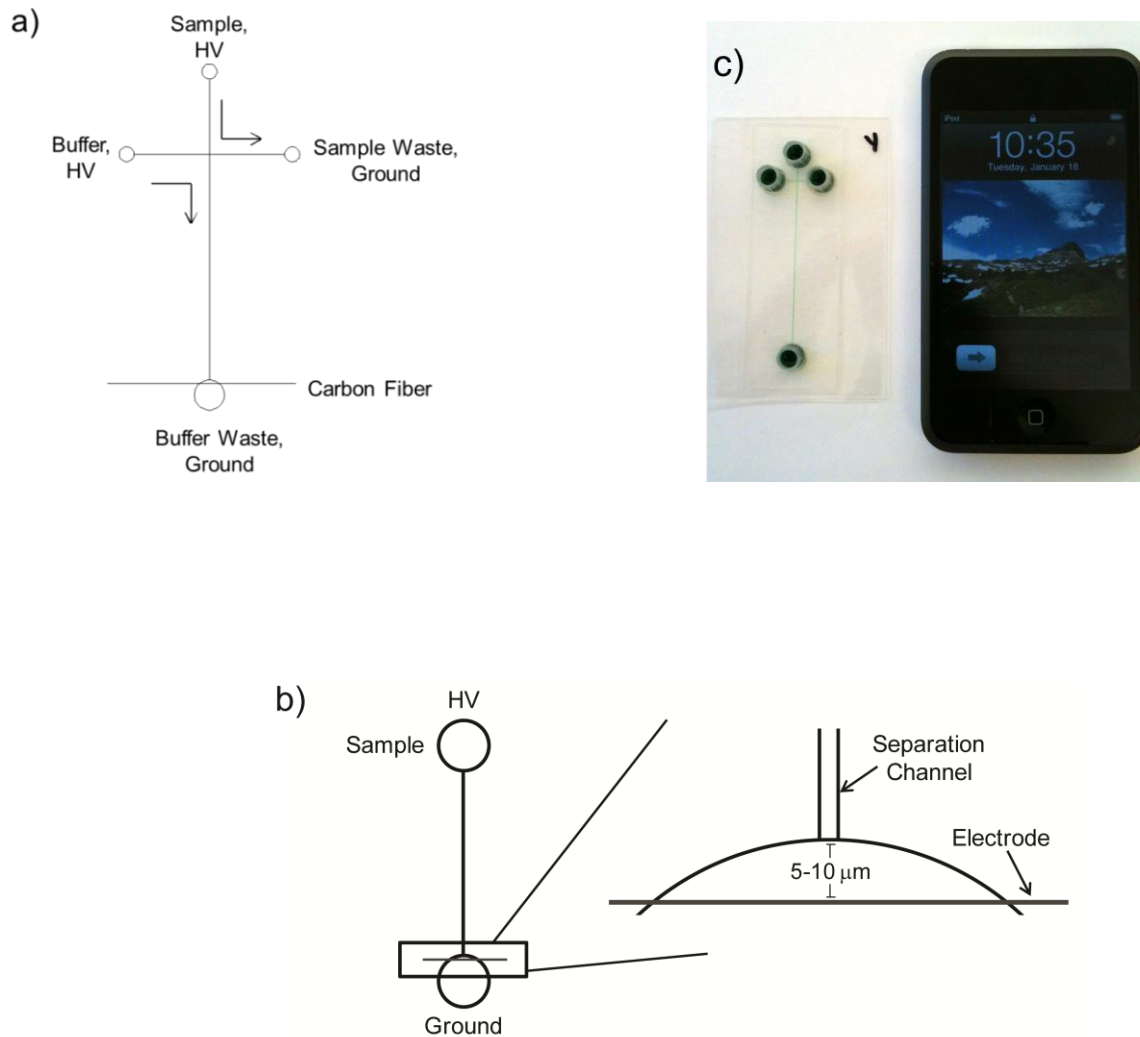


Figure 6.2 Schematic of the fluidic channels and the electrode alignment used for (a) microchip electrophoresis and (b) electrokinetic flow injection analysis. The inset in (b) shows the electrode alignment which was identical between set-ups. The image in (c) depicts a microfluidic device next to a cell phone for size comparison.

material used in conventional CE separations. Glass chips provide a stable, renewable surface which helps maintain good run-to-run precision and provides devices with long life-times [12]. However, glass chips are also more difficult to fabricate and are considerably more costly than those made from PDMS. Glass microchips cannot be mass-produced by replica molding, unlike with PDMS. Each chip must be made individually which increases the total fabrication time per device. The difficulty of fabrication is a predominant reason why PDMS is still more commonly used in most applications; however, if a reliable separation is desired, glass is still the best material to use.

Fabrication of glass MCE devices was accomplished using photolithography and wet chemical etching [13, 14]. Borofloat glass substrates coated with chromium and AZ 1518 positive photoresist were purchased from Telic (Valencia, CA). Photomasks were put into hard contact with the glass and exposed to UV radiation from the mask aligner for 4 s. The glass substrate was then put into 300 MIF developer (AZ; Somerville, NJ) where the exposed photoresist was developed away. Chromium etchant (Cyantek; Fremont, CA) was then used to remove the exposed chromium. Following this step, the design from the photomask was now exposed on the bare glass surface and the channels were ready to be etched. A wet-etching procedure was used here where the substrate was submerged into a 20:14:66 solution of hydrofluoric acid (Acros Organic; Pittsburgh, PA), nitric acid (Fisher Scientific), and water, respectively, to create recessed channels in the glass. The solution was agitated until the exposed surface was etched down to the desired depth (~15 μm) as verified by a profilometer (Tencor; Milpitas, CA). The depth of this etch dictated the height of the microfluidic channels. Once the channels were etched into the glass, the remaining photoresist and chromium were removed, and

access holes were drilled to create fluid reservoirs using a diamond-tipped drill bit. A schematic of glass chip fabrication is shown in Figure 6.3.

To complete fabrication of the MCE device, a coverplate of glass was thermally bonded to the channel substrate to create a sealed device. To accomplish this, a blank plate of glass and the etched plate were slowly sealed together under running deionized water while being careful not to introduce any air bubbles. Pressure was then applied to the plates using binder clips, and put into the vacuum desiccator to remove water from the channels and help seal the plates together. The device was inspected to ensure no air bubbles formed and then put into a low temperature oven (80 °C) for 1-2 hours. If after this time period no pockets of air formed, the temperature was increased to 110 °C and left overnight. The following morning, the binder clips were removed and the device was placed into a programmable furnace (Fisher Scientific) for a full thermal bonding cycle.

For borofloat glass bonding, the temperature was initially ramped at 3 °C/min from room temperature to 540 °C where it was further increased to 630 °C at 4 °C/min. The oven temperature was held at 630 °C for 3 hours to complete the bonding. The temperature was then slowly ramped down to 540 °C at 3 °C/min and then to 510 °C at 1.5 °C/min to ensure the plates did not crack during the cooling process. After holding at 510 °C for 30 min, the chip was cooled from 510 °C to 460 °C at 0.5 °C/min. At this point, the glass was below the transition temperatures and could be cooled to room temperature at a faster rate of 5 °C/min. Following the thermal bonding, the pieces of glass were fused together and could be utilized as a MCE device.

MCE devices typically employ separation channels in a simple T design (Figure 6.2a). This is due to the ease of fabrication and its general applicability for most analyses. While simple T microchips are useful, they may not provide sufficient separation efficiency for the analysis of



Figure 6.3 Schematic of the steps involved in the fabrication of glass MCE devices. A side view of the glass substrate is displayed.

MAs in blood samples. Serum is a complex matrix, so the separation will be complicated. As a result, additional peak capacity may be necessary to resolve all of the components present in the sample as well as to resolve the structurally similar MAs. Therefore, a MCE device containing a serpentine separation channel was fabricated to provide additional separation length (Figure 6.4). Serpentine channels afford superior resolution while preserving the small size of the MCE device [15]. The final channel dimensions were 15 x 45 μm with a 14 cm separation channel (13 cm to detector). The sample reservoir side-arm was 1 cm in length, while the buffer and sample waste side-arms were 4 cm long.

6.2.4 Microchip Operation

6.2.4.1 PDMS Microchip Operation

For EFIA, the fluidic channel and detection reservoir were filled with 20 mM pH 9.2 borate, and the derivatization reagents were added to the sample reservoir as described in 6.2.1. A lead from a Spellman high voltage (HV) power supply (Hauppauge, NY) was placed in the sample reservoir while the detection reservoir was grounded (Fig 6.2b). Once all derivatization solutions had been mixed, HV was applied to the sample reservoir to drive fluid flow. A field strength of 300 V/cm was chosen for electrophoresis since it is comparable to those typically employed in MCE. A potentiostat (BAS; West Lafayette, IN) was connected to the copper lead and used to measure current at the working electrode at the onset of HV application. The carbon fiber was employed as the working electrode, a Ag/AgCl electrode (BAS) served as the reference electrode, and a platinum wire was used as a counter electrode. EC data was collected using ChromGraph software (BAS).

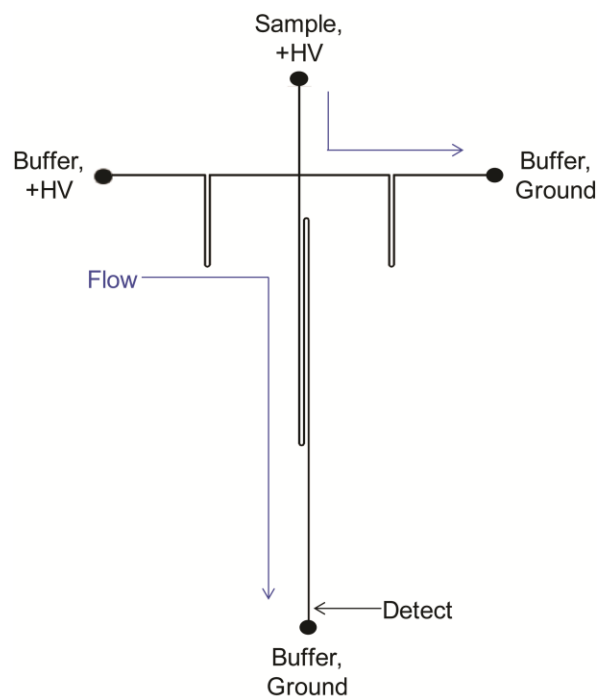


Figure 6.4 Design of the glass MCE-LIF device used for MA analysis.

For MCE experiments, the system was set up in a similar manner. However, a gated injection scheme was used where two HV electrodes were required to drive fluid flow. A potential of 1200 V was applied to the sample reservoir and 1600 V was applied to the buffer reservoir to create the gate. Sample was injected into the separation channel by floating the HV to the buffer reservoir for 3 s. The detection setup was identical to the EFIA experiments.

6.2.4.2 Glass Microchip Operation

Once the conventional capillary electrophoresis separation method had been optimized (Chapter 3), similar separation parameters were evaluated using a MCE device. Because the glass channels of the microchip are analogous in composition to the walls of the silica capillary, the EOF for the two methods should be similar, and a comparable separation should be achieved. To perform a gated injection on a microchip, however, two high voltage electrodes were required to produce the two different flow streams as opposed to the linear electric field necessary for a conventional CE separation. To obtain the peak capacity that would likely be necessary for resolving MAs from components in serum, a serpentine separation channel was employed immediately instead of a simple T design.

The operation of the glass microchip device was analogous to that of the PDMS chips. Channels were first filled with a 30 mM borate/ 1.5 mM SBEC run buffer and derivatized sample was loaded into the sample reservoir. An UltraVolt high voltage power supply (Ronkonkoma, NY) was used to apply 7.8 kV to the sample reservoir and 13.5 kV to the buffer reservoir while the other two reservoirs were held at ground to establish a robust gate. Injections were made into the separation channel by floating the HV in the buffer reservoir for 0.2 s. The HV was then reapplied to reestablish gating and also allow the components of the sample plug to separate as

they were electrokinetically driven down the separation channel. A custom program to control the high voltage application and data collection was written in-house using Labview software (National Instruments; Austin, TX).

To collect the fluorescence signal from the microchip device, a 445 nm PhoxX diode laser (Market Tech; Scotts Valley, CA) was directed into an epifluorescence microscope (Nikon; Melville, NY) via a fiber optic cable [16]. This allowed laser light to reflect off of a dichroic mirror and be directed up toward the sample stage, as shown in Figure 6.5. The laser spot emanating from the microscope objective was focused onto the MCE device 1 cm upstream from the buffer waste reservoir. As NDA-labeled analytes flowed through the laser spot, their fluorescent emission passed back through the dichroic to a photomultiplier tube where the response was detected using the aforementioned Labview program. Careful selection of the dichroic excitation and emission wavelengths allowed for selective monitoring of only NDA-labeled analytes, which led to excellent limits of detection (LODs).

6.3 Results and Discussion

6.3.1 Microchip Electrophoresis with Electrochemical Detection

Given that substantial effort has been invested by our group into the fabrication of a miniaturized EC detection system, an initial investigation was made into determining whether MCE-EC could be used in a POC system. All data presented in previous chapters utilized LIF as the detection scheme; however, switching to EC should be feasible. The derivatization reagent for all the previous studies was NDA. An additional benefit of NDA is that not only are its derivatized complexes fluorescent, they are also electroactive. This opens up the possibility of

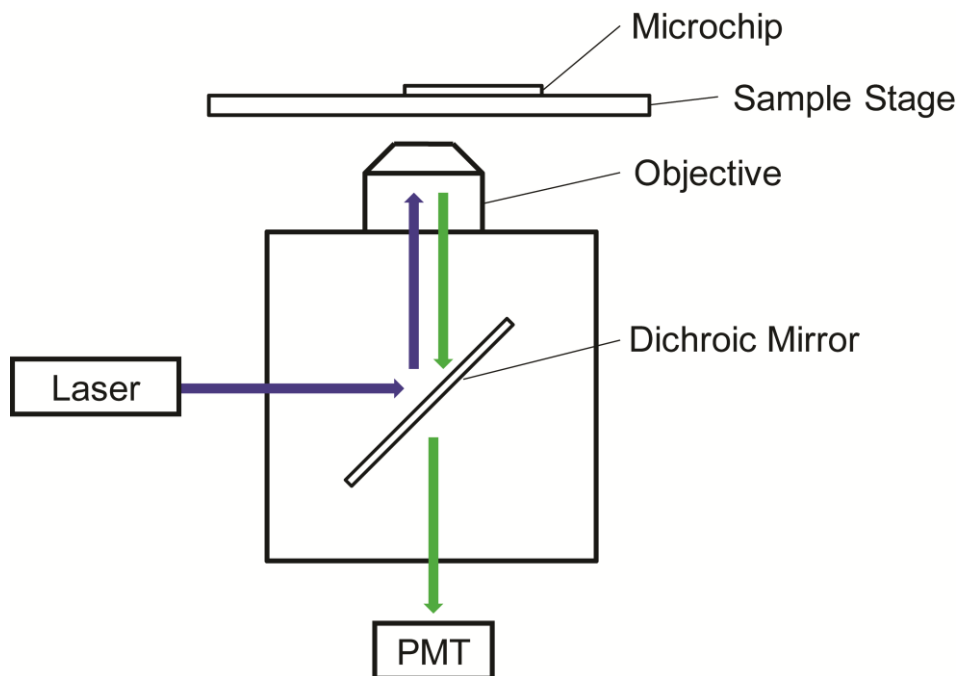


Figure 6.5 Microscope set-up for collecting fluorescence emission from a MCE device.

measuring the derivatized analytes with EC detection while still preserving the good peak capacity and resolution afforded by the optimized CE-LIF separation.

6.3.1.1 Electrochemical Response of NDA-Labeled Analytes

Prior to determining how reliably the separation transferred from CE to a MCE-EC platform, an initial investigation had to be made into how well the NDA-derivatized analytes responded at the surface of an electrode. Because NDA-labeled compounds are organic molecules, the use of carbon-based electrodes to oxidize them is more favorable than metal electrodes. Carbon electrodes can be integrated into PDMS much more readily than into glass, so for ease of fabrication, PDMS was selected as the substrate material for the analysis.

After construction of the device, an initial MCE separation was performed. Rather than beginning with more expensive MA standards, lower cost compounds were initially analyzed. Specifically, a separation between the NOS reaction products arginine and citrulline was performed to validate the performance of the system. The resulting peak currents at the carbon fiber electrode were monitored. Sample electropherograms of the separation of NDA/CN⁻-derivatized arginine and citrulline are shown in Figure 6.6.

The data shown in Figure 6.6 illustrates some potential drawbacks with using EC detection. First, much higher concentration standards needed to be introduced into the device to produce a reasonable signal. At these higher concentrations, peak shape was found to deviate from ideal. While this problem could be corrected with buffer modification, a more concerning problem was found in the form of the relatively high detection potential necessary to oxidize the labeled analytes. While the response at 700 mV vs. Ag/AgCl was strong, no response was observed at 400 mV. This high potential can reduce the selectivity of the analysis and may

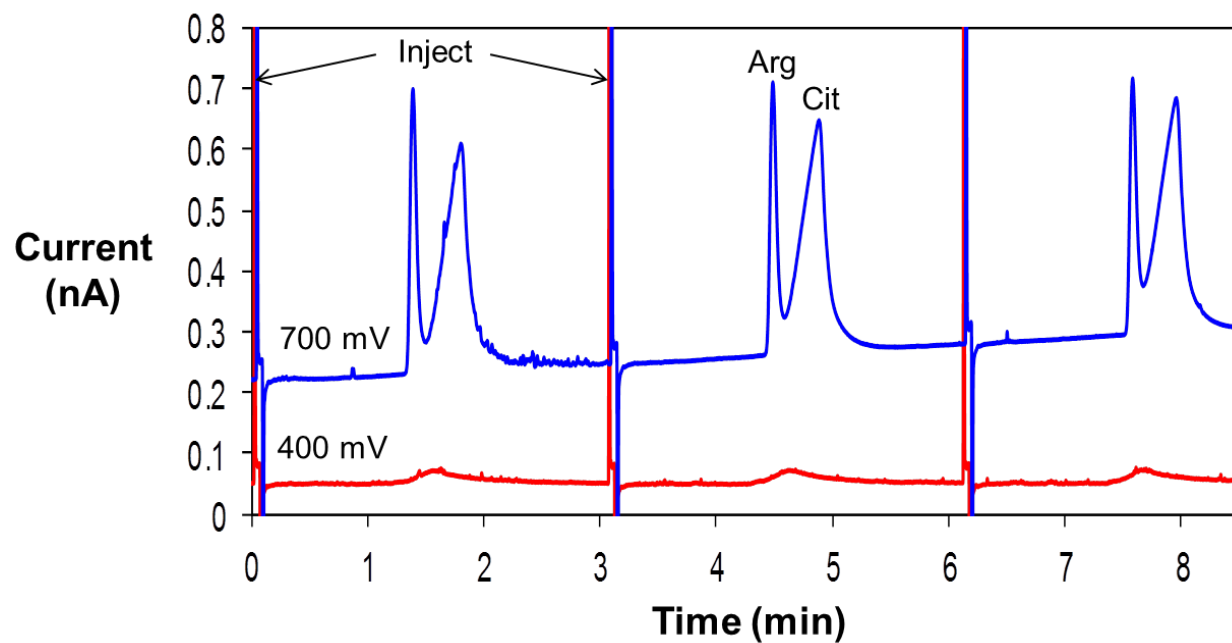


Figure 6.6 Sample electropherograms of a separation of 40 μM NDA-labeled Arg and Cit using MCE-EC in a 15 mM borate run buffer. The detection potentials were 700 mV (top) and 400 mV (bottom) vs. Ag/AgCl.

render quantitation difficult due to the presence of potentially interfering species. The largest drawback to this MCE-EC method, however, stemmed from the high detection limits of the method. The LOD for arginine at 800 mV was determined to be 600 nM which unfortunately is above the endogenous concentrations of MAs in serum samples. To overcome this severe limitation, a modification of the system was required if serum samples could ever be analyzed with this technique.

Other groups have reported that electrode modification can be performed to lower the detection limits of carbon electrodes. Depositing carbon nanotubes onto the carbon fiber [17] or employing a boron-doped diamond electrode [18] could help improve the limits of detection significantly; however, these methods require sophisticated equipment for fabrication. Also, the resulting electrodes are not as robust as standard carbon fibers which could result in variable response over time. So rather than attempt to modify the electrode to lower the LOD, an investigation into improving the derivatization chemistry was performed instead.

6.3.1.2 Evaluation of Alternative Nucleophiles

Cyanide has been used as the standard nucleophile in the NDA reaction since it was first reported in 1986 [19]. However, NDA/CN⁻ derivatization requires relatively lengthy reaction times and high oxidation potentials. These traits complicate the analysis of complex sample mixtures. Longer reaction times diminish throughput and hinder near real-time analyses from being performed. The use of higher redox potentials results in increased background currents and also limits the selectivity by allowing more potentially interfering species to be detected. As a result of these problematic characteristics of NDA/CN⁻, a different nucleophile was sought out for the derivatization reaction. Compounds were selected based on their nucleophilicity, charge,

solubility, and size. Only small molecules with high aqueous solubility were evaluated. Furthermore, anionic thiols were preferentially selected due to the high reactivity of thiols with NDA, and their ability to preferentially derivatize cationic species due to electrostatic attraction.

As mentioned in Chapter 2, NDA labels primary amines in the presence of a nucleophile to form a fluorescent/ electroactive product (Figure 6.7). Cyanide is the nucleophile that has most commonly been employed with NDA derivatization since the dye was first invented [20]. While CN^- may be satisfactory for LIF detection, it is not ideal for EC detection. Looking at the final derivatized species shows that the CN^- is covalently bonded to the isoindole ring that undergoes oxidation. The presence of this electron withdrawing group destabilizes the ring which makes oxidation more difficult. If a different nucleophile were used in place of CN^- , possibly with electron donating effects, the ring system would be stabilized thereby decreasing the potential necessary for oxidation. Not only would this improve the selectivity of the analysis (by decreasing the likelihood that non-derivatized species generate a response at the electrode), but it may also improve the limits of detection. If the signal could be enhanced while reducing the background noise at the electrode by operating at a lower potential, then a better LOD could be achieved.

6.3.1.2.1 Electrokinetic Flow Injection Analysis

To evaluate the abilities of various nucleophiles to improve the NDA electrochemistry, an EFIA system was designed. This system allowed the effectiveness of various nucleophiles to catalyze the formation of an electrochemically active product to be characterized. EFIA was used in place of conventional flow injection analysis to better mimic MCE analyses. When an electrode is placed near an electric field, a bias may be established at the electrode. To

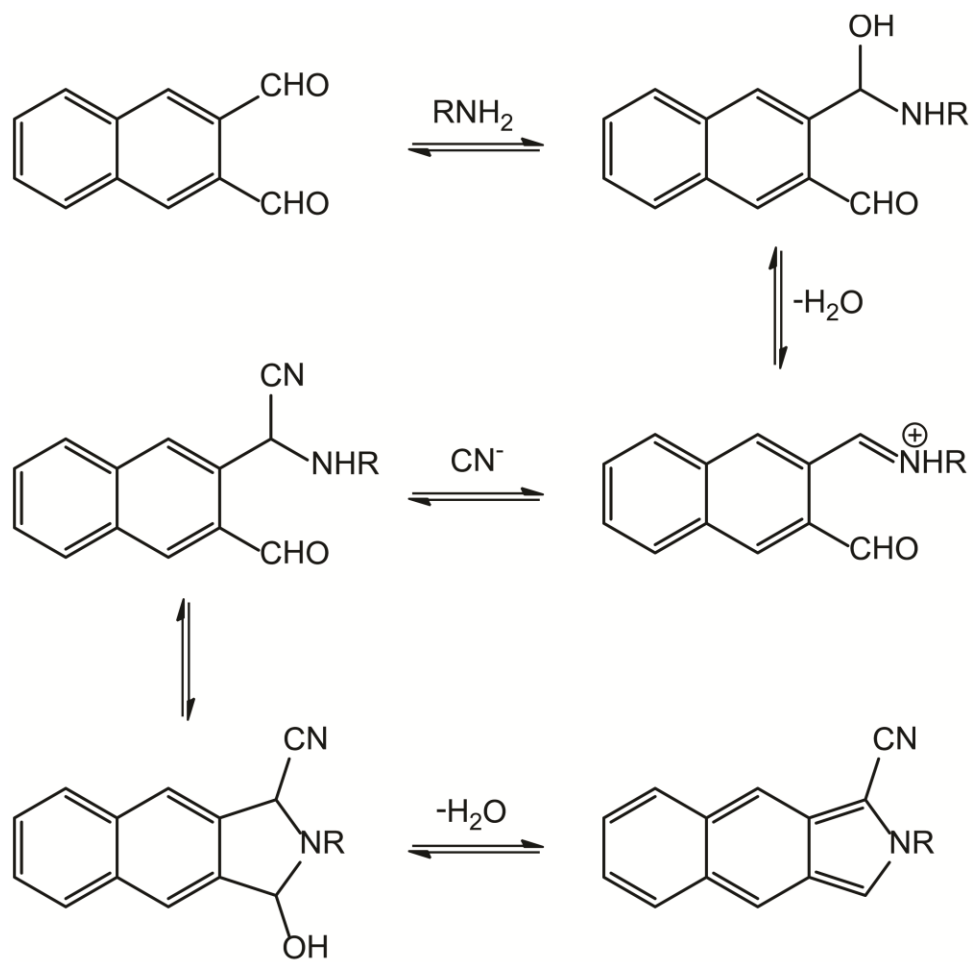


Figure 6.7 Mechanism of the NDA derivatization reaction.

compensate for the effect this field has on the electrode, derivatized sample was flowed down the channel electrokinetically using field strengths similar to those used in MCE. By constructing the experiment in this manner, any electric field-induced shift in oxidation potential would already be accounted for prior to switching to MCE analysis.

EFIA was utilized to evaluate the efficacy of each nucleophile to derivatize a 100 μM arginine sample. Following HV application, derivatized species passed over the electrode and the resulting current was monitored to determine which nucleophile was most promising for subsequent studies. Detection potentials of 700 mV and 250 mV were evaluated for each nucleophile. The primary parameter considered when evaluating nucleophile efficacy was the impartment of a lower oxidation potential on the derivatized species. Table 6.1 lists the nucleophiles that were used in this study and the average peak current produced from their derivatized complexes. Signals were normalized to the nucleophile that produced the largest response. Figure 6.8a depicts sample data from this study.

The data demonstrated that CN^- gave the largest response at high detection potentials but another reagent was best at lower ones. Since CN^- is the most commonly used nucleophile in NDA derivatization, its strong performance at relatively high potentials was not surprising. However, at lower oxidation potentials, CN^- produced one of the weakest signals. This indicates the relatively high amount of energy required to oxidize NDA/ CN^- -labeled species. At low detection potentials, the nucleophile that generated the highest response was MESA. This sulfur-containing molecule stabilized the derivatives and allowed more facile oxidation. 2-ME produced reasonably high responses at both potentials which demonstrated the reason it is typically the only other nucleophile used in NDA derivatization [21]. However, there were problems associated with 2-ME. Blank EFIA analyses were also performed with each

Table 6.1 Normalized peak currents of NDA-derivatized arginine with the indicated nucleophiles at 700 mV and 250 mV detection potentials.

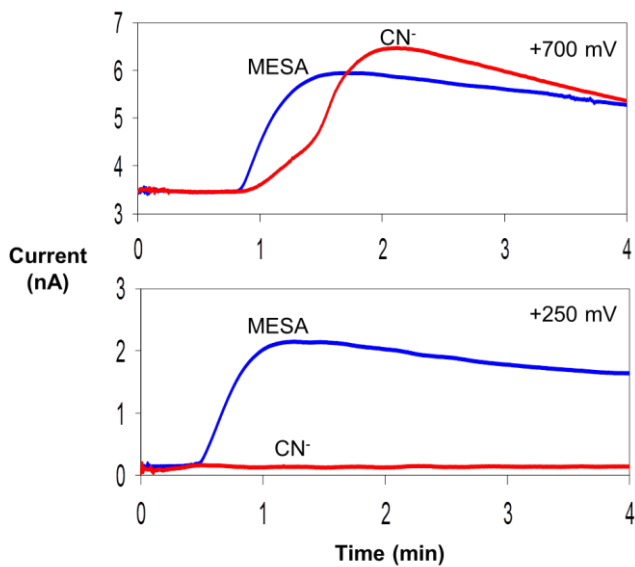
+700 mV

Nucleophile	Normalized Current
Potassium Cyanide	1.000
2-ME	0.930
MESA	0.541
Mercaptosuccinic Acid	0.195
Chlorobenzenethiol	0.073
Fluorothiophenol	0.045
Sodium Azide	0.016

+250 mV

Nucleophile	Normalized Current
MESA	1.000
2-ME	0.502
N-Acetylcysteine	0.451
Penicillamine	0.322
Potassium Cyanide	0.013

a)



b)

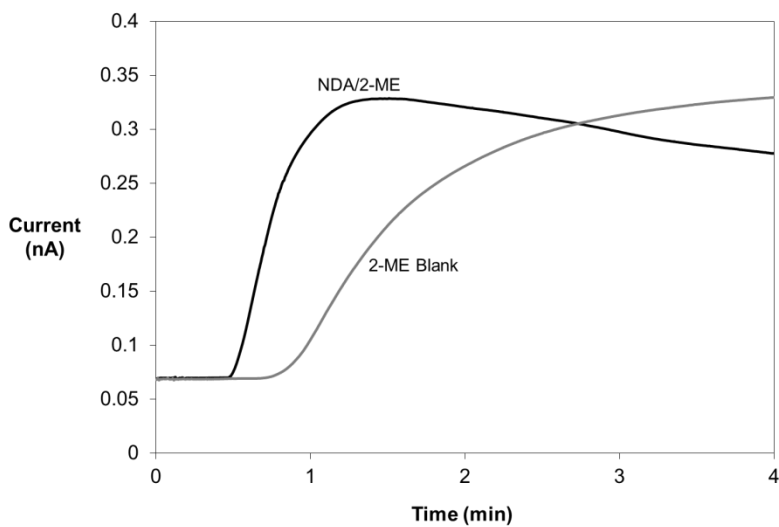


Figure 6.8 (a) Responses of arginine labeled with NDA and either MESA or CN⁻ at a detection potential of 700 mV (top) or 250 mV (bottom). (b) NDA/2-ME-labeled arginine and a NDA/2-ME blank detected at 250 mV. It can be seen the 2-ME produces a large amperometric response without labeling an analyte.

nucleophile, and the blank response produced by 2-ME was quite high. Figure 6.8b illustrates the high current produced by 2-ME, indicating that this molecule is electroactive itself. The use of this compound as a nucleophile in the labeling reaction is not ideal since its peak will have to be resolved from those of the derivatized components. MESA was found to not contribute significantly to the background current even with the high excess concentrations used for derivatization. Based on these studies, MESA was selected as the most promising nucleophile that warranted further investigation.

6.3.1.2.2 Cyclic Voltammetry

Based on the high response of MESA at a low oxidation potential, further studies were conducted on the use of MESA in the NDA reaction. Cyclic voltammetry was used to further characterize the electrochemical properties of the labeled species. It was determined that arginine derivatized with NDA/MESA produced a complex that had an average peak potential (E_p) of 300 mV. The E_p for arginine labeled with NDA/ CN^- was 650 mV. Sample CVs are shown in Figure 6.9. Other amino acids were also analyzed by CV to determine their E_p values. These results are shown in Table 6.2. The data demonstrates that MESA oxidized all species at lower potentials compared to their CN^- -derivatized counterparts.

The utilization of MESA as the nucleophile helped decrease the potential required to oxidize the NDA complex. Benz[f]isoindole derivatives undergo irreversible one electron oxidations independent of pH. Therefore, oxidation is thought to occur through the removal of an electron from the lone pair on the isoindole nitrogen thus forming a radical cation [22]. The high electron density in the ring system helps stabilize the radical cation which makes electrochemical removal of the electron favorable; however, the radical species is still highly reactive and does

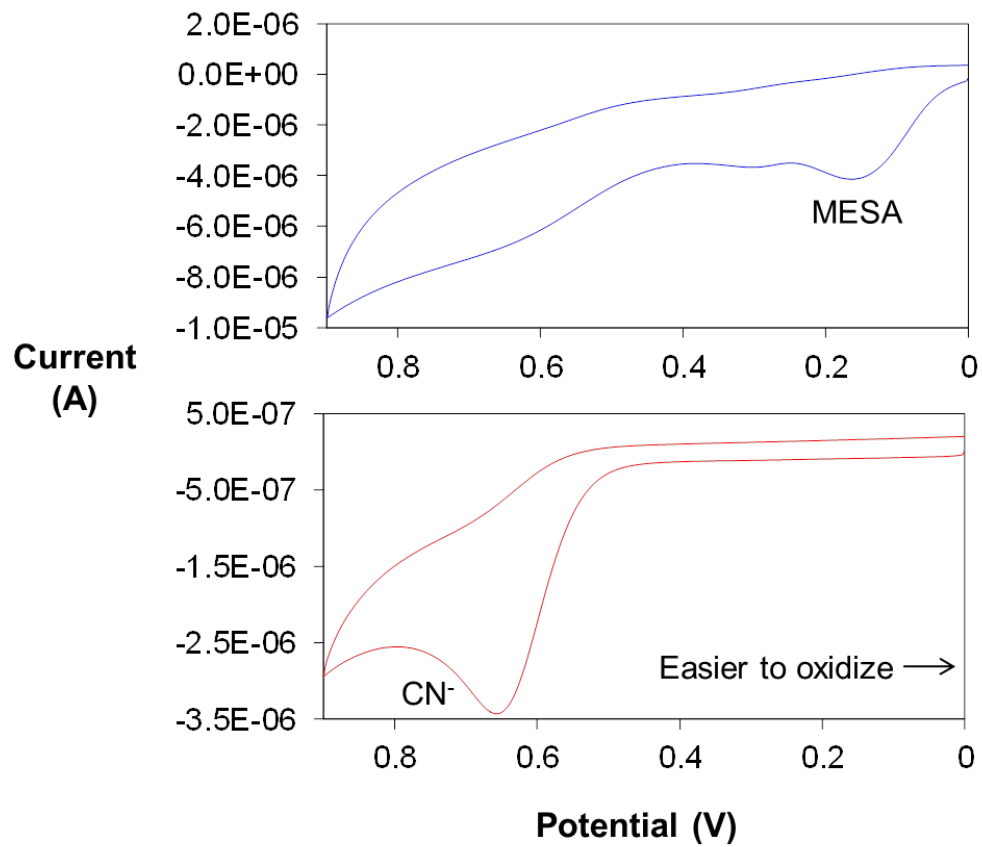


Figure 6.9 Cyclic voltammograms of arginine derivatized with NDA and either (a) MESA or (b) CN^- in 15 mM borate. A carbon fiber electrode (vs. Ag/AgCl) was used scanning at 100 mV/s.

Table 6.2 Peak potentials (vs. Ag/AgCl) for NDA-derivatized amino acids using either MESA or CN⁻ as the nucleophile.

Analyte	Nucleophile	Avg E _p (mV)
Arg	MESA	200 ± 17
	KCN	654 ± 3
Cit	MESA	256 ± 41
	KCN	559 ± 11
Glu	MESA	276 ± 8
	KCN	624 ± 10
Gly	MESA	227 ± 16
	KCN	556 ± 19
Lys	MESA	264 ± 12
	KCN	617 ± 18
Trp	MESA	221 ± 16
	KCN	498 ± 36

not have sufficient lifetime for subsequent reduction in a CV [23]. This logic explains the benefit of utilizing MESA as a nucleophile over CN^- . Cyanide is a strong electron-withdrawing group which depletes the ring system of electron density and destabilizes the radical cation generated at the electrode. This lack of stabilization forces more energy to be used to remove the electron from the NDA complex, requiring relatively high potentials to be used. MESA is an electron-donating group because of the electron-rich sulfur atom that covalently binds to the NDA. The added electron density provides additional stability to the complex which allows it to be oxidized more easily at lower potentials. However, unlike 2-ME, MESA itself produces only a minimal EC response.

6.3.1.2.3 Microchip Electrophoresis

Upon completing nucleophile characterization using EFIA and CV, it was discovered that MESA produced the most favorable responses at low detection potentials. Further studies were then performed comparing CN^- and MESA using MCE. Hydrodynamic voltammograms were first generated to determine the optimal detection potential of derivatized arginine in MCE separations. Arginine labeled with NDA/ CN^- showed that a relatively high detection potential of 750 mV was required to obtain an optimal signal. When using MESA, however, the HDVs indicated a potential of only 400 mV was needed. Figure 6.10 shows the HDVs for NDA-labeled arginine with the different nucleophiles.

Differences exist in the reaction kinetics when derivatizing arginine with MESA versus CN^- . It has been reported that the use of thiols in NDA derivatization produces fluorescent species more quickly than with CN^- but that the species decompose much more rapidly [24]. When using MESA as the nucleophile, our data agrees with these findings. Figure 6.11 illustrates

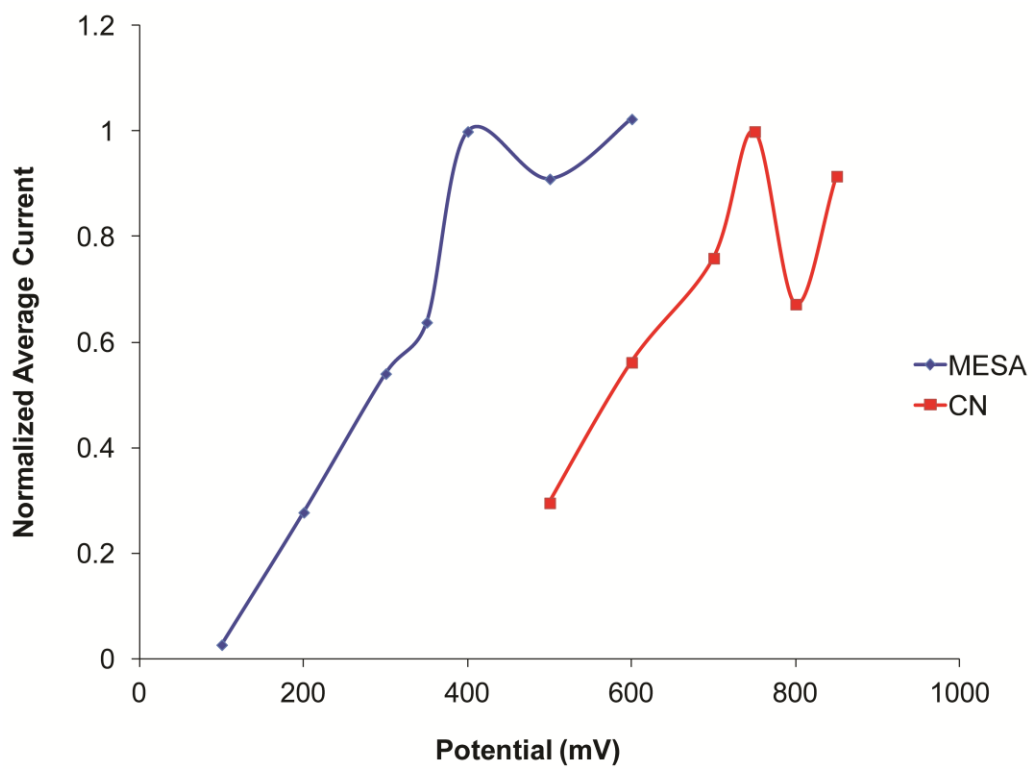


Figure 6.10 HDVs for NDA-derivatized arginine with either MESA or CN^- as the nucleophile.

that the rate of formation of NDA/MESA-derivatized analytes is quite rapid when compared to NDA/CN⁻ derivatives, which require longer times to reach maximum signal. However, the slope of the decay curve for MESA derivatives is steeper which indicates that the derivatized product is less stable. The rapid completion of the derivatization reaction is beneficial because it allows samples to be analyzed without significant delay. The short lifetimes of the derivatives are actually of little consequence because of the fast analysis times afforded by MCE.

After MESA had been identified as an effective nucleophile and its performance characterized, NDA/MESA-labeled MAs were prepared and subjected to a MCE-EC separation (Figure 6.12). The MAs exhibited derivatization kinetics similar to arginine and produced good responses at the carbon electrode. However, the analytes in a mixture were not well-resolved from one another under simple run buffer conditions. While the addition of buffer modifiers could have been explored, it was determined that a longer separation distance was probably necessary to attain good resolution between the components.

Given the lack of resolution between the MAs, an investigation was made into the use of a serpentine separation channel that would provide additional separation length. For this experiment, a PDMS chip containing the features illustrated in Figure 6.4 was fabricated. To ensure good adhesion between the channel and electrode layers, a ratio of 20:1 base:curing agent was employed to produce tackier PDMS. The electrode was aligned per usual, and an initial separation of the electroactive molecules dopamine and norepinephrine was attempted with good results (Figure 6.13a). Peaks for the two analytes were nicely separated, indicating the feasibility of this serpentine MCE-EC design.

During the time when this chip design was being evaluated for the analysis of NDA-derivatized analytes, a serious problem arose. The electricity in the lab building was becoming

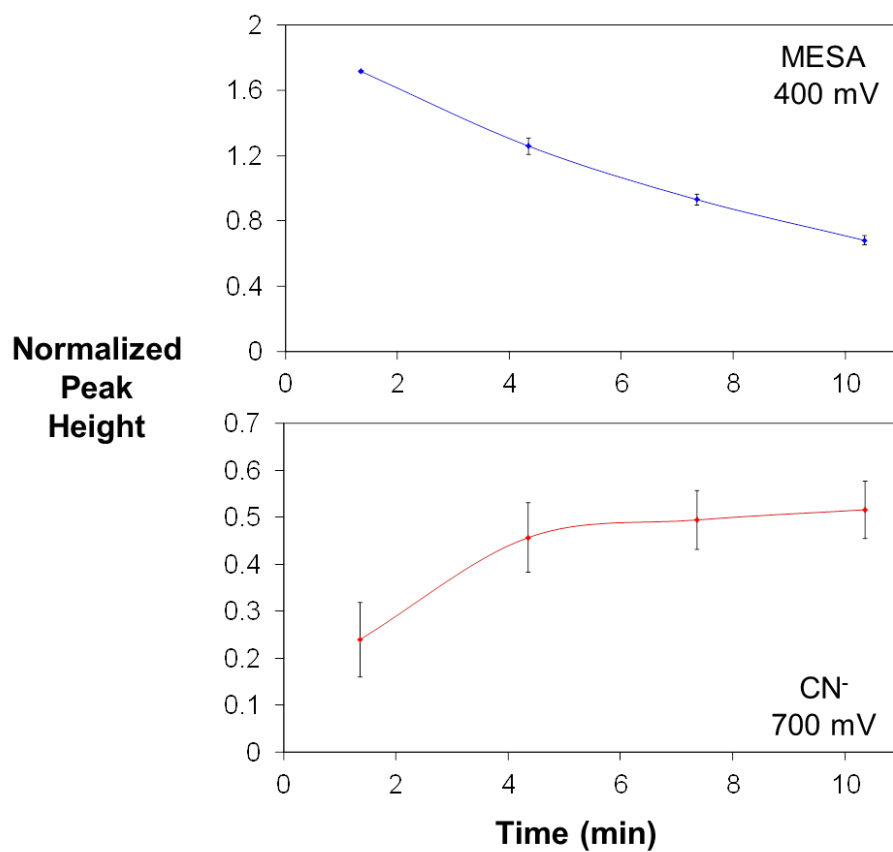


Figure 6.11 Reaction kinetics profile of the reaction of arginine with NDA and either MESA (top) or CN⁻ (bottom).

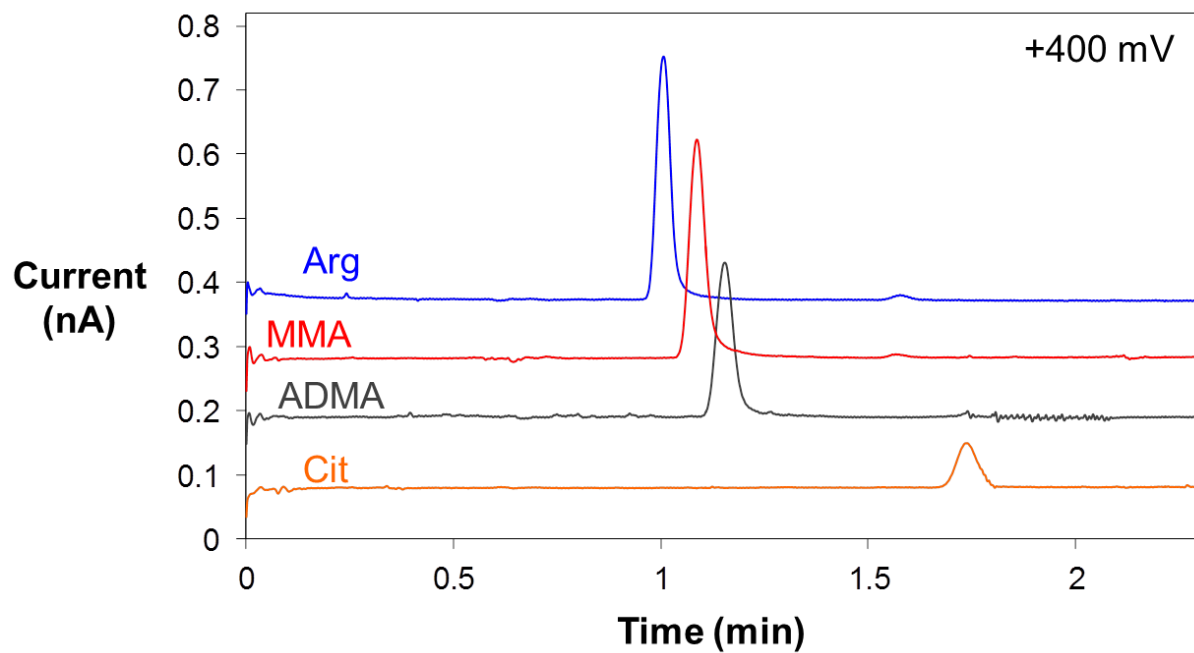


Figure 6.12 Separation of NDA/MESA-derivatized analytes at 20 μM concentrations. The separation buffer contained 20 mM borate.

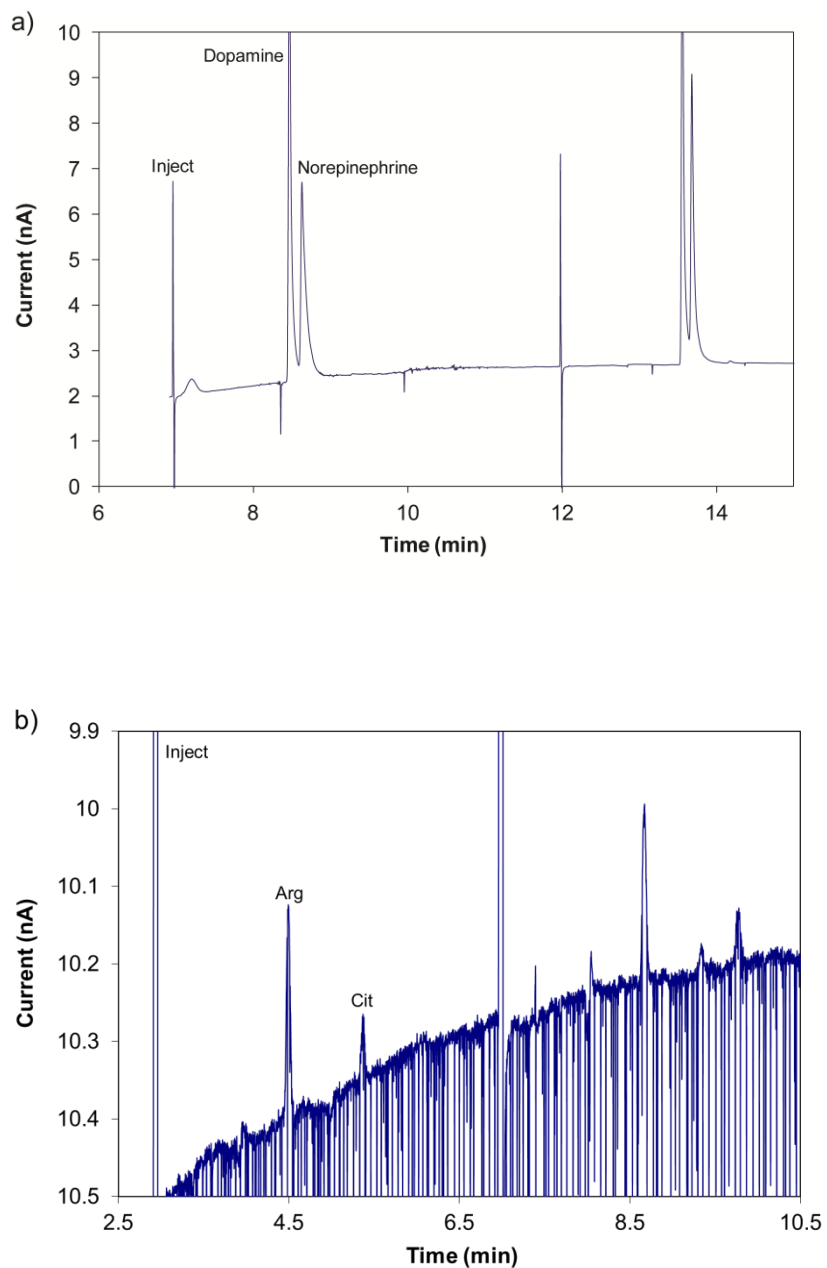


Figure 6.13 Separation of (a) dopamine and norepinephrine and (b) NDA/MESA-derivatized arginine and citrulline on a serpentine MCE-EC device. Evidence of building electrical issues can be seen in the baseline of (b).

increasingly inconsistent. For example, electrical outlet grounds were measured to be >1 V on several occasions. As one may imagine, these electrical issues caused chaos in the EC detection systems. Figure 6.13b shows a separation of arginine and citrulline on the serpentine chip; however, the baseline was incredibly noisy. Vigorous bubbling was observed between the counter electrode and HV ground during these experiments which undoubtedly caused the instability of the baseline current. Unfortunately, these electrical problems precluded EC detection from being used as a detection mode in MCE.

However, before the electrical problems in the building prevented EC experiments from being conducted, a severe limitation of MCE-EC was discovered in the analysis of NDA-derivatized analytes. When detection limits were being characterized for the derivatized complexes, it was found that they depended on the identity of the nucleophile used and the detection potential. At 800 mV detection potentials, both nucleophiles provided good LODs. The LOD ($S/N = 3$) for arginine derivatized with NDA/ CN^- was 600 nM while the LOD for NDA/MESA at that potential was 400 nM. At 400 mV oxidation potentials, however, the LODs were very far from similar. Detection limits for arginine derivatized with MESA and CN^- were 200 nM and 80 μ M, respectively. This data highlights the drastic difference the choice of nucleophile makes in the oxidation potentials of the derivatized species. NDA/MESA-derivatized analytes produced good responses at low detection potentials. This is highly beneficial since many interfering species will not be capable of producing a current at the electrode since the detection potential will be below their E_p values. This mitigates their impact on the separation and will provide less complex electropherograms. However, even though the LOD with NDA/MESA was significantly lower than with NDA/ CN^- , it was still too high to quantify endogenous concentrations of MAs. This derivatization chemistry would be beneficial

in the analysis of amino acids such as arginine since it is present at concentrations in the tens of micromolar. Unfortunately, since MA quantitation is central to the goal of this project, alternative analytical methods with lower LODs must be established.

6.3.2 Microchip Electrophoresis with Fluorescence Detection

Upon discovering that MCE-EC lacked the requisite detection limits to monitor endogenous levels of MAs, a transition was made to MCE-LIF since fluorescence detection has been shown to provide superior LODs [3]. The devices used for the MCE-LIF study were fabricated from glass substrates because of their higher optical clarity and ability to aid the precision of the separation.

Once the chip was fabricated and ready for use, an initial analysis using a simpler run buffer (from Figure 3.5) was first evaluated. Sample containing 1 μM of each MA analogue was derivatized with NDA/CN⁻ and loaded into the sample reservoir for analysis. A sample electropherogram depicting the resulting separation is shown in Figure 6.14. It was found that under these conditions, baseline resolution was achieved for the MAs on a MCE device in approximately three minutes. The good resolution between peaks demonstrates the high separation efficiency achieved in chips even though the separation distance was almost four-fold less than that in the conventional CE system. The fast analysis times also demonstrate the viability of incorporating MCE-LIF into a POC analysis system for MA analysis. However, in order to be able to serve as a POC system, the LOD of the method must be sufficient to measure endogenous concentrations. A LOD study was then performed where it was found that the detection limits for each MA was 10 nM. This is well-below the expected serum concentrations which suggests that this system could be used in a clinical assay.

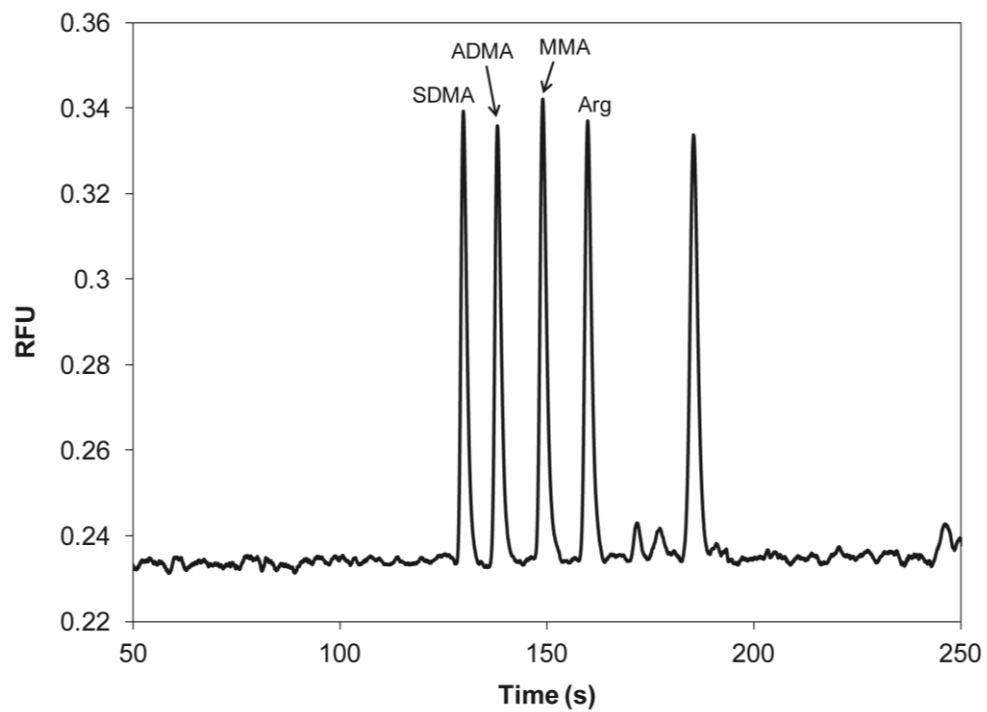


Figure 6.14 MCE-LIF separation of NDA/CN⁻-derivatized MAs.

While the system was found to be capable of measuring endogenous MA concentrations, improvements could still be made. The separation efficiency and analysis times could be improved by increasing the field strengths in the microchip. In this study, the separation current in the channels was limited to a 100 μA maximum. This limit was set as an arbitrary threshold to prevent Joule heating from producing bubbles in the chip. As a result, gating voltages of 7.8 kV and 13.5 kV were chosen because they provided the highest field strengths while preventing the current from exceeding the maximum threshold. The 7.8/13.5 kV voltage scheme corresponded to field strengths of 700 V/cm. However, field strengths well over 1000 V/cm are theoretically possible before boiling the buffer [25]. Because no significant bubble formation occurred under our conditions and because higher electric fields have been reported, higher voltages could be applied to our chip to help increase the rate of analysis and improve separation efficiency. This would help increase peak capacity which may be necessary for the analysis of serum-derived samples.

6.4 Conclusions

MCE is an attractive platform for achieving high efficiency separations with fast analysis times. Therefore, this technology was evaluated for the determination of MAs towards the development of a point-of-care screening system. Experiments were first conducted using MCE-EC since the miniaturization of EC systems is more easily accomplished than with LIF systems. Unfortunately, it was found that utilizing EC detection required high detection potentials for NDA/ CN^- labeled analytes which produced high LODs. This led to a study conducted to determine if an alternative nucleophile could be used in place of CN^- . It was discovered that MESA imparted beneficial traits onto the analysis. NDA/MESA-labeled analytes required lower

detection potentials, labeled analytes more quickly, and produced better peak shapes during electrophoretic separations. However, even despite the benefits of NDA/MESA, the LOD with this EC method was still insufficient to detect endogenous concentrations of MAs. To overcome the limitations of EC detection, a MCE-LIF method was evaluated. This method provided promising results in the analysis of MAs. A good separation of MAs was achieved on-chip and the LODs were found to be at levels conducive to the determination of MAs in clinical samples.

6.5 References

- [1] D. Janasek, J. Franzke, A. Manz, Scaling and the design of miniaturized chemical-analysis systems, *Nature*, 442 (2006) 374-380.
- [2] L.J. Kricka, Miniaturization of analytical systems, *Clin. Chem.*, 44 (1998) 2008-2014.
- [3] G.J.M. Bruin, Recent developments in electrochemically driven analysis on microfabricated devices, *Electrophoresis*, 21 (2000) 3931-3951.
- [4] X. Lin, C.L. Colyer, J.P. Landers, Electrophoresis in microfabricated devices, *Encyclopedia of Chromatography*, CRC Press, 2010, pp. 716-725.
- [5] W.R. Vandaveer, S.A. Pasas-Farmer, D.J. Fischer, C.N. Frankenfeld, S.M. Lunte, Recent developments in electrochemical detection for microchip capillary electrophoresis, *Electrophoresis*, 25 (2004) 3528-3549.
- [6] S. Pasas, B. Fogarty, B. Huynh, N. Lacher, B. Carlson, S. Martin, W. Vandaveer, S. Lunte, Detection on microchips: principles, challenges, hyphenation, and integration, *Separation Methods in Microanalytical Systems*, CRC Press LLC, 2006, pp. 433-497.
- [7] Y.F. Cheng, N.J. Dovichi, Subattomole amino acid analysis by capillary zone electrophoresis and laser-induced fluorescence, *Science*, 242 (1988) 562-564.
- [8] D.C. Duffy, J.C. McDonald, O.J.A. Schueller, G.M. Whitesides, Rapid Prototyping of Microfluidic Systems in Poly(dimethylsiloxane), *Anal. Chem.*, 70 (1998) 4974-4984.
- [9] S.K. Sia, G.M. Whitesides, Microfluidic devices fabricated in poly(dimethylsiloxane) for biological studies, *Electrophoresis*, 24 (2003) 3563-3576.
- [10] R. Mukhopadhyay, When PDMS isn't the best, *Anal. Chem.*, 79 (2007) 3248-3253.

- [11] D.J. Fischer, M.K. Hulvey, A.R. Regel, S.M. Lunte, Amperometric detection in microchip electrophoresis devices: Effect of electrode material and alignment on analytical performance, *Electrophoresis*, 30 (2009) 3324-3333.
- [12] L.A. Legendre, J.P. Ferrance, J.P. Landers, Microfluidic devices for electrophoretic separations: fabrication and use, *Handbook of Capillary and Microchip Electrophoresis and Associated Microtechniques*, CRC Press LLC, 2008, pp. 335-358.
- [13] B.H. Huynh, B.A. Fogarty, P. Nandi, S.M. Lunte, A microchip electrophoresis device with on-line microdialysis sampling and on-chip sample derivatization by naphthalene 2,3-dicarboxaldehyde/2-mercaptoethanol for amino acid and peptide analysis, *J. Pharm. Biomed. Anal.*, 42 (2006) 529-534.
- [14] T.H. Linz, C.M. Snyder, S.M. Lunte, Optimization of the separation of NDA-derivatized methylarginines by capillary and microchip electrophoresis, *J. Lab. Autom.*, 17 (2012) 24-31.
- [15] S.C. Jacobson, R. Hergenroder, L.B. Koutny, R.J. Warmack, J.M. Ramsey, Effects of Injection Schemes and Column Geometry on the Performance of Microchip Electrophoresis Devices, *Anal. Chem.*, 66 (1994) 1107-1113.
- [16] P. Nandi, D.P. Desai, S.M. Lunte, Development of a PDMS-based microchip electrophoresis device for continuous online in vivo monitoring of microdialysis samples, *Electrophoresis*, 31 (2010) 1414-1422.
- [17] P.J. Britto, K.S.V. Santhanam, P.M. Ajayan, Carbon nanotube electrode for oxidation of dopamine, *Bioelectrochem. Bioenerg.*, 41 (1996) 121-125.
- [18] J. Park, Y. Show, V. Quaiserova, J.J. Galligan, G.D. Fink, G.M. Swain, Diamond microelectrodes for use in biological environments, *J. Electroanal. Chem.*, 583 (2005) 56-68.

- [19] R.G. Carlson, K. Srinivasachar, R.S. Givens, B.K. Matuszewski, New derivatizing agents for amino acids and peptides: Facile synthesis of N-substituted 1-cyanobenz[f]isoindoles and their spectroscopic properties, *J. Org. Chem.*, 51 (1986) 3978-3983.
- [20] B.K. Matuszewski, R.S. Givens, K. Srinivasachar, R.G. Carlson, T. Higuchi, N-substituted 1-cyanobenz[f]isoindole: evaluation of fluorescence efficiencies of a new fluorogenic label for primary amines and amino acids, *Anal. Chem.*, 59 (1987) 1102-1105.
- [21] M. Lacroix, V. Poinot, C. Fournier, F. Couderc, Laser-induced fluorescence detection schemes for the analysis of proteins and peptides using capillary electrophoresis, *Electrophoresis*, 26 (2005) 2608-2621.
- [22] M.A. Nussbaum, J.E. Przedwiecki, D.U. Staerk, S.M. Lunte, C.M. Riley, Electrochemical characteristics of amino acids and peptides derivatized with naphthalene-2,3-dicarboxaldehyde: pH effects and differences in oxidation potentials, *Anal. Chem.*, 64 (1992) 1259-1263.
- [23] S.M. Lunte, T. Mohabbat, O.S. Wong, T. Kuwana, Determination of desmosine, isodesmosine, and other amino acids by liquid chromatography with electrochemical detection following precolumn derivatization with naphthalenedialdehyde/cyanide, *Anal. Biochem.*, 178 (1989) 202-207.
- [24] P. de Montigny, J.F. Stobaugh, R.S. Givens, R.G. Carlson, K. Srinivasachar, L.A. Sternson, T. Higuchi, Naphthalene-2,3-dicarboxyaldehyde/cyanide ion: a rationally designed fluorogenic reagent for primary amines, *Anal. Chem.*, 59 (1987) 1096-1101.
- [25] N.J. Petersen, R.P.H. Nikolajsen, K.B. Mogensen, J.P. Kutter, Effect of Joule heating on efficiency and performance for microchip-based and capillary-based electrophoretic separation systems: A closer look, *Electrophoresis*, 25 (2004) 253-269.

Chapter Seven

Conclusions and Future Directions

7.1 Dissertation Summary

The purpose of this dissertation was to describe the efforts made towards the development of analytical methods for the determination of methylarginines (MAs) in serum. Initial studies were concerned with optimization of the electrophoretic separation of the different MAs of interest. It was discovered that an optimal separation was achieved when sulfobutylether- β -cyclodextrin and dimethylsulfoxide were employed as additives to the run buffer. Neither of these compounds are typically utilized in CE experiments but were found to be crucial for the separation method. Under these optimized conditions, excellent peak capacity was realized. This enabled near-baseline resolution to be obtained for the MAs and the internal standard from the other components in complex serum-derived samples.

A novel method was also developed to permit rapid preparation of serum samples. Serum samples were subjected to a thermal coagulation procedure to induce protein aggregation. Small molecules were able to be isolated from the gelatinous serum samples via solid-liquid extraction. This optimized procedure was compared to a commonly employed solid-phase extraction (SPE) procedure to ensure analytical suitability. The results from both methods were in agreement with one another; however, the novel heat-assisted extraction method was substantially faster, less expensive, and more precise than the SPE method.

Following the development and characterization of the sample preparation and separation methods, they were applied to the analysis of clinical samples. MAs were measured in samples from patients potentially suffering from either cardiovascular or respiratory diseases. Both types of diseases stem from underlying nitric oxide (NO) deficiency, and therefore, patients may exhibit clinically-relevant elevations in the concentrations of MAs in their systems. From these preliminary studies, it was determined that patients diagnosed with coronary artery disease

(CAD) did have higher average MA concentrations than those without CAD; however, the differences were not significant. Additionally, MAs were measured in critically ill infants and interesting variations were found based on their ages. The plasma MA concentrations were much higher over the first few months of life when compared to adults. These levels eventually dropped off as age increased, and once an infant was six months old, their MA concentrations were similar to those of adults. These findings illustrate but two of the interesting MA-related applications of the novel analytical methods.

Finally, the separation method was transferred to a microfluidic platform as a first step towards the development of a point-of-care diagnostic device. Microchip electrophoresis (MCE) coupled to either electrochemical (EC) or fluorescence (LIF) detection was evaluated to determine its ability to provide sufficient limits of detection (LODs) for the measurement of MAs in clinical samples. MCE-EC separations were found to produce poor peak shape and high LODs, so an investigation was initiated to improve both the separation and electrochemical characteristics of the derivatized analytes. This study identified a novel nucleophile that was superior in the derivatization scheme because it imparted beneficial properties onto the analytes. However, the detection limits were still insufficient for clinical analyses. Therefore, a MCE-LIF analysis was implemented to determine its ability to separate the analytes. With this system, good resolution between MAs was achieved, and the system was found to have adequate detection limits to permit quantitation of MAs in serum samples.

7.2 Future Directions

While the methods developed in this dissertation demonstrated significant advances in the quantitation of MAs in complex serum samples, additional studies are still warranted. Brief descriptions related to improvements and applications of MA analyses will be discussed here.

7.2.1 Analytical Advances

Efforts can be made towards the development of an autonomous point-of-care system by integrating the sample preparation and analysis components into a single microfluidic device. A method could be implemented to prepare serum gel off-line but then introduce the gel into a microfluidic device to carry out the extraction. Extracted analytes could then be directly derivatized on-chip by mixing the sample flow with streams of NDA and CN⁻. Our lab has already developed similar microchips that demonstrate the feasibility of achieving this goal [1]. Further investigations could also be made into creating a microchip device with multiple separation channels for multiplexed analysis [2, 3]. This would allow the simultaneous analysis of samples from several patients, which would further improve throughput. The miniaturization of the entire analytical system can also be undertaken such that sample analysis could be performed in clinical labs. The construction of a self-contained system incorporating a diode laser, optics cube, objective lens, and PMT detector would allow the entire setup to be readily transported to hospitals to analyze patient samples on-site.

This analytical device could also be used in the analyses of other potential biomarkers of cardiovascular and respiratory diseases. The use of a separation technique would allow other biological amines to be quantified to determine whether a positive correlation could be made between the biomarker concentration and disease progression. Extraction and separation

conditions could be slightly modified as necessary to obtain optimal results, but the general analytical protocol would essentially remain the same.

7.2.2 Biochemical Mechanism Elucidation Studies

The analytical methods described in Chapters 3 and 4 were successfully implemented in the analysis of clinical samples from two small-scale studies described in Chapter 5. The preliminary data derived from those studies provided interesting results for which to base subsequent studies. The results from these experiments would offer additional information regarding the development of cardiovascular and respiratory diseases.

7.2.2.1 Cardiovascular Disease

A larger scale study exploring the effects of heart medication on MA concentrations could be initiated in which patients are divided into groups based on their past coronary health. Those who have an established history of CAD and are currently receiving medication would be in one group while newly diagnosed patients who are not yet receiving treatment would be in a second group. Comparing the amounts of MAs between these two groups (along with a control group) would provide insight into the impact of the medication on systemic levels of MAs. This could aid in better understanding the biochemical pathways affected by commonly prescribed cardiac drugs whose mechanisms of action are not well known. Further studies can also be conducted to determine a threshold concentrations of MAs that indicate CVD. These values could be used as early screening diagnostic markers to predict CVD before a patient presents with a heart attack or stroke. This would allow the initiation of a medication regimen before a potentially life-threatening event occurs.

7.2.2.2 Respiratory Disease

Preliminary results obtained from critically ill newborns indicated that MA levels are quite high within the first few months of life. Therefore, conducting a study with a larger patient population would be prudent to determine if this trend holds true over a larger sample size and to determine whether healthy infants yield similar values. This study should also be designed to specifically enroll newborns with respiratory failure and not merely critically ill infants.

If it is determined that MAs are present at significantly different concentrations between healthy infants and those with respiratory distress, further studies should be undertaken to investigate the nitric oxide synthase (NOS) pathway. A pulmonary endothelial cell culture model could be developed to monitor the enzymes responsible for the production and degradation of the MAs as well as the bipterins. Expression levels of these enzymes can be measured to determine if they differ between healthy and diseased cells. This model system would allow the enzymes to be interrogated in a controlled manner to elucidate the root cause of NOS dysfunction. Nitric oxide could also be added into the cell culture incubator to determine its effect on enzyme expression. Understanding how the presence of excess NO affects NOS activity will aid in determining the mechanism of action of inhaled nitric oxide (iNO) therapy.

Additionally, if it is discovered that endogenous BH₄ concentrations are diminished in infants with respiratory distress, an investigation can be made into the effects of iNO administration on oxidative stress damage in the lungs. Since it has been established that NOS produces superoxide if depleted of BH₄, an influx of NO (from iNO therapy) could react with the superoxide to generate large amounts of peroxynitrite. Peroxynitrite can cause a number of problems in cells including lipid peroxidation, protein oxidation or nitration, and DNA degradation [4]. This irreversible damage to vital cellular components can lead to cellular

dysfunction or cell death [5]. Although previous studies have shown no significant increase in proinflammatory cytokines in tracheal aspirate fluid (TAF) [6] nor increased peroxynitrite biomarkers in plasma [7] in patients suffering from respiratory distress, the administration of iNO could increase peroxynitrite production. The resulting peroxynitrite-induced tissue damage may be responsible for the onset of asthma and other breathing disorders that these infants develop later in life [8].

To determine whether lung damage occurs following iNO therapy, analytical methods can also be developed to monitor the biomarkers malondialdehyde (MDA) [9] and 3-nitrotyrosine (3-NT) which have been shown to serve as indicators of oxidative stress damage. MDA is formed as a byproduct of reactive oxygen species-induced peroxidation of polyunsaturated lipids and is a common biomarker for oxidative stress damage. Increased concentrations of MDA have been shown to correlate to increased amounts of peroxynitrite-induced oxidative stress damage in respiratory disorders and heart disease [10-12]. 3-NT is a more specific marker for peroxynitrite damage and has also been shown to be present at higher levels during conditions of oxidative stress [5, 8]. TAF can be collected from intubated infants suffering from respiratory distress before and after initiation of iNO to determine whether the concentrations of oxidative stress biomarkers change following treatment. Analysis of the biomarkers in TAF, rather than plasma, would provide a more accurate understanding of localized oxidative stress than would be gained by monitoring those compounds in systemic circulation.

7.3 References

- [1] P. Nandi, D.P. Desai, S.M. Lunte, Development of a PDMS-based microchip electrophoresis device for continuous online in vivo monitoring of microdialysis samples, *Electrophoresis*, 31 (2010) 1414-1422.
- [2] J.F. Dishinger, K.R. Reid, R.T. Kennedy, Quantitative monitoring of insulin secretion from single Islets of Langerhans in parallel on a microfluidic chip, *Anal. Chem.*, 81 (2009) 3119-3127.
- [3] N.R. Munce, J. Li, P.R. Herman, L. Lilge, Microfabricated system for parallel single-cell capillary electrophoresis, *Anal. Chem.*, 76 (2004) 4983-4989.
- [4] W.A. Pryor, K.N. Houk, C.S. Foote, J.M. Fukuto, L.J. Ignarro, G.L. Squadrito, K.J.A. Davies, Free radical biology and medicine: it's a gas, man!, *Am. J. Physiol. Regul. Integr. Comp. Physiol.*, 291 (2006) R491-511.
- [5] G. Ferrer-Sueta, R. Radi, Chemical Biology of Peroxynitrite: Kinetics, Diffusion, and Radicals, *ACS Chem. Biol.*, 4 (2009) 161-177.
- [6] W.E. Truog, P.L. Ballard, M. Norberg, S. Golombek, R.C. Savani, J.D. Merrill, L.A. Parton, A. Cnaan, X. Luan, R.A. Ballard, Inflammatory markers and mediators in tracheal fluid of premature infants treated with inhaled nitric oxide, *Pediatrics*, 119 (2007) 670-678.
- [7] P.L. Ballard, W.E. Truog, J.D. Merrill, A. Gow, M. Posencheg, S.G. Golombek, L.A. Parton, X. Luan, A. Cnaan, R.A. Ballard, Plasma biomarkers of oxidative stress: relationship to lung disease and inhaled nitric oxide therapy in premature infants, *Pediatrics*, 121 (2008) 555-561.
- [8] F.L.M. Ricciardolo, A. Di Stefano, F. Sabatini, G. Folkerts, Reactive nitrogen species in the respiratory tract, *Eur. J. Pharmacol.*, 533 (2006) 240-252.

- [9] J.C. Cooley, C.E. Lunte, Detection of malondialdehyde in vivo using microdialysis sampling with CE-fluorescence, *Electrophoresis*, 32 (2011) 2994-2999.
- [10] O. Koksel, I. Cinel, L. Tamer, L. Cinel, A. Ozdulger, A. Kanik, B. Ercan, U. Oral, N-acetylcysteine inhibits peroxynitrite-mediated damage in oleic acid-induced lung injury, *Pulm. Pharmacol. Ther.*, 17 (2004) 263-270.
- [11] S. Levrard, C. Vannay-Bouchiche, B. Pesse, P. Pacher, F. Feihl, B. Waeber, L. Liaudet, Peroxynitrite is a major trigger of cardiomyocyte apoptosis in vitro and in vivo, *Free Radical Biol. Med.*, 41 (2006) 886-895.
- [12] F.D. Saunders, M. Westphal, P. Enkhbaatar, J. Wang, K. Pazdrak, Y. Nakano, A. Hamahata, C.C. Jonkam, M. Lange, R.L. Connelly, G.A. Kulp, R.A. Cox, H.K. Hawkins, F.C. Schmalstieg, E. Horvath, C. Szabo, L.D. Traber, E. Whorton, D.N. Herndon, D.L. Traber, Molecular biological effects of selective neuronal nitric oxide synthase inhibition in ovine lung injury, *Am. J. Physiol. Lung Cell Mol. Physiol.*, 298 (2010) L427-436.